GROIN HERNIA: THE ROLE OF DIAGNOSTIC IMAGING

J.C. van den Berg

GROIN HERNIA: THE ROLE OF DIAGNOSTIC IMAGING

J.C. van den Berg

GROIN HERNIA
THE ROLE OF DIAGNOSTIC IMAGING

Een wetenschappelijke proeve op het gebied
van de Medische Wetenschappen

Proefschrift

Ter verkrijging van de graad van doctor
aan de Katholieke Universiteit Nijmegen,
volgens besluit van het College van Decanen
in het openbaar te verdedigen op

dinsdag 24 april
des namiddags om 1.30 uur precies

door

Josua Cornelis van den Berg
Geboren op 20 september 1961 te Leiden

Promotores: prof. dr. G. Rosenbusch
prof. dr. J.B.M.J. Jansen

Co-promotor: dr. F.B.M. Joosten

Manuscriptcommissie: prof. dr. Th. Wobbes (voorzitter)
prof. dr. J.H.J.M. van Krieken
prof. dr. M.A.M. Feldberg

Het verschijnen van dit proefschrift werd mede mogelijk gemaakt door de steun van: Agfa Gevaert, ATL, BARD, Byk, Boston Scientific, Cook, Cordis, Edwards Lifesciences, Guidant, Jomed, Medtronic AVE, Philips Medical Systems, Raad van Bestuur St. Antonius Ziekenhuis Nieuwegein, Schering, Sigma Medical, Terumo, W.L. Gore & Associates.

CIP-gegevens Koninklijke Bibliotheek, Den Haag.
Groin hernia: the role of diagnostic imaging/J.C. van den Berg. - [Nieuwegein; s.n.], met samenvatting in het Nederlands. 2001.-135 pagina's: ill; 24 cm.
ISBN: 90-9014635-0
Subject headings: groin hernia, ultrasound, MRI

Drukkerij : EPC, Nieuwegein

Omslag:
Pl II : canalis inguinalis et femoralis, uit : Recherches anatomiques sur les hernies de l'abdomen ; Jules Cloquet-Paris : Méquignon-Marvis, 1817 (Museum Boerhaave, Leiden).

CONTENTS

1

INTRODUCTION

The role of diagnostic imaging in general has changed rapidly over the last decade. With the advent of new imaging techniques, like ultrasound, CT and magnetic resonance imaging, a whole new world had to be discovered. Radiologists also became more involved in therapeutic decision making. This not only because the development of various (therapeutic) interventional procedures (abscess drainage, percutaneous biliary drainage and vascular interventional procedures) urged them to do, but also because diagnostic imaging is playing an increasing and important role in planning of surgery and radiotherapy. Extensive radiological work-up (including CT and MRI) is now performed routinely prior to institution of therapy in patients with (malignant) tumours, abscesses etc.

As for general radiology, diagnostic imaging of the groin region has been changed. In the past (the pre-ultrasound, pre-CT and pre-MRI era) the only question from the surgeon that had to be answered was: is there an inguinal hernia, or not?

Before 1961, in the early years of radiology the groin hernia could only be demonstrated indirectly by depicting the contents of a hernial sac using plain abdominal radiography, barium examinations of the digestive tract or contrast enhanced examinations of the urinary tract [**1,2,3**]. For direct demonstration of the hernial sac itself herniography was the first available diagnostic modality. The first in vivo delineation of the peritoneal cavity was achieved by intraabdominal inflation of air (negative contrast peritoneography) [**4,5,6**]. Main indications for this diagnostic procedure were the evaluation of abdominal or pelvic masses noted on plain abdominal films or physical examination, evaluation of the extension of malignant disease and the determination of the presence of subphrenic or subhepatic abscess. Positive contrast was first used in peritoneography in the early sixties by Birzle, and later by many others [**5,7,8,9**].

Later ultrasound, CT and MRI were successfully used in the diagnosis of abdominal wall hernias [**10,11,12,13,14,15**], and the new techniques also allowed establishment not only of the presence of a mass but also the nature of any mass lesion in the groin [**16,17,18,19,20**].

The first report describing the sonographic appearance of a hernia was published in 1975 [**21**]. Technical developments of ultrasound equipment (i.e. high frequency transducers) made it possible to obtain high resolution images of anatomic structures as small as peritoneum [**17**].

The use of CT in the diagnosis of hernias was initially described in case reports and later in pictorial essays [**12,22,23**], or in cases of clinically hard to diagnose entities such as obturator hernias [**15,24,25**]. With the advent of helical CT it became also possible to obtain high resolution images by scanning a small volume with thin slices. Multiplanar reconstructions added to the advantages of helical CT scanning. With the reduction of the time

needed to scan such a volume, nowadays images obtained during one breathhold or during straining are available [**26,27**].
The first description of an inguinal hernia on MRI was made in 1989 using standard, non-dynamic, scanning sequences [**12**]. By shortening of the acquisition time dynamic MRI that is used in studies of pelvic descent became feasible [**28**].
Advantage of ultrasound, CT and MRI is the ability to reveal other causes of groin pain [**29,30**]. Despite the extensive use in clinical practice, however, the diagnostic accuracy of these techniques and their value was not established systematically.
As the majority of patients presenting with inguino-femoral disease have clearcut findings at clinical history and physical examination, indications for all the above mentioned diagnostic imaging modalities are limited. Only in clinically doubtful cases there is a role for diagnostic imaging.
Recent developments in minor access surgery, such as laparoscopic hernia repair show the need of a more detailed anatomic depiction of the groin pre-operatively. This is a new indication for imaging of the inguinal region and it requires a thorough knowledge of the specific anatomy and pathology from the radiologist [**31,32**].
This applies for clinically doubtful cases too, in which the radiologist must be familiar with the differential diagnosis of a groin mass as well as the advantages and limitations of various radiological modalities.

Aim and purpose of this thesis is:
-To give an overview of the key anatomic structures of the groin region as seen on gross anatomy, and the appearance of these anatomic structures on herniography, ultrasound, CT and MRI.
-To present the differential diagnosis of masses and pain in the groin, by giving an overview of the imaging characteristics of several disease entities in the inguinofemoral region including herniations, neoplasms, joints disease and vascular abnormalities.
-To make a validation of imaging modalities used in the preoperative diagnosis of inguinal hernias including herniography, ultrasound and MRI.
-To evaluate the role of MRI in the postoperative period after surgical inguinal hernia repair.

Chapter 2 and 3 present a pictorial review of groin anatomy and disease of the inguinofemoral region respectively.
Chapter 4 to 7 focus on the diagnosis of groin hernias:
-Herniography will be discussed in Chapter 4. This technique was and still is a very reliable modality in the diagnosis of herniations of the abdominal wall [**33,34**]. Technique of herniography and its diagnostic yield are evaluated.

-The description and use of a new dynamic MRI is presented in chapter 5 and 6, reporting the first clinical experience and description of the anatomy of the inguinal canal and its surroundings on coronal MRI images. In these chapters the diagnostic potential of the technique by correlation with surgery is evaluated.
-In chapter 7 a comparative study is made of MRI, ultrasound and physical examination in patients with clinically evident groin hernia.
Finally the role of MRI in the postoperative patient is described in chapter 8. The last chapters present a general discussion and summary as well as a practical guide to the work-up of the patient suspected of a groin hernia

REFERENCES

1. Laurell H (1929) Über die Röntgenuntersuchung von Brüchen, insbesondere klinisch schwer zu diagnostizierende Formen. Acta Radiol 10:462.
2. Zausner J, Dumont AE, Ring SM (1972) Obturator hernia.AJR 115:408-410.
3. Glicklich M, Eliasoph J (1989) Incarcerated obturator hernia: case diagnosed at barium enema fluoroscopy. Radiology 172:51-52.
4. Meyers MA (1973) Peritoneography, normal and pathologic anatomy.AJR 117:353-365.
5. Birzle H (1961) Ist die Peritoneographie als röntgenologische Untersuchungsmethode möglich und brauchbar. Fortschr. Röntgenstr. 95:824-829.
6. Arner O, Fernstrom I (1970) The value of pneumoperitoneum in the diagnosis of hernia in the inguinal region. Surgery 67:741-747.
7. Ekberg O, Fork FT (1979) Röntgenologische Leisten-bruchdiagnostik-Erfahrungen mit intraperitonealer Jodkontrast-instillation. Fortschr. Röntgenstr 131: 166-168.
8. Oh KS, Dorst JP, White JJ, Haller JA, Heller RM, James AE, Johnson BA, Strife JL (1973) Positive-contrast peritoneography and herniography. Radiology 108-:647-654.
9. White JJ, Haller JA, Dorst JP (1970) Congenital inguinal hernia and inguinal herniography. Surg Clin North Am 50:823-837.
10. Maglinte DDT, Miller RE, Lappas JC (1984) Radiological diagnosis of occult incisional hernias of the small intestine. AJR 142:931-932.
11. Gharemani GG, Jimenez MA, Rosenfeld M, et al. (1987) CT diagnosis of occult incisional hernias. AJR 148:139-142.
12. Wechsler RJ, Kurtz AB, Needleman L, et al. (1989) Cross-sectional imaging of abdominal wall hernias. AJR 153:517-521.
13. Zarvan NP, Lee FT, Yandow DR, Unger JS (1995) Abdominal hernias: CT findings. AJR 164:1391-1395.

14. Deitch EA, Soncrant MC (1981) Ultrasonic diagnosis of surgical disease in the inguino-femoral region. Surg Gyn Obst 152:319-322.
15. Harrison LA, Keesling CA, Martin NL, Lee KR, Wetzel LH (1995) Abdominal wall hernias: Review of herniography and correlation with cross-sectional imaging. Radiographics 15:315-332.
16. Gitschlag KF, Sandler MA, Madrazo BL, Hricak H, Eyler WR (1982) Disease in the femoral triangle:sonographic appearance. AJR 139:515-519.
17. Truong S, Pfingsten FP, Dreuw B, Schumpelinck V (1993) Stellenwert der Sonographie in der Diagnostik von unklaren Befunden der Bauchwand und Leistenregion. Chirurg 64:468-475.
18. Erez I, Schneider N, Glaser E, Kovalivker M (1992) Prompt diagnosis of 'acute groin' conditions in infants. Eur J Radiology 15:185-189.
19. Nguyen KT, Sauerbrei EE, Lewandowski BJ, Nolan RL (1991) The abdominal wall. In: Rumack CM, Wilson SR, Charboneau JW. Diagnostic ultrasound. Mosby Year Book, St. Louis, pp353-363.
20. Heiken JP (1989) Abdominal wall and peritoneal cavity. In: Lee JKT, Sagel SS, Stanley RJ. Computed body tomography, 2nd edition. Raven Press, New York, pp661-666.
21. Spangen L (1975) Ultrasound as a diagnostic aid in ventral abdominal hernia J Clin Ultrasound 3:211-213.
22. Lee G-H M, Cohen AJ (1993) CT imaging of abdominal hernias. AJR 161:1209-1213.
23. Yeh HC, Lehr-Janus C, Cohen BA, Rabinowitz JG (1984) Ultrasonography and CT of abdominal and inguinal hernias. J Clin Ultrasound 12:479-486.
24. Megibow AJ, Wagner AG (1983) Obturator hernia. JCAT 7:350-352.
25. Cubillo E (1983) Obturator hernia diagnosed by computed tomography. AJR 140:735-736.
26. Hahn-Pedersen J, Lund L, Hansen Højhus J, Bojsen-Møller F (1994) Evaluation of direct and indirect inguinal hernia by computed tomography. British Journal Surgery 81: 569-572.
27. Højer AM, Rygaard H, Jess P (1997) CT in the diagnosis of abdominal wall hernias: a preliminary study. Eur Radiol 7:1416-1418.
28. Vanbeckevoort D, Van Hoe L, Oyen R, Ponette E, De Ridder D, Deprest J (1999) Pelvic floor descent in females: comparative study of colpocystodefecography and dynamic fast MR imaging. J Magn Reson Imaging 9: 373-377.

29. Tuite MJ, DeSmet AA (1994) MRI of selected sports injuries: muscle tears, groin pain, and osteochondritis dissecans. Semin Ultrasound CT MR 15:318-340.
30. Ekberg O, Sjoberg S Westlin N (1996) Sports-related groin pain: evaluation with MR imaging. Eur Radiol 6:52-55.
31. Liem MSL, van Vroonhoven ThJMV (1996) Laparoscopic inguinal hernia repair. Br J Surg 83:1197-1204.
32. Nyhus LM (1993) Individualization of hernia repair: a new era. Surgery 114: 1-2.
33. Jones RL, Wingate JP (1998) Herniography in the investigation of groin pain in adults. Clin Radiol 53:805-808.
34. Hamlin JA, Kahn AM (1998) Herniography: a review of 333 herniograms. Am Surg 64:965-969.

2

RADIOLOGICAL ANATOMY OF THE GROIN REGION

ABSTRACT
The purpose of this paper is to give an overview of the anatomy of the inguinal region, and to discuss the value of various imaging modalities in the diagnosis of groin hernias. After description of the gross anatomy of the groin, attention is focussed on the anatomic features of conventional herniography, ultrasound (US), computed tomography (CT) and magnetic resonance imaging (MRI). Advantages, disadvantages and accuracy of each technique are discussed briefly.

Keywords
hernia, inguinal
abdominal wall, anatomy
ultrasound
CT
MRI
herniography

INTRODUCTION

The anatomy of the inguinal region is complex and unique in the fact that on one hand several muscular and vascular structures have to pass from the abdominal cavity into the upper leg, whereas on the other hand structures such as bowel and other internal organs have to be withheld from passing beyond the borders of the peritoneal cavity.

In the evaluation of groin masses, and of inguinal hernias in particular, several diagnostic modalities are available. Most important in day-to-day clinical practice is physical examination. In doubtful cases radiological imaging techniques (conventional radiography, US, CT or MRI) can be helpful. In these patients precise knowledge of the anatomy is the key to diagnostic success.

In this study a review of the gross anatomy of the groin is described, with specific attention to findings at herniography, US, CT and MRI.

GROSS ANATOMY

The inguinofemoral region is bordered by the anterior superior iliac spine and pubic crest superiorly, and includes the upper thigh region as well as the caudal part of the anterior abdominal wall. The abdominal wall and the groin region are composed of several layers from outer to inner side: skin, superficial fascia, subcutaneous fat, various muscle groups, extraperitoneal fat, and peritoneum. The muscles of the abdominal wall include the external and internal oblique, transversus abdominis and rectus abdominis (figure 1A). The *external oblique* is the most superficial of the three anterolateral muscles. Part of the fibres of this muscle give way to a thin, strong aponeurosis [**1**]. In the region of the groin the fibres of the external oblique aponeurosis form a free border, known as Poupart's ligament [**1,2**]. The *internal oblique muscle* is situated between the external oblique and *transversalis muscle*. The major vessels are the *external iliac artery and vein*; these vessels run along the medial side of the *psoas major muscle* and enter the leg by passing under the iliopubic tract (a reinforced band of fibres at the interior aspect of the peritoneal cavity at the level of the inguinal ligament) and into the femoral sheath (figure 1B). In the preperitoneal space there are two major arterial branches, the *inferior epigastric and the deep circumflex iliac artery* [**3**]. The inferior epigastric vessels are behind the inguinal canal, at the medial aspect of the internal inguinal ring. They originate from the external iliac artery and vein, reside along the anterior abdominal wall coursing upwards and medially to a position dorsally of the m. rectus abdominis (figure 1B, 1C) [**2,4**].

Laterally under the inguinal ligament is the iliopsoas muscle (and its bursa). The medial extent of Poupart's ligament is over the femoral vessels and the *pectineus muscle*. The *greater or long saphenous vein* passes through the fascia

lata to empty into the femoral vein (figure 1B) [**2**].

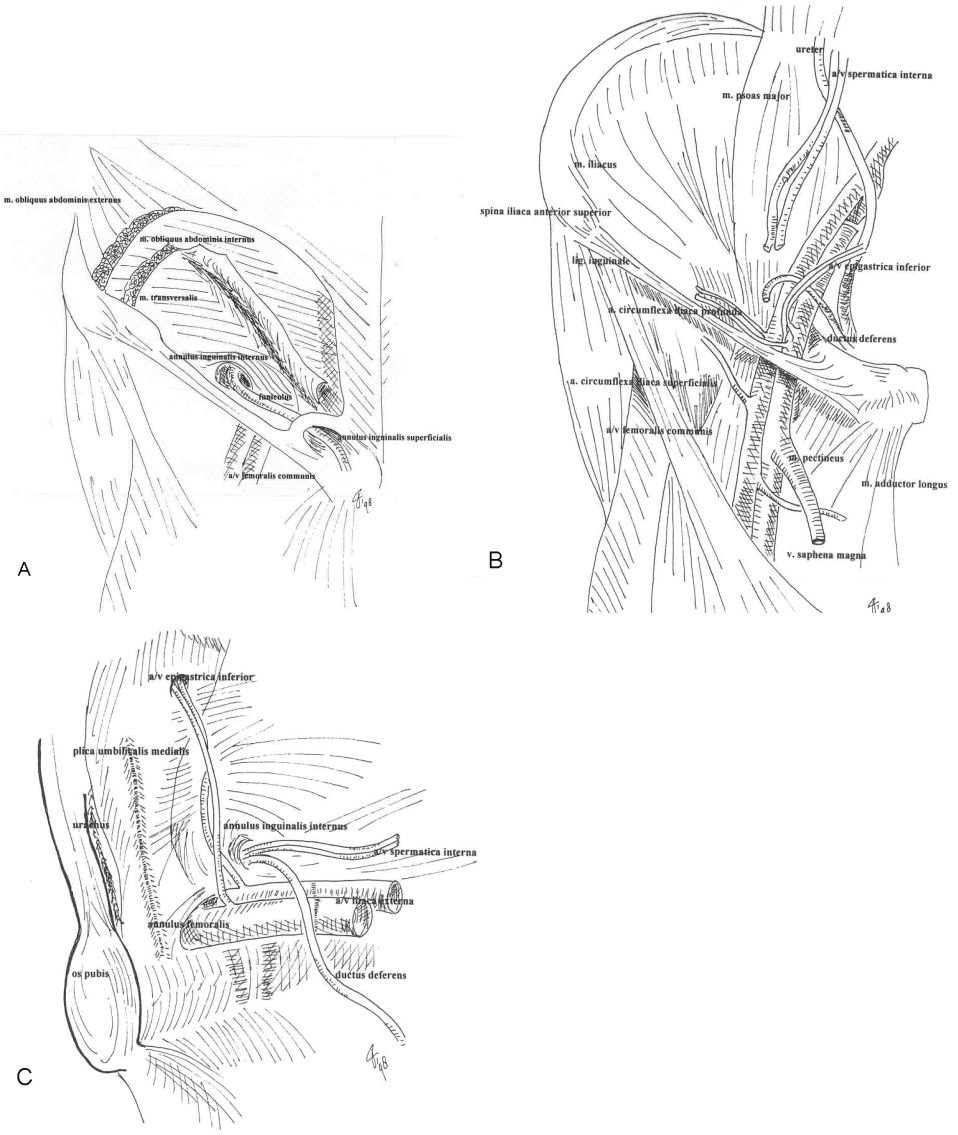

Figure 1
A-Oblique view of a dissection of external and internal oblique muscle, showing transversalis muscle and fascia, internal and external inguinal ring.
B-Major anatomic retroperitoneal structures and vessels of the groin region and femoral canal without the muscles of the anterior abdominal wall.
C-Medial view from internal aspect of right inguinal region (adapted from reference 1, 5 and 31).

On a view of the anterior abdominal wall from its internal aspect, the peritoneal tissue of the anterior abdominal wall will be seen to be raised into five vertical ligaments (folds), with intervening depressions (figure 1C) [**4,5**]. The *median umbilical ligament* (lig. umbilicale medianum/plica urachi)

is situated in the median line, and is caused by the urachus, the remnant of the allantois. It is attached to the apex of the bladder and produces a fold in the midline with peritoneal covering. On each side of the median umbilical fold a prominent band, caused by the fibrous remains of the obliterated umbilical arteries, passes just laterally to the bladder obliquely upward and inward to the umbilicus: the *medial umbilical fold* (lig. umbilicale mediale). To either side of these three cords are the inferior epigastric vessels, which ascend obliquely upward and inward from a point midway between the symphysis pubis and the anterior superior spine of the ilium. A fold of peritoneum, which is known as the *lateral umbilical fold* (lig. umbilicale laterale), covers it [**4,5**]. Between these raised folds are depressions of the peritoneum, constituting so-called fossae (from medial to lateral the supravesical fossa or internal inguinal fossa, the medial inguinal and lateral inguinal fossa) [**5**].

The inguinal canal (figure 1A, 1B) is occupied by the ilioinguinal nerve, and in the male by the *spermatic cord* structures and in the female by the round ligament of the uterus. It commences above at the *internal or deep inguinal ring* (located laterally in the transversalis fascia [**1,5**]), which is the point where the cord enters the inguinal canal, and terminates below at the *external or superficial ring* (a triangular opening in the aponeurosis of the external oblique [**1,2,3**]). The *ductus deferens* snakes around the posterior aspect of the bladder, crossing above and medial to the *ureter* to enter the lateral ligaments of the bladder [**4**]. It then continues to course along the lateral pelvic wall and subsequently hooks around the lateral side of the inferior epigastric artery. Here it joins the *testicular vessels* and nerves to form the spermatic cord. The spermatic cord traverses the deep inguinal ring, and then runs obliquely downward and medially in the inguinal canal and emerges through the superficial inguinal ring [**1,2,3**].

RADIOLOGICAL ANATOMY

The diagnosis of inguinal hernias is usually made on clinical grounds. Presently the role of additional diagnostic imaging is limited to cases with doubtful or inconclusive findings at physical examination. At present the treatment of direct and indirect inguinal hernias can differ considerably with the advent of new laparoscopic surgical techniques [**6**]. This development may influence the need of more extensive preoperative assessment of the patient's anatomy before deciding how to intervene.

HERNIOGRAPHY

The technique of herniography has been described extensively [**7,8,9, 10,11,12,13**]. After intra-peritoneal administration of 50 mL of non-ionic contrast medium, a standard series of views of both groins is obtained during

straining with the patient prone and in a slightly elevated position, as follows: posteroanterior, posteroanterior with caudocraniad angulation of the tube (15°), two oblique views, and a lateral view.
The folds (plicae) and fossae as described previously can be identified, as well as the osseous structures (figure 2). Douglas' pouch can be discerned on lateral and oblique views.

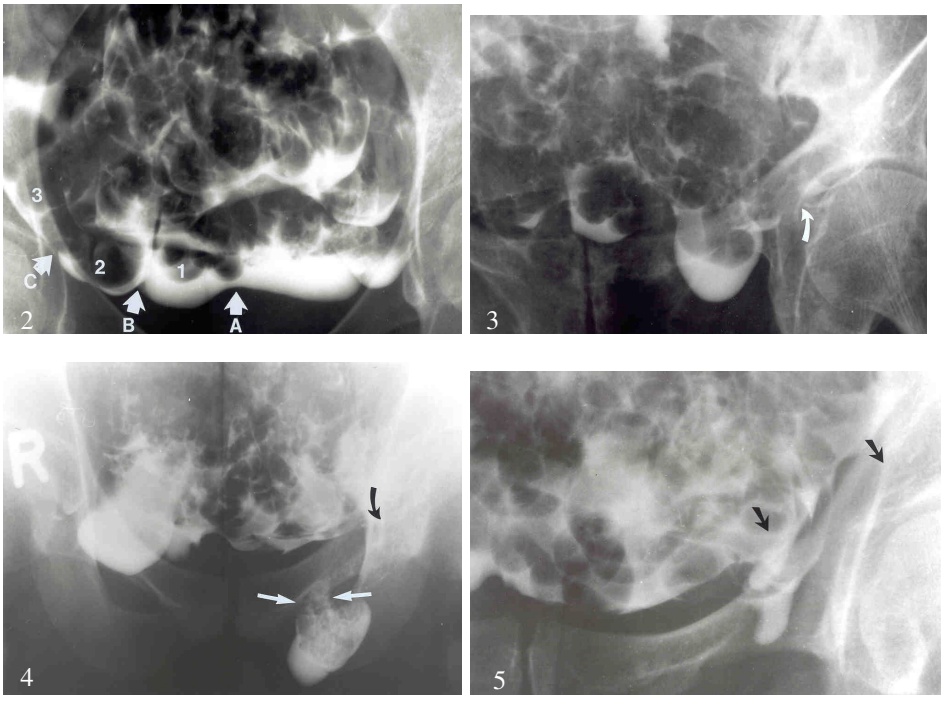

Figure 2
Normal herniography; A= median umbilical fold, B= medial umbilical fold, C= lateral umbilical fold, 1= supravesical fossa, 2= medial inguinal fossa, 3= lateral inguinal fossa.
Figure 3
Herniographic appearance of a left-sided direct inguinal hernia, originating from the medial inguinal fossa; the lateral inguinal fold (= inferior epigastric vessels) is indicated by the arrow.
Figure 4
Herniography demonstrating the typical course within the left inguinal canal of an indirect inguinal hernia; arrows indicate the location of the external inguinal ring, the curved arrow points at the site of the inferior epigastric vessels.
Figure 5
Example of a left-sided femoral hernia demonstrated herniographically; the typical origin below the inguinal ligament (indicated with arrows) is clearly seen.

A hernia is defined as a pathologic protrusion of one of the fossae beyond the boundaries of the inguinal ligament (imaginary line coursing from the anterior superior iliac spine to the pubic tubercle) or into the femoral canal, foramen obturatorium or abdominal wall (Spigelian hernia). The direct (acquired) inguinal hernias always originate medial to the lateral umbilical fold (inferior epigastric vessels), usually from the medial inguinal fossa

(sometimes from the supravesical fossa; figure 3). The indirect inguinal hernia protrudes from the lateral inguinal fossa. It follows the course of the inguinal channel (figure 4). Femoral hernias originate below the inguinal ligament from the inferior aspect of the peritoneal cavity (figure 5).
Disadvantage of herniography is its invasiveness and its inability to depict pathological conditions other than hernias.
Herniography is known to be highly reliable in diagnosing hernias in patients with unequivocal findings at physical examination, revealing hernias in about one-third of patients [**7**]. However to date the diagnostic accuracy of herniography is still not known [**14**].

ULTRASOUND

The muscular and fascial layers of the abdominal wall and groin region are best depicted with high-frequency (7.5-10 MHz), short-focused transducers [**9**]. In obese patients 5 MHz or even 3.5 MHz transducers may be needed (resulting however in low resolution images). With a high-frequency transducer, the midline and anterolateral muscle groups can be identified beneath the superficial fascia and subcutaneous tissue (figure 6a). On both longitudinal and transverse images, the peritoneal line is seen as a discrete linear echogenicity (figure 6b, c).

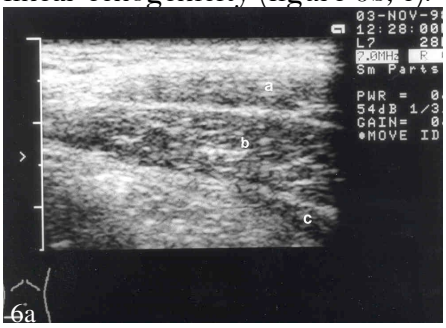

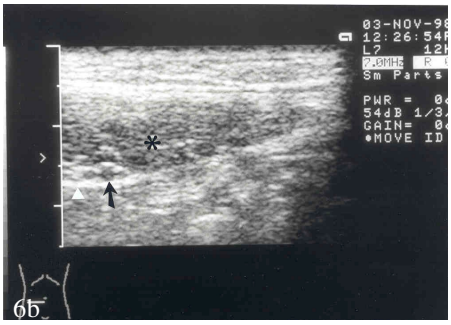

Figure 6
a-Ultrasound image of the anterolateral muscle groups of the abdominal wall at the level of the umbilicus; a= m.obliquus abdominis externus, b= m.obliquus abdominis internus, c= m.transversalis.
b-Medially obtained transverse image at the same level demonstrating the position of the inferior epigastric vessels (arrow) relative to the rectus muscle (asterisk); the peritoneal line is clearly seen (arrowhead).
c-Extended field-of-view ultrasound image demonstrating the entire anterior abdominal wall; a= m.obliquus abdominis externus, b= m.obliquus abdominis internus, c= m.transversalis, d= m. rectus abdominis.

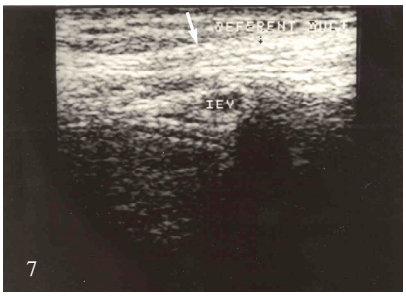

Figure 7
Ultrasound appearance of the deferent duct (arrow) and the inferior epigastric vessels (iev).

This line usually represents a combination of the peritoneum and the deep abdominal fascia. However, in patients with abundant extraperitoneal fat the peritoneum and deep fascia can be appreciated as two separate linear echodensities. Major advantage is the possibility to perform the examination in supine and upright position as well as at rest and during straining, the so-called dynamic scanning technique [**15**]. Comparison with the abdominal wall on the asymptomatic side may be necessary to help define the normal abdominal wall anatomy [**9**]. US is non-invasive and, like herniography, allows examination of the patient in a physiologic manner. Disadvantage is the high operator dependency of ultrasound, which can be partially caused by unfamiliarity with sonographic anatomy and partially by the great variation of ultrasound imaging quality with body habitus.

Evaluation of the inguinal region is best performed by oblique scanning between the easily identifiable bony landmarks of the anterior superior iliac spine and the pubic crest. The other anatomic structures for sonographic orientation are the lateral margin of the rectus abdominis muscle, iliac and femoral vessels and inferior epigastric artery and vein [**16**]. The femoral artery and vein can be identified just anterior to the iliopubic junction. The inferior epigastric vessels (figure 7) can be seen coursing upwards to the umbilicus (behind the rectus muscle) [**17,18**].

The superficial inguinal ring itself is not easily seen sonographically [**17,19**]. The region of the superficial inguinal ring can be identified easily on short axis real time views of the inguinal canal at a point just lateral to the pubic tubercle. At this point the posterior inguinal wall is concave anteriorly and the inguinal canal is ovoid in shape [**15**]. The deep inguinal ring lies anterior to the femoral vessels above the inguinal ligament, and can be identified at the point where the tubular structures of the spermatic cord can be seen to enter the inguinal canal (figure 7, 8a) [**17,20**]. Ultrasound allows differentiation between direct and indirect inguinal herniations by identifying the origin of the hernia (fig 8a), the typical course of an indirect inguinal hernia (figure 8b) or the position of the herniation relative to the inferior

epigastric vessels (figure 8c).

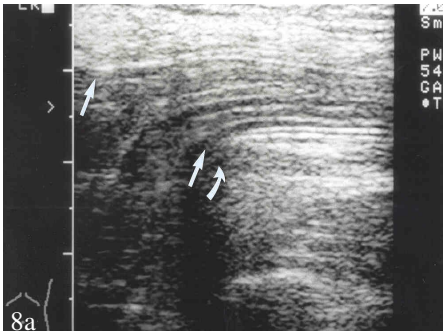

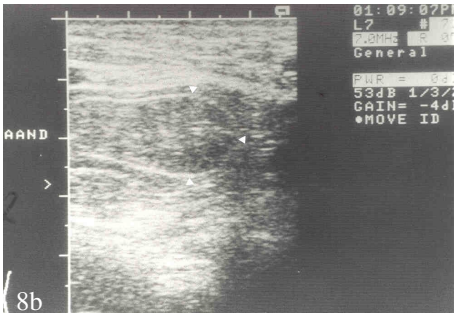

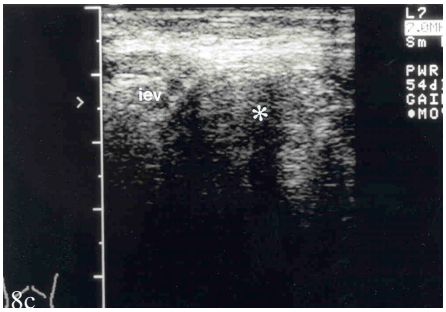

Figure 8
a-Ultrasound appearance of an indirect inguinal hernia demonstrating the location of the internal inguinal ring (between arrows) and the inferior epigastric vessels (curved arrow).
b-Indirect inguinal hernia coursing within the inguinal canal containing bowel (arrowheads) in another patient demonstrated ultrasonographically (image obtained during straining).
c-Transverse ultrasound image of a direct inguinal hernia (hypoechogenic, asterisk) clearly originating medially from the inferior epigastric vessels (image obtained during straining).

Although ultrasound is reported to be very useful in the evaluation of groin masses [**21**], little is known about the accuracy of ultrasound in diagnosing hernias. A recent report indicates that it may be sufficiently able to pick up hernias before they become symptomatic, thus suggesting a very high sensitivity, however specificity of ultrasound has not been discussed [**15**].

COMPUTED TOMOGRAPHY

CT of the inguinal region or pelvis is usually performed during breathhold, without straining. Reports dealing with CT (slice to slice) performed during Valsalva manoeuvre have been published, the use of helical CT has thusfar not been reported [**22,23**]. CT is capable in demonstrating the muscular, fascial and vascular structures [**9,24**]. Most adults have sufficient body fat to allow identification of the subcutaneous fat layer and individual muscles on CT (figure 9). In very thin or very muscular individuals, the three anterolateral muscles can appear as one single muscular mass [**25**]. In the normal CT anatomy the rectus abdominis muscle can be seen on both sides of

the umbilicus. The external oblique, internal oblique and transversus abdominis muscles are separated from the rectus muscles by the linea semilunaris. Asymmetry of the abdominal wall muscles is common **[26]**. The aponeuroses of the anterolateral muscles can be seen to unite at the lateral border of the rectus muscles. The anterior and posterior wall of the inguinal canal (the aponeurosis of the external oblique and the transversalis fascia respectively) can be identified, as well as the internal inguinal ring (figure 10) **[25]**.

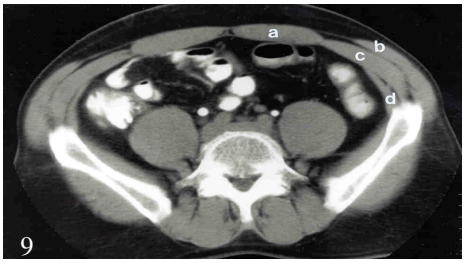

Figure 9
CT scan demonstrating normal anatomy of the muscles of the abdominal wall; a= m. rectus abdominis, b= m.obliquus abdominis externus, c= m.obliquus abdominis internus, d= m.transversalis.

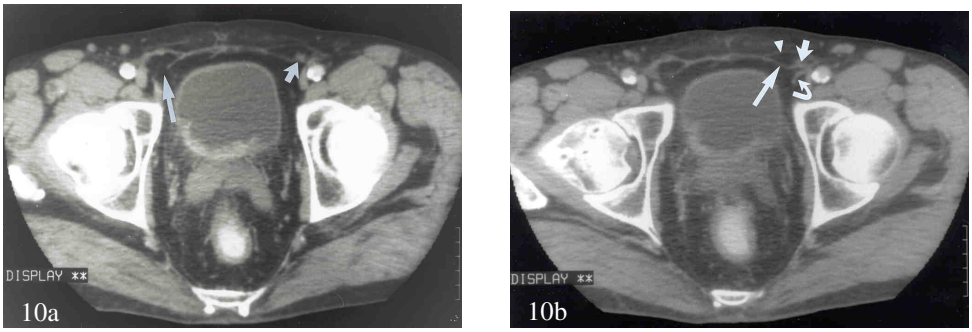

Figure 10
a-CT scan in a male patient clearly showing the location of the internal inguinal ring (annulus inguinalis internus) on the right side (large arrow); on the left side part of the deferent duct is seen within the inguinal canal (small arrow).
b-Slice obtained 5 mm lower demonstrating another part of the deferent duct (small arrow), as well as the epigastric vessels (curved arrow); at this level the anterior wall of the inguinal canal on the left side is formed by the aponeurosis of the external oblique (arrow-head), the posterior wall by the transversus aponeurosis and transversalis fascia (arrow).

The vas deferens and the pampiniform plexus can be seen, the latter even better after intravenous contrast agents (figure 11, 12) **[22]**.

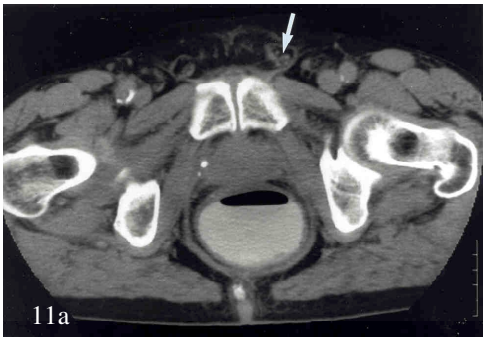

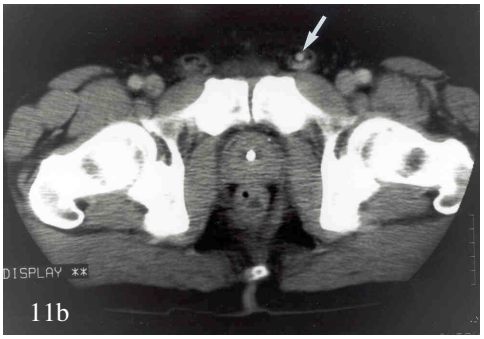

Figure 11
a-CT scan at the level of the distal part of the inguinal canal; the contents of the left inguinal canal (deferent duct and testicular/spermatic vessels) is clearly seen (arrow).
b-CT scan at the same level in another patient with a varicocele; after intravenous contrast administration the left testicular vein (arrow) enhances.

In females the round ligament can be seen coursing towards the labium (fig 13). The inferior epigastric vessels (forming the lateral umbilical folds) that play an important role in the differentiation of direct from indirect inguinal hernias can be easily identified, both on CT and MR [**24**].

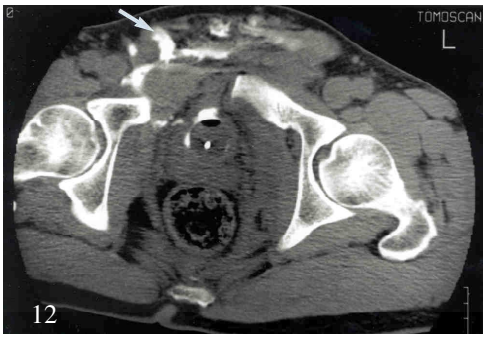

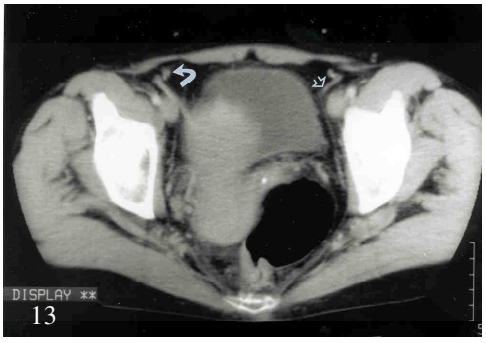

Figure 12
CT scan in a patient with bladder perforation, after administration of contrast through a urinary catheter; the extravasated contrast follows the course of the deferent duct and inguinal canal on the right (arrow).
Figure 13
CT scan in a female patient demonstrating the course of the round ligament on the left side (arrow) from the uterus towards the internal inguinal ring (curved arrow: right inferior epigastric vessels).

Direct inguinal hernial sacs are behind the spermatic cord and hence are unlikely to reach the scrotum, thus creating another way to differentiate direct from indirect inguinal hernias (figure 14,15) [**27**].
The median and medial umbilical folds (urachus and obliterated umbilical arteries respectively) are generally not identified on CT [**28**].

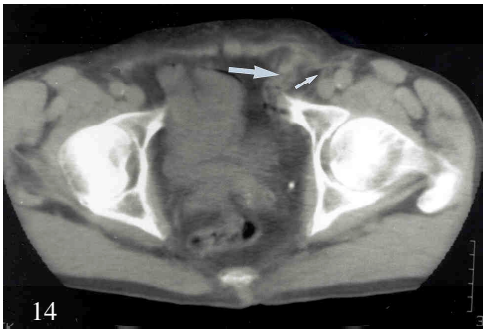

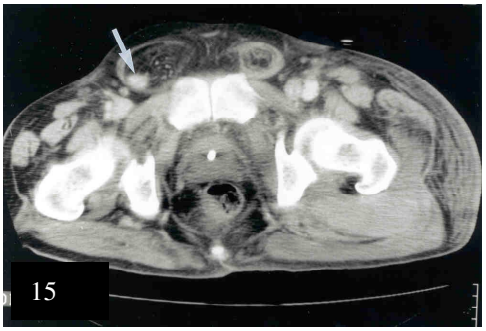

Figure 14
CT scan in a patient with a left sided direct inguinal hernia (arrow); the origin of the hernia medial to the inferior epigastric vessels (small arrow) is clearly seen.
Figure 15
CT scan in a patient with a bilateral indirect inguinal hernia, the course within the inguinal canal is clearly seen on the right side (arrow).

A sensitivity of 83% and specificity ranging from 67-83% in detecting hernias has been described [**22,23**].

MAGNETIC RESONANCE IMAGING

Major advantage of MRI is the possibility to obtain images in any plane, either by directly scanning in different planes or by making multiplanar reconstructions on a workstation (also possible with CT imaging). In addition MRI can be used to perform dynamic examinations during straining [**29**]. Like CT, MRI is able to depict the layers of the anterior abdominal wall (skin, superficial fascia, subcutaneous fat, anterolateral muscle and midline muscle groups, transversalis fascia, extraperitoneal fat, and peritoneum; figure 16, 17) [**30**].

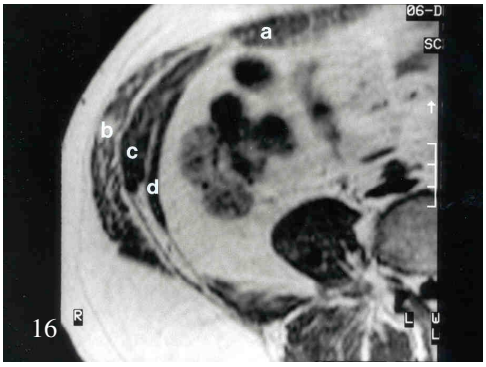

Figure 16
Transverse T-2 weighted MR image depicting the muscles of the anterior abdominal wall; a= m. rectus abdominis, b= m.obliquus abdominis externus, c= m.obliquus abdominis internus, d= m.transversalis (R=right, L=left).

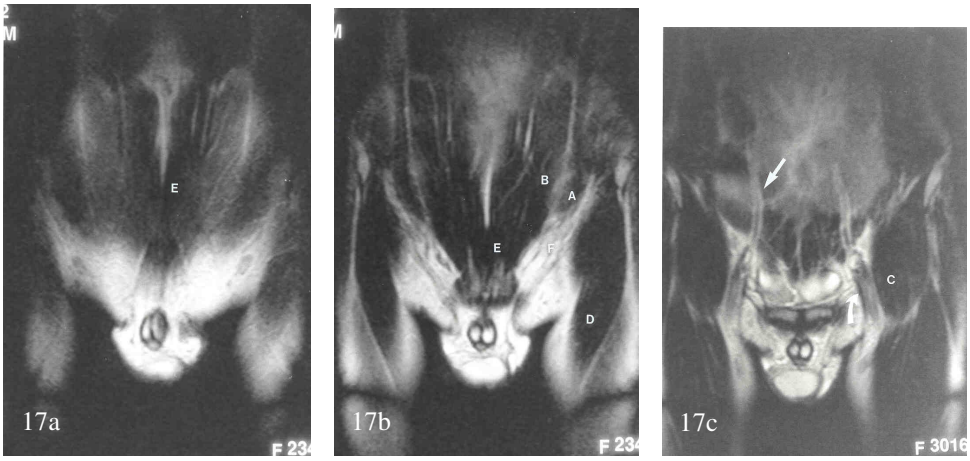

Figure 17
Three coronal T-1 weighted MR images (A to C= anterior to posterior) showing the course of the inferior epigastric vessels on the right side (small arrow), femoral vessels on the left side (curved arrow) and major muscle groups; A= m. obliquus abdominis externus, B= m. obliquus abdominis internus, C= m. iliopsoas, D= m. sartorius, E= m. rectus abdominis, F= inguinal canal.

The median and medial umbilical folds can not be identified with MRI [**29**]. The contents of the inguinal canal and the inguinal ligament can be demonstrated clearly using MRI, as well as the course of the inferior epigastric vessels that are of importance in the differentiation of direct from indirect inguinal hernias (figure 18, 19, 20).

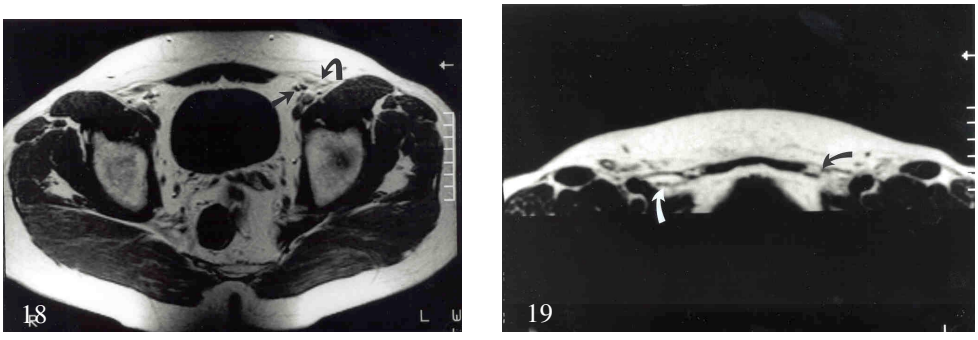

Figure 18
Transverse T-2 weighted MR image in a male patient at the same level as figure 10A, demonstrating the epigastric vessels (arrow) and lateral part of the left inguinal canal (curved arrow); R=right, L=left.
Figure 19
Transverse T-2 weighted MR image in a female patient at the level of the inferior epigastric vessels on the right side (curved white arrow) and the left inguinal canal (curved black arrow); note the relative paucity of structures as compared to figure 18.

Furthermore MRI is able to depict inguinal hernias [**24**], and to differentiate the several types of hernias (figure 21, 22, 23, 24). Sensitivity and specificity of MRI in the diagnosis of groin hernias is not known. A preliminary report indicates that MRI is a promising imaging modality for the diagnosis of

groin hernia, with 84.6% of hernias being diagnosed correctly prospectively on coronal scans of both groins [**29**].

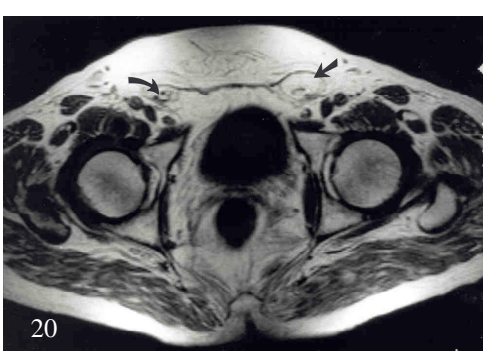

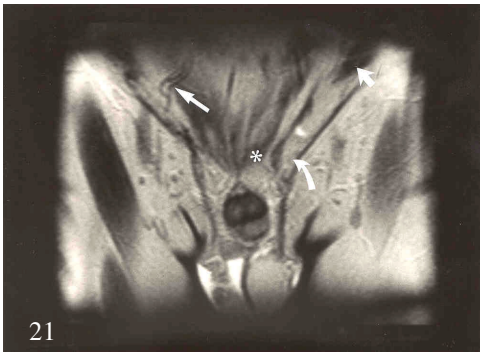

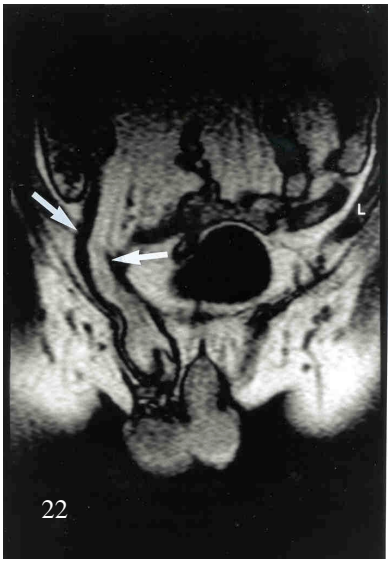

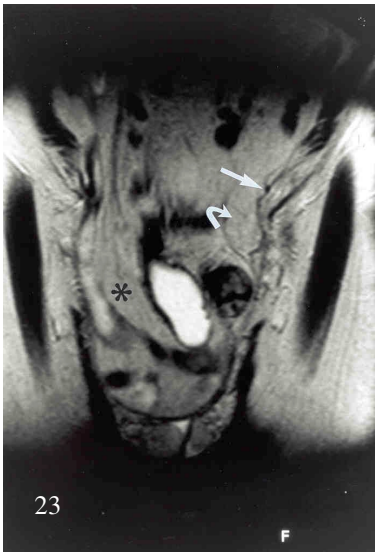

Figure 20
Transverse T-2 weighted depicting abnormal fatty content in the left inguinal canal (straight arrow); on the right side the spermatic cord structures (curved arrow) is seen.
Figure 21
Coronal T-1 weighted MR image clearly demonstrating the course of the inguinal canal by the presence of a left sided indirect inguinal hernia (curved arrow); furthermore the rectus muscles (asterisk), inferior epigastric vessels (straight arrow) and external oblique muscle (small arrow) is seen.
Figure 22
Coronal MR image (Turbo Field Echo; TE=8 ms, TR=16 ms) obtained during straining showing the internal inguinal ring as outlined by a large right-sided indirect inguinal hernia (arrows); L=left.
Figure 23
Coronal T-2 weighted image demonstrating a large scrotal hernia on the right side containing bowel, mesentery and fat (asterisk); left sided direct inguinal hernia is also present (curved arrow), originating medially from the inferior epigastric vessels (straight arrow).

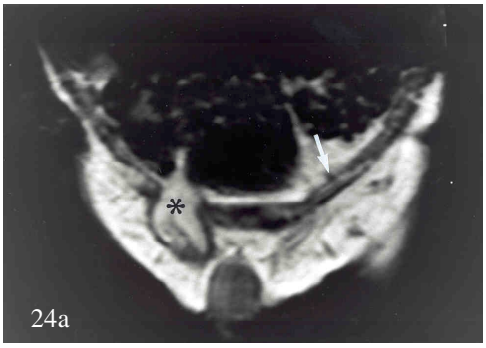

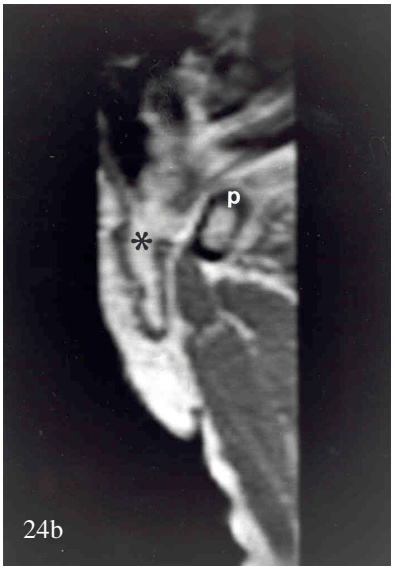

Figure 24
Coronal (A) and curved oblique sagittal reconstruction (B) of a T-1 weighted volume MR scan in a patient with a right-sided direct inguinal hernia (asterisk); p= pubic bone; the inferior epigastric vessels on the left can be seen on the coronal image (arrow).

CONCLUSION

In the radiological diagnosis of inguinal disease exact knowledge of the anatomy of the groin is of great importance. Diagnostic imaging now plays a minor role in the primary diagnosis of most inguinal hernias, but herniography, ultrasound and to a lesser extent CT are useful in doubtful cases. The information that is needed by the surgeon can be obtained using state-of-the-art imaging techniques, such as CT, ultrasound and MRI, and a thorough knowledge of anatomy in these imaging modalities.

REFERENCES

1. Gardner DJ, Gray DJ, O'Rahilly R (1975) Abdominal walls. In: Gardner, Gray and O'Rahilly. Human Anatomy. 3rd ed. W.B. Saunders Company, Philadelphia, pp 351-362.
2. Ponka JL (1980) Anatomy. In: Ponka JL. Hernias of the abdominal wall. W.B. Saunders, Philadelphia, pp18-39.
3. Condon RE (1994) The anatomy of the groin: the basis for anatomical repair of groin hernias.In: Arregui ME, Nagan RF. Inguinal hernia: advances or controversies? Radcliff Medical Press, Oxford, New York, pp7-9.

4. Rosser J (1994) The anatomical basis for laparoscopic hernia repair revisited. Surgical Laparosopy & Endoscopy 4:36-44.
5. Gray H (1977) The surgical anatomy of hernia. In: Pick TP, Howden R eds. Anatomy, descriptive and surgical. Bounty Books, New York, pp 1041-1062.
6. Nyhus LM (1993) Individualization of hernia repair: a new era. Surgery 114: 1-2.
7. Ekberg O (1981) Inguinal herniography in adults:technique, normal anatomy and diagnostic criteria for hernias. Radiology 138:31-36.
8. van den Berg JC, Strijk SP (1992) Groin hernia: Role of herniography. Radiology 184: 191-194.
9. Harrison LA, Keesling CA, Martin NL, Lee KR, Wetzel LH (1995) Abdominal wall hernias: Review of herniography and correlation with cross-sectional imaging. Radiographics 15:315-332.
10. Jones RL, Wingate JP (1998) Herniography in the investigation of groin pain in adults. Clin Radiol 53:805-808.
11. Hamlin JA, Kahn AM (1998) Herniography: a review of 333 herniograms. Am Surg 64:965-969.
12. MacArthur DC, Grieve DC, Thompson AM, Greig JD, Nixon SJ (1997) Herniography for groin pain of uncertain origin. Br J. Surg 84:684-685.
13. Makela JT, Kiviniemi H, Palm J, Myllyla V (1996) The value of herniography in the diagnosis of unexplained groin pain. Ann Chir Gynaecol 85:300-304.
14. Oh KS, Dorst JP, White JJ, Haller JA, et al (1973) Positive-contrast peritoneography and herniography.Radiology 108:647-654.
15. Orchard JW, Read JW, Neophyton J, Garlick D (1998) Groin pain associated with ultrasound finding of inguinal canal posterior wall deficiency in Australian Rules footballers. Br J Sports Med 32:134-139.
16. Furtschegger A, Sandbichler P, Judmaier W, Gstir H, Steiner E, Egender G (1995) Sonography in the postoperative evaluation of laparoscopic inguinal hernia repair. J Ultrasound Med 14: 679-684.
17. Engel JM, Deitch EE (1981) Sonography of the anterior abdominal wall. AJR 137:73-77.
18. Vincent LM (1992) Peritoneal cavity and abdominal wall. In: Mittelstaedt C. General ultrasound. Churchill Livingstone, New York, pp 639-651.
19. Nguyen KT, Sauerbrei EE, Lewandowski BJ, Nolan RL. The abdominal wall. In: Rumack CM, Wilson SR, Charboneau JW (1991) Diagnostic ultrasound. Mosby Year Book, St. Louis, pp 353-363.

20. Chou TY, Chu CC, Diau GY, Wu CJ, Gueng MK (1996) Inguinal hernia in children: US versus exploratory surgery and intraoperative contralateral laparoscopy. Radiology 201:385-388.
21. Arregui ME (1994) The value of ultrasound in the diagnosis of hernias. In: Arregui ME, Nagan RF.Inguinal hernia: advances or controversies? Radcliff Medical Press Oxford, New York, pp 73-79.
22. Hahn-Pedersen J, Lund L, Hansen Højhus J, Bojsen-Møller F (1994) Evaluation of direct and indirect inguinal hernia by computed tomography. British Journal Surgery 81: 569-572.
23. Højer AM, Rygaard H, Jess P (1997) CT in the diagnosis of abdominal wall hernias: a preliminary study. Eur Radiol 7:1416-1418.
24. Wechsler RJ, Kurtz AB, Needleman L, et al (1989) Cross-sectional imaging of abdominal wall hernias.AJR 153:517-521.
25. Heiken JP (1989) Abdominal wall and peritoneal cavity. In: Lee JKT, Sagel SS, Stanley RJ. Computed body tomography, 2nd ed. Raven Press, New York, 661-666.
26. Marn CS (1994) Anterior abdominal wall. In: Gore, Levine and Laufer. Textbook of gastrointestinal radiology, 1st ed. Saunders, Philadelphia, pp 2401-2410.
27. Zarvan NP, Lee FT, Yandow DR, Unger JS (1995) Abdominal hernias: CT findings. AJR 164:1391-1395.
28. Khati NJ, Enquist EG, Javitt MC (1998) Imaging of the umbilicus and periumbilical region. Radiographics 18:413-431.
29. van den Berg JC, de Valois JC, Go PMNYH, Rosenbusch G (1997) Dynamic magnetic resonance imaging in the diagnosis of groin hernia.Investigative Radiology 32: 644-677.
30. Bennett HF, Balfe DM (1995) MR imaging of the peritoneum and abdominal wall. MRI Clin North Am 3:99-120.
31. Wind GG, Valentine RJ (1998) I vasi femorali. In Wind GG, Valentine RJ, Cassina I. Anatomia descrittiva e vie di accesso in chirurgia vascolare. GC Medical Books, Palermo, pp 335-372.

3

MASSES AND PAIN IN THE GROIN: A REVIEW OF IMAGING FINDINGS

ABSTRACT

The inguinofemoral region is a crossroads of numerous vascular, nervous and muscular structures. As even the most astute clinician can have difficulty in correctly diagnosing the cause of complaints or a mass in the groin and thigh region, radiological investigation is frequently warranted. For the radiologist involved, knowledge of the anatomy and specific pathology of the groin is essential. This paper deals with the imaging characteristics of the various diseases in the inguinofemoral triangle. Furthermore this article provides an overview of the role of the various imaging modalities in the evaluation of disease in the groin and upper thigh.

A sound working knowledge of groin anatomy and pathology is mandatory. The various imaging modalities used should be considered complementary.

Keywords

Hip, abnormalities
Hernia, inguinal
Abdomen, abnormalities
Neoplasms, diagnosis

INTRODUCTION

Pathology in the groin can be of very diverse etiology. In daily clinical practice the methods for diagnosing the presence or absence of disease in the inguinofemoral region are based upon a knowledge of anatomy combined with clinical acumen. The differential diagnosis will largely depend on the patient's clinical presentation. In patients presenting with a lump in the groin and signs of intestinal obstruction, the diagnosis of incarcerated inguinal hernia can be made straightforward, thus obviating the need for further diagnostic imaging. In patients with pain related to movement of the hip, diagnostic imaging is needed more frequently, in order to differentiate articular from periarticular disease. Furthermore groin complaints can be caused by various diseases having a similar clinical presentation, and clinical findings may be nonspecific in many cases, thus making differentiation of the pathology involved difficult or even impossible [1]. In those patients a careful history and a physical examination do not provide sufficient information for therapeutic decisions [2]. Except for the accuracy in the diagnosis of hernias (discussed below), the diagnostic accuracy of physical examination itself is not known, and thus the number of cases in which the clinician has to resort to diagnostic imaging is not known. In cases in which the exact nature of a palpable mass in the groin is sometimes difficult to establish, and clinical diagnosis is obscured by obesity, previous surgery, radiation or trauma, imaging modalities such as conventional radiography, ultrasound, CT and MRI play an important role in the assessment of the correct diagnosis [3]. In general the goals of imaging can be fourfold. First the lesion can be exactly localized. Second, evidence for underlying causative disease should be looked for (e.g. Crohn's disease (see below)). Third, differentiation of solid from fluid containing, cystic lesions can be made. Finally, in the case of a fluid containing lesion ultrasound or CT-guided aspiration can be performed, and percutaneous drainage can be offered [4]. The appearance of the various pathologic entities in the groin and upper thigh region on the various imaging modalities are discussed.

ANATOMY

The inguinofemoral region is bordered by the anterior superior iliac spine and pubic crest superiorly, and includes the upper thigh region as well as the caudad part of the anterior abdominal wall. The abdominal wall and the groin region are composed of several layers: skin, superficial fascia, subcutaneous fat, various muscle groups, extraperitoneal fat, and peritoneum. The muscles of the abdominal wall include the external and internal oblique, transversus abdominis and rectus abdominis. In the region of the groin the

fibres of the external oblique aponeurosis form a free border, known as Poupart's ligament. The inguinal canal begins at the internal inguinal ring (situated laterally in the transversalis fascia), at the level of the anterior superior iliac spine and extends medial and inferiorly to the pubic tubercle. The anterior wall of the canal is formed by the aponeurosis of the external oblique, its posterior wall by the transversalis fascia. In the medial aspect of the inguinal canal an aperture in the external oblique aponeurosis is recognized as the superficial, or external inguinal ring. Lying laterally under the inguinal ligament is the iliopsoas muscle (and its bursa). The medial extent of Poupart's ligament lies over the femoral vessels and the pectineus muscle. The greater saphenous vein passes through the fascia lata to empty into the femoral vein. The inferior epigastric vessels originate from the external iliac vein and artery coursing upwards to a position dorsally of the musculus rectus abdominis. Lymphatics from the lower extremity, the perineum, the external genitalia, the anus and the abdomen below the level of the umbilicus drain into the inguinal lymphnodes [**5,6**]. The anatomy of the inguinofemoral region is represented in figure 1a, and figures 1b-1e demonstrate the imaging characteristics of these structures.

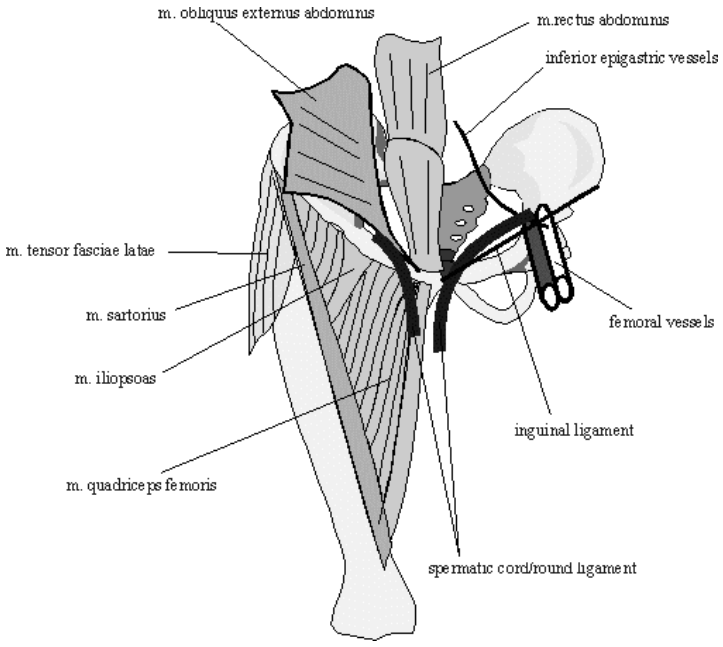

Figure 1a
Drawing of the major anatomical landmarks in the inguinofemoral region.

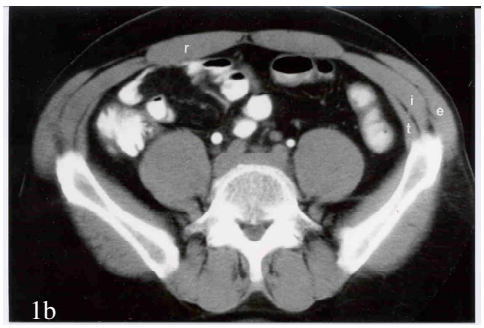

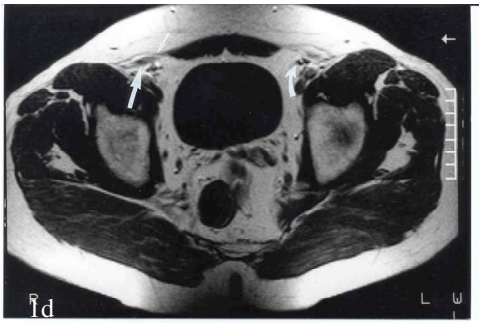

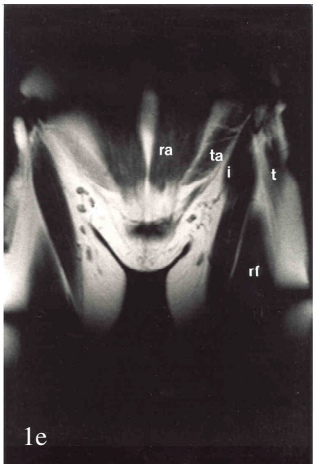

Figure 1b
CT at the level of the anterior superior iliac spine, demonstrating the abdominal wall muscles: m. rectus abdominis (r); m. obliquus internus abdominis (i); m. obliquus externus abdominis (e); m. transversus abdominis (t).
Figure 1c
CT in another patient at a level just cranial from the symphysis, showing the m. rectus abdominis (r), as well as the transversalis fascia (arrow) and deferent duct (small arrow).
Figure 1d
Transverse T1-weighted MRI demonstrating the passage of the deferent duct (arrow) through the inguinal canal (bounded anterior by the external oblique aponeurosis (small arrow)); the epigastric vessels are shown (curved arrow).
Figure 1e
Coronal T1-weighted MRI of the pelvis in a female patient demonstrating the m. iliopsoas (i), m. tensor fasciae latae (t), m. rectus femoris (rf), m. transversus abdominis (ta), m. rectus abdominis (ra) and inguinal ligament (arrow).

PATHOLOGY

Pathology of the groin is very diverse. The various disease entities that can be discerned are now discussed.

HERNIAS

Hernias may cause diagnostic problems, particularly in obese patients, patients with scars, or those in whom a herniated sac protrudes between muscle layers [7]. Arregui has pointed out that 70% of non-obstructed femoral hernias are misdiagnosed by referring non-surgical medical

practitioners. Even when symptoms are severe enough to warrant surgical intervention, 20-25% of femoral hernias are not diagnosed preoperatively by surgical staff [**3**]. Clinical diagnosis of inguinal hernias has a higher accuracy of 97% [**3,8**].

Figure 2
Indirect inguinal hernia containing large bowel (sigmoid and part of descending colon) as depicted on barium enema.

Although hernias may be demonstrated indirectly on intravenous urography and barium enema, by depicting their contents (bladder, ureter, large or small bowel; figure 2), diagnosis is done preferably by means of ultrasound, CT, MRI or herniography [**7,9,10,11,12,13,14**]. Although herniography is minimally invasive, and lacks the visualization of adjacent soft tissue structures, it is easy to perform and is a sensitive imaging modality. Other diagnostic imaging modalities are indicated in patients with a negative herniography [**2,7,9,11,15,16,17,18**]. Crucial in the differentiation of the various types of herniations in the inguinofemoral region is identification of several anatomical landmarks. Medial (direct) and lateral (indirect) inguinal hernias are separated from each other by the inferior epigastric vessels, which can be readily identified on herniography, ultrasound, CT and MR. A *lateral inguinal hernia* typically follows the course of the inguinal canal (figure 3,4,5), whereas a *medial inguinal hernia* protrudes at a right angle to the inguinal channel (figure 6).

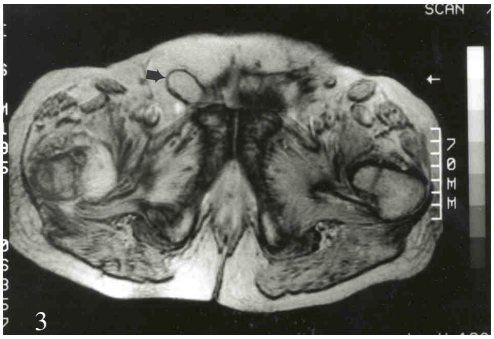

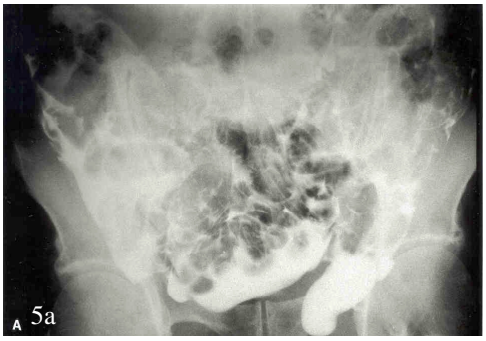

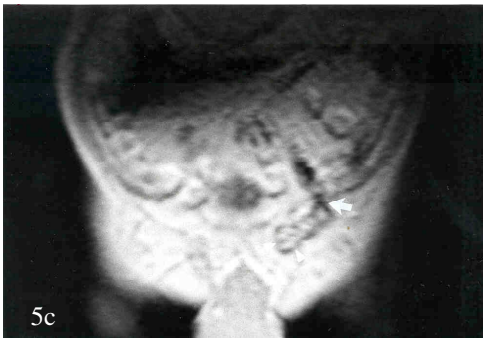

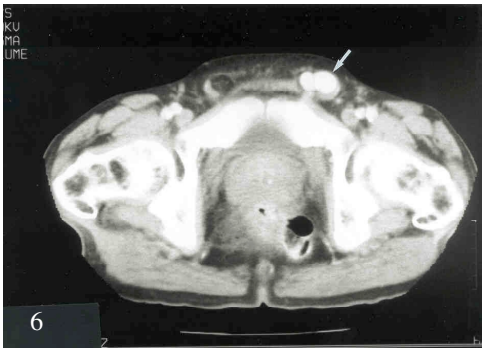

Figure 3
Transverse T2-weighted MR image showing an indirect inguinal hernia containing fat; clear delineation of the hypointense hernial sac (arrow).
Figure 4
CT appearance of indirect inguinal hernia containing ovarian cyst (arrowheads)(courtesy J.P.M. van Heesewijk, MD, Nieuwegein, The Netherlands).
Figure 5
Indirect inguinal hernia as shown on herniography (a) and MRI (b); poor delineation on MRI of the hernial sac (arrowheads) on T1-weighted volume can as compared with figure 2. On a dynamic MR study (c; performed during straining) better delineation of the hernial orifice (arrow) as well as the hernia sac itself (arrowheads).
Figure 6
Appearance of direct inguinal hernia on CT containing contrast opacified small bowel (arrow), typically originating medially from the epigastric vessels (courtesy R. van den Berg, MD, Leiden, The Netherlands).

A *femoral hernia* protrudes medially, is located in the femoral canal, medial to the femoral vein, and is usually pear-shaped. An *obturator hernia* passes through the canal between the superior ramus of the pubic bone and the

obturator membrane and emerges under the cover of the pectineal muscle. A *patent vaginal process* finally is considered a potential pathway for herniation of peritoneal contents, thus being a precursor of an indirect inguinal hernia. It typically has a very slender neck, sometimes with a ballooning bird-beaked end (figure 7).

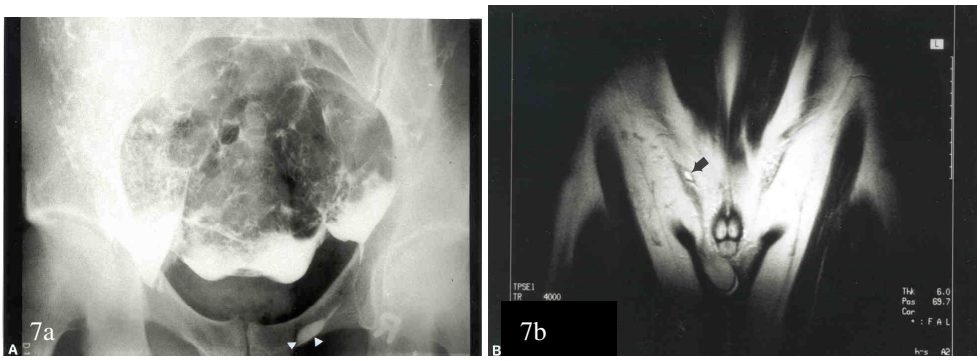

Figure 7
Herniography (PA view) revealing a patent vaginal process (a) with typical ballooning end (arrowheads). Herniographically proven patent vaginal process in another patient, delineated on T2-weighted MR image as a hyperintense lesion (b; arrow).

The appearance of any hernia on various imaging modalities is uniform. The peritoneal lining and hernial contents is depicted indirectly on herniography (figure 5a) and can be directly shown with ultrasound, CT and MRI (figure 5b). On ultrasound the defect in the (hyperechoic) fascia can be visualized, the peritoneum itself is hardly discernible as a hyperreflective line. The hernial contents can either be hyperechoic (omental or mesenterial fat) or of varying echogenicity with reverberations due to air in bowel loops, creating the so-called target lesions with strong reflective central echoes in the bowel lumen. With ultrasound, as well as with CT the hernial contents can be depicted clearly. The hernial sac, mostly a thin peritoneal layer, may be very hard to discern on ultrasound and CT studies, especially when it is not filled with bowel or other structures. Care should be taken to look for signs of strangulation, such as thickening of bowel loops, whirl-sign, U-shaped bowel loop, beak-sign, triangular loop, two adjacent collapsed loops, coexisting inflammatory changes and finally the presence of free air intraperitoneally, indicative of perforation [**19,20**].

NEOPLASMS

Primary soft tissue tumors find their origin in skin, subcutaneous fat, or muscular structures. In case of a *lipoma* a specific diagnosis can be made on ultrasound, CT or MR appearance (figure 8), however differentiation from liposarcoma can be very difficult or even impossible. In all other cases most neoplasms are relatively non-specific in appearance [**21**], and primary malignancies are relatively rare [**4**]. Extensive discussion of the differential

rs is beyond the scope of this paper.

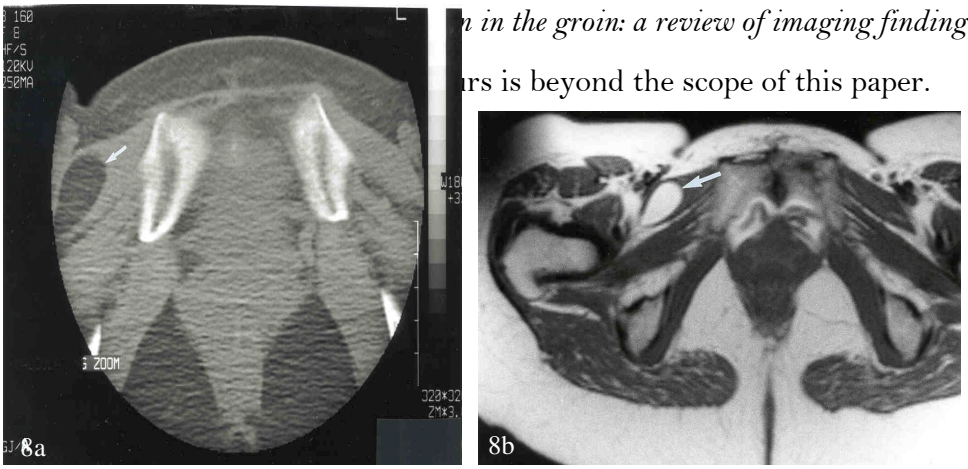

Figure 8
Intramuscular lipoma (arrows) in pectineus muscle as shown on CT (a; hypodense) and MRI (b; T1 and T2 characteristics of fat (only T1 presented)).

Secondary metastatic disease is more common and usually clinically evident. They may be overlooked, particularly in the obese patient. The changes of the lesion at US, CT or MR over time can be used as a marker of response to chemotherapy. The most frequent malignant nodules located in the subcutaneous tissues are due to *metastases* of malignant melanoma [**4,22**]. Subcutaneous nodules due to metastatic spread from lymphoma (figure 9), carcinoma of the lung, breast, ovary and colon are less frequent. Direct spread of intraabdominal malignancies is common. Furthermore muscles about the groin may be involved by metastatic deposits [***23***].

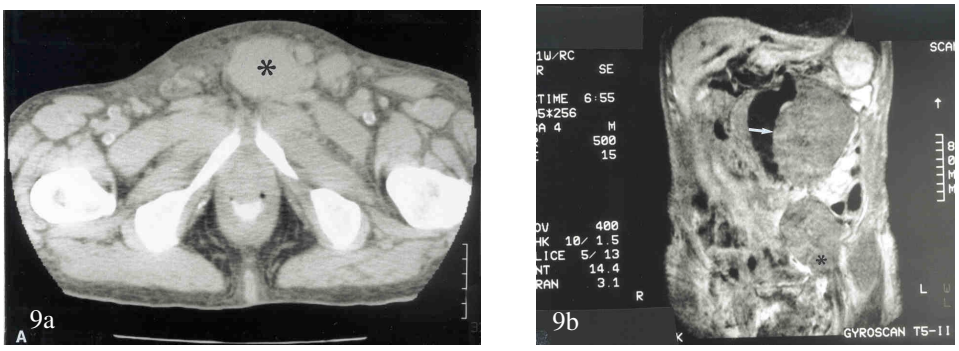

Figure 9
CT (a) and MRI (b) appearance of a mass due to non-Hodgkin lymphoma in the lower abdomen (arrow), with extension into the inguinal canal on the left side (asterisk).

Lymphnodes in the groin region are part of the superficial inguinal pathway and thus are the primary pathway for metastasis of tumors of the perineum (vulva, penis, lower vagina, lower rectum, anus), and lower extremity [**5,6**]. One must be aware that an enlarged lymphnode may be easily confused clinically with a femoral hernia [***5***]. Therefore additional imaging may be

necessary, either to categorize a palpable mass as lymphadenopathy, or it can be used to detect lymphadenopathy when there is no palpable mass [**22**]. The normal appearance of lymphnodes at ultrasonography consists of an oval shaped, hypoechoic peripheral zone and echogenic center. With extensive *lipomatosis* the node may become indistinguishable from the surrounding subcutaneous tissue [**22**]. *Confluent necrotizing lymphadenitis* is characterized ultrasonographically as multiple sonolucent circumscribed lesions with internal echoes [**8**]. Although benign nodes tend to be more oval, and malignant nodes to be round, nor size or any other criterion (such as the presence or absence of the fatty center) can differentiate sufficiently between reactive hyperplasia and metastatic spread of tumor into a lymphnode [**24**]. In fact malignant lymphnodes as small as 8mm, and benign nodes as large as 3 cm in long-axis diameter have been described [**25**]. Color Doppler imaging and Doppler spectral waveform analysis may be helpful in making this differentiation. Color Doppler sonography can show flow in all lymph nodes, regardless of whether they are affected by a benign or malignant process, and spectral waveform analysis allows distinction between lymphnodes affected by benign versus malignant processes. Lymphnodes involved with metastases show a high resistive index, a high pulsatility index and a low end diastolic velocity [**1,26**]. The appearance of lymphnodes at CT or MRI is mostly nonspecific (figure 10).

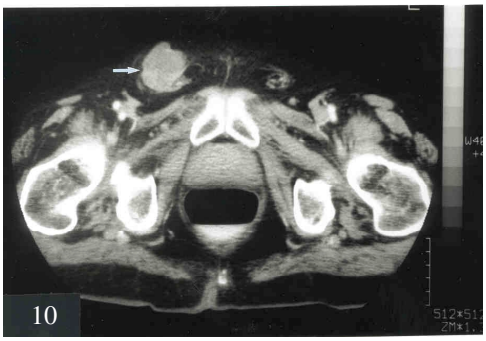

Figure 10
CT scan demonstrating metastatic deposit in inguinal lymphnode (arrow) in patient with adenocarcinoma of the lung.

Two common benign masses of the abdominal wall and the groin region are cysts and *desmoid tumors*. Desmoid tumors are low in signal intensity on both T1- and T2-weighted images [**4,23**]. The ultrasound appearance is usually anechoic or hypoechoic, typically with smooth and sharply defined margins [**27**].
Endometriosis in the superficial soft tissues is an uncommon occurrence. The sonographic appearance is variable. Primarily anechoic mixed with solid-type

echopatterns are found [**27**]. On MRI endometriomas commonly will demonstrate increased signal intensity on T1-weighted images due to the presence of blood [**23**].

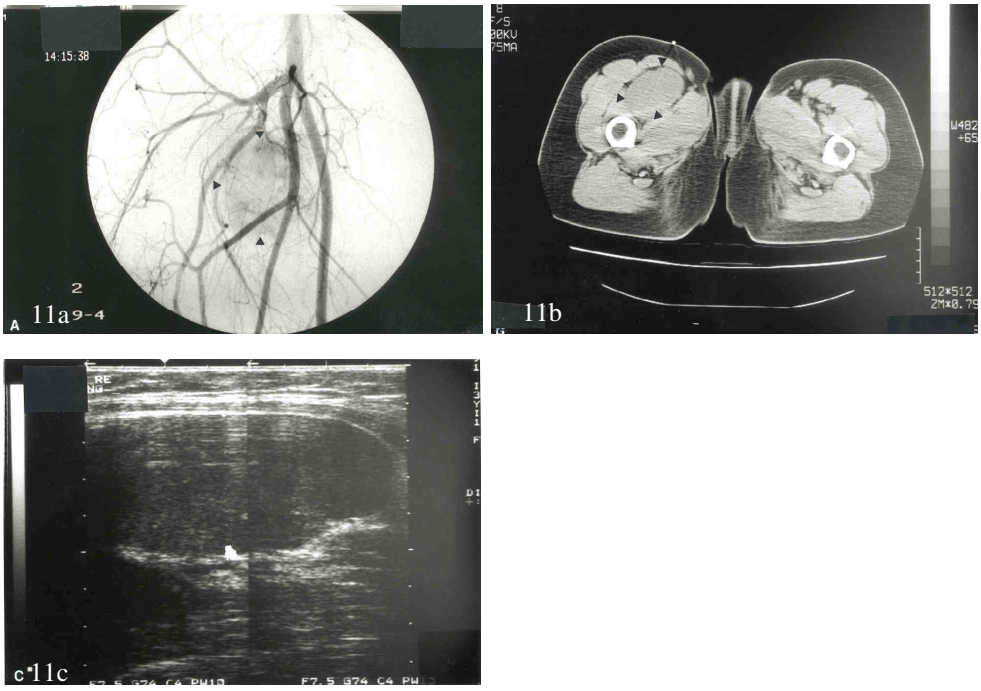

Figure 11
Angiographic (a) and CT features (b) of a neurofibroma in the upper thigh, showing a solid, homogeneous, uniformly enhancing mass (arrowheads). On ultrasound (c) no posterior acoustic enhancement is shown, a feature that, however can occur in these tumors, thus making differentiation from cystic masses difficult.

Tumors of the peripheral nervous system are relatively rare and form a heterogeneous group of tumors originating from neurectoderm tissue. Peripheral nerve tumors are mostly round, oval or fusiform. All benign and some malignant peripheral nerve tumors have well-defined margins. *Neurofibromas* present as well defined lesions with low-to-moderate signal intensity on T1-weighted images and high signal intensity on T2-weighted images, frequently showing a characteristic target appearance on T2-weighted images. *Schwannomas* (or neurinomas) originate from Schwann cells of peripheral nerves. They have a high water content, resulting in hyperintensity on T2-weighted images. Ultrasonographically as well as with MR imaging, a distinction between neurofibromas and Schwannomas cannot always be made reliably: both appear fusiform in shape and present sonographically as lesions with decreased echogenicity and increased through transmission (figure 11). The relation of the tumor to the peripheral nerve however may be of help in this regard. A neurofibroma is located

concentrically to the nerve, whereas a schwannoma is located eccentrically. Frequently peripheral nerve tumors are multifocal or appear like a string of beads. Neurofibrosarcomas can often not be differentiated from neurofibromas and schwannomas. However ill-defined margins and an inhomogeneous texture are features of malignancy [28,29].
Severe stinging, circumscribed pain occurring 1 to 2 months after surgical intervention (in the groin) is highly suspicious for a *posttraumatic neuroma.* Sonographically a neuroma presents as a hypoechoic mass, in most cases continuous with a (hyperechoic) nervous structure (figure 12). Differentiation between peripheral nerve (sheath) tumors and other soft tissue masses (e.g. small cysts or abscesses, reactive lymphadenopathy) may be very difficult on both ultrasound and MR imaging. Especially soft tissue or bone masses causing nerve entrapment and foreign bodies can mimic a peripheral nerve tumor clinically as well as radiologically [30,31,32,33,34].

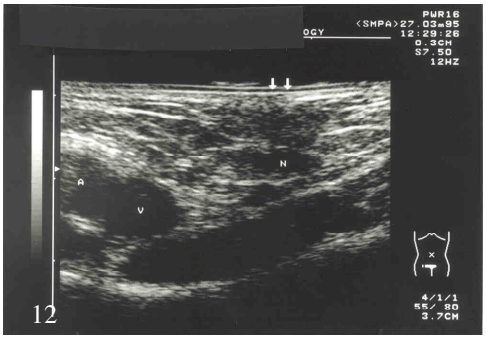

Figure 12
Transverse sonogram of a histologically proven posttraumatic neuroma (N): spindle-shaped, extremely tender hyporeflective structure in a patient after classic inguinal hernia repair (arrows indicate point of tenderness; A/V= common femoral artery and vein).

JOINT DISEASE

In the evaluation of joint disease the role of arthrography and CT (arthrography) is limited presently. Imaging modalities of choice are ultrasound and MR [21,35]. With MRI joint and synovial effusions can be seen best on T2-weighted images. The soft tissue lesions of (hypertrophied) synovium have intermediate signal on both T1- and T2-weighted images, and show marked enhancement after intravenous administration of Gadolineum [21].
The value of ultrasound in the evaluation of pain or swelling in the hip region lies in its ability to differentiate between intra-articular and periarticular pathology. It is extremely sensitive in the detection of joint effusion (amounts as small as 1 ml can be demonstrated), although the specific diagnosis of either a bacterial or viral arthritis or joint effusion on the

basis of synovitis cannot be made [36,37]. Furthermore the presence of loose bodies can be easily demonstrated (dynamic US; figure 13).

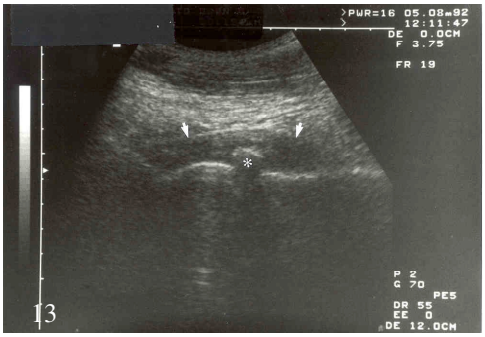

Figure 13
Longitudinal ultrasound of the right hip demonstrating intraarticular fluid (arrows) and loose body (asterisk); diagnosis: arthritis.

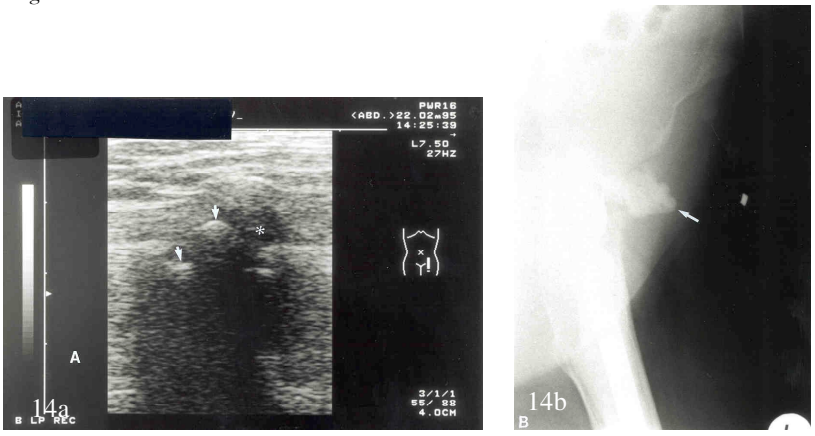

Figure 14
Ultrasound of the left hip (after total hip replacement) showing an irregularly outlined, hyperreflective structure (arrows), with an overlying small, sonolucent bursa (asterisk; a), and plain radiograph of the same patient (b), demonstrating cement (arrow) ventrally from the hip joint: a bursa has formed at an unusual place, where frictional forces occur.

Bursae are present in places where frictional forces occur. This is illustrated in figure 14. More commonly however, bursae are located about the joints (e.g. iliopsoas bursa). The iliopsoas bursa is located in front of the capsule of the hip joint, beneath the iliopsoas muscle, just posterolateral to the common femoral artery (figure 15,16). An enlarged iliopsoas bursa presents ultrasonographically as a cyst like mass. The trochanteric bursa is the most common site of frictional bursitis of the hip (figure 17).

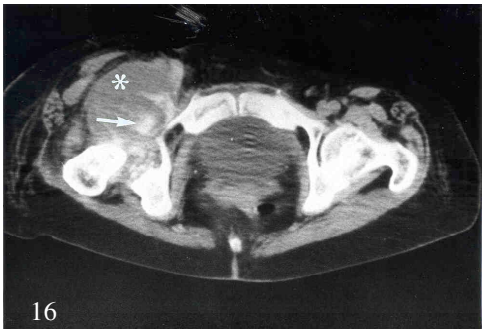

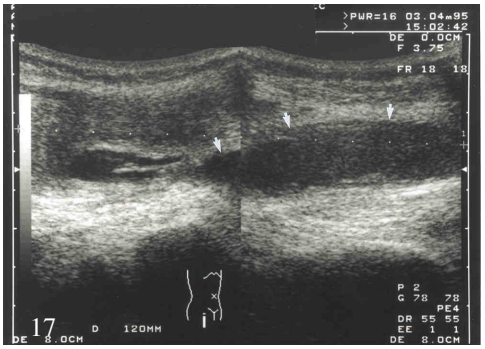

Figure 15
CT appearance of iliopsoas bursitis in an osteoarthritic hip, showing a mass with fluid density (HU 17; arrow) in the typical location posterolateral to the common femoral artery.
Figure 16
Unenhanced CT scan of bleeding (hyperdense; arrow) in an enlarged iliopsoas bursa of the right hip (asterisk)(courtesy G.J. Jager, MD, Nijmegen, The Netherlands).
Figure 17
Longitudinal ultrasound of the right hip showing a fluid collection (arrows) lying dorsolaterally from the greater trochanter, painful at palpation. No hydrops of the hip joint could be demonstrated. Findings consistent with trochanteric bursitis.

In *acute traumatic bursitis*, the fluid is usually anechoic and is markedly hypoechoic compared with normal bursal fluid. Walls of the bursa are thin, which can be an important factor in differentiating this condition from chronic bursitis. In *chronic bursitis* often debris as well as calcifications can be found in the bursal fluid, leading to increased echogenicity of the bursal fluid. With the advent of non-invasive imaging techniques the role of contrast bursography seems to be limited to selected cases of the snapping hip syndrome [**38**], although ultrasound seems to be valuable in these cases as well [**39,40**]. In these patients subsequent therapeutic injections may be performed.

VASCULAR ABNORMALITIES

False aneurysm is a wellknown but uncommon (incidence of 0.1%) complication of femoral artery catheterization [**22**]. Due to an increasing number of vascular interventional procedures, and the increasing use of anticoagulant therapy the occurrence of false aneurysms will increase. A false

aneurysm is a pulsatile hematoma, secondary to bleeding in the soft tissue, with fibrous encapsulation, thrombus formation and a persistent communication between the artery and the extraarterial fluid space [**41**]. The vessel wall does not heal and the blood flows back and forth between the two spaces. The color and pulsed-wave Doppler criteria of a false aneurysm include swirling flow within a cystic cavity (to and fro sign, ying-yang), expansile pulsatility, anechoic mass and a visible tract (figure 18a and 18b).

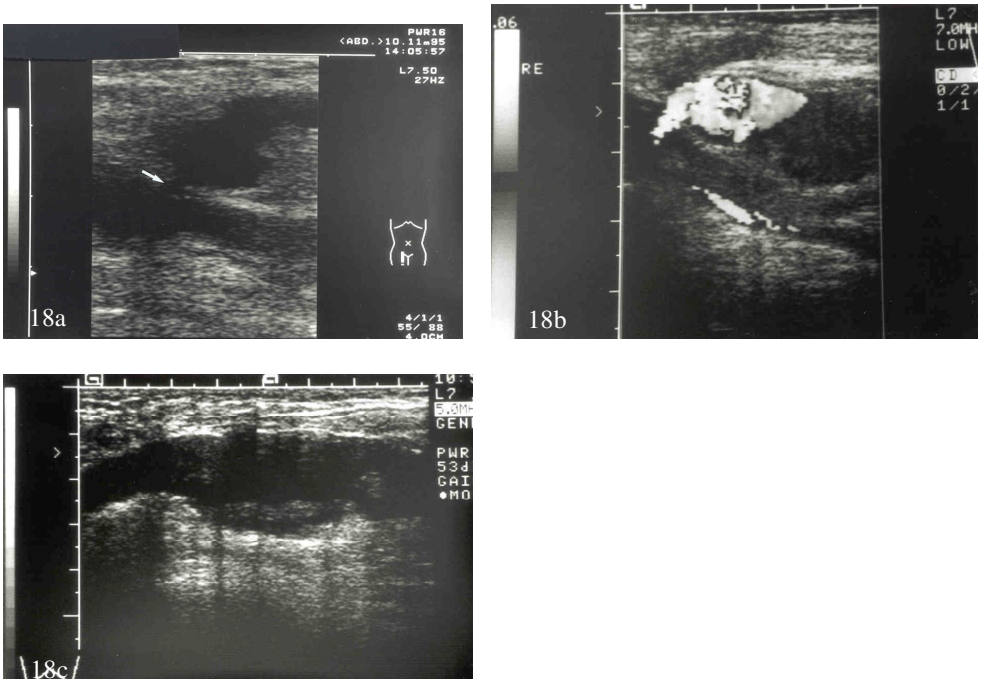

Figure 18
Ultrasound appearance of a false aneurysm of the common femoral artery (a), showing a visible, though slender tract (arrow; at color Doppler swirling flow could be demonstrated (b)), and a true aneurysm of the common femoral artery (c), with clear demonstration of the continuity of the vessel lumen with the aneurysm and mural thrombus.

The swirling flow should be differentiated from the "to and fro" pattern seen in fluid filled hernial sacs; the latter will pulsate with respect to the respiratory cycle, and lack coincidence of pulsations with the cardiac cycle [**42**]. Ultrasound offers the possibility of ultrasound-guided compression therapy. *True aneurysms* are usually the result of atherosclerosis, but may be caused by iatrogenic trauma. In the femoral vessels, they may present as a pulsatile groin mass, and thus may mimic a false aneurysm. Because there is a disruption in the laminar arterial flow within a true aneurysm, a swirling, turbulent blood flow pattern may be seen at color Doppler sonography. However, confusion can be avoided by recognizing that a true aneurysm is in continuity with the arterial lumen, rather than outside (figure 18c) [**41**].
AV-fistulae are rare and occur also mostly iatrogenically, when both the

femoral artery and vein are punctured simultaneously. At the site of the fistula arterial blood preferentially shunts into the vein. The shunting results in decreased blood flow in the artery distal to the fistula, and increased pulsatile blood flow in the vein proximal to the fistula [41].
A varix of the great saphenous vein can be visualized ultrasonographically as an oval, anechoic mass in the groin continuous with the femoral vein (figure 19) [43]. A varicosity in this area may be confused clinically with a femoral hernia [5].

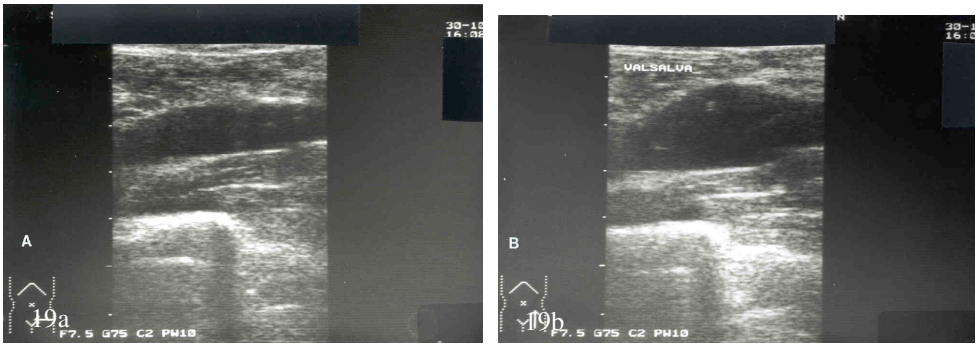

Figure 19
Sonographic visualization of a saphenous varix, depicted at rest (a) and during straining (b).

High resolution ultrasound is ideal in imaging subcutaneous arterial bypass grafts, such as the axillofemoral graft, whereas CT is better in depicting deeper lying grafts (e.g. obturator bypass, figure 20) [4].

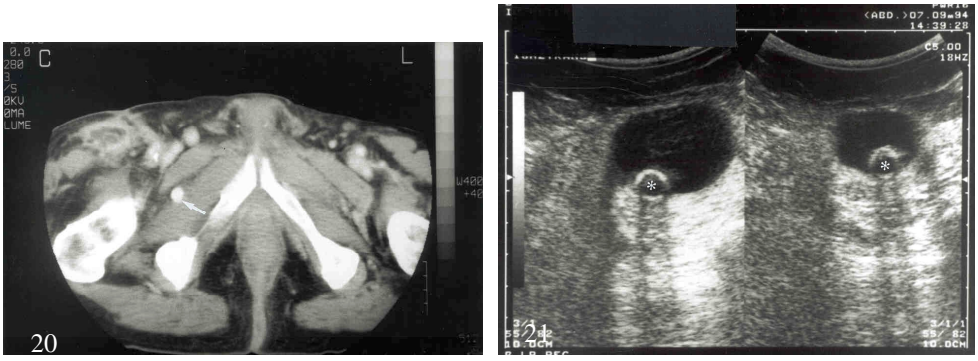

Figure 20
Obturator bypass as depicted by CT in a patient with infected aortic bifurcation prosthesis (note abscess, with irregular enhancing margin, in the right femoral region). The graft (arrow) follows the course of part of the obturator canal in this section lying between the pectineus muscle and the obturator externus muscle.
Figure 21
Transverse sonogram of a sonolucent persistent perigraft fluid collection in a patient after femoropoliteal bypass graft (asterisk); at Doppler examination no flow could be demonstrated; diagnosis: seroma.

Postoperatively small transient perigraft fluid collections can be visualized at

the level of the surgical tunnels, which disappear as the graft is incorporated into the subcutaneous tissues. Persistent perigraft fluid collections, or other localized fluid collections are abnormal, and are usually seromas or abscesses (figure 21).

MISCELLANEOUS

Fluid collections are usually seromas, liquifying hematomas, or abscesses related to previous surgery or trauma. Sterile fluid collections are usually anechoic. When complicated by hemorrhage or infection, they appear more complex, not echo-free, with septations and/or layering low-level echoes representing blood or debris. Although irregular margins of a fluid collection might suggest infection, absence of all these findings does not permit unequivocal differentiation between hematomas, wound seromas or infected fluid collections.

Figure 22
Large hematoma (arrowheads) in the obturator region, as depicted on CT, displaying mixed density, origin of bleeding remained unknown, spontaneous regression.

Hematomas in the acute phase present as fluid collections on ultrasound while they become lesions of mixed echogenicity in the subacute and chronic phase. The CT appearance of a hematoma is that of an abnormal mass, often elliptical or spindle-shaped, enlarging, obliterating, or displacing normal structures (figure 22).

An acute hematoma displays a density equal to or greater than the density of muscle because of the high protein content of hemoglobin. Most of the hematomas imaged within the first two weeks after initial hemorrhage are hyperdense and often inhomogeneous. On occasion, a fluid-fluid level can be seen on CT, MRI, and ultrasound (figure 23) (the so-called hematocrit effect). By 2-4 weeks density falls to values of 20-30 Hounsfield Units (i.e., that of serum).

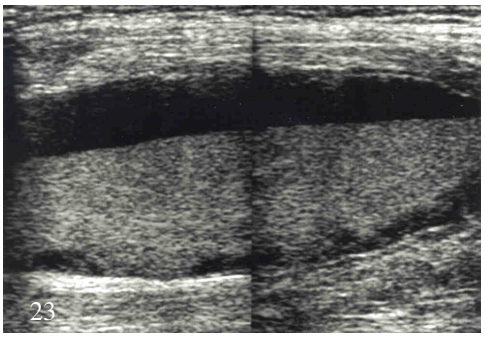

Figure 23
Ultrasound examination of a patient with a large hematoma lateral of the common femoral artery (after cardiac catheterization), displaying hematocrit effect (fluid-fluid layer).

Hematomas follow a characteristic evolution when examined with MRI and show typical time dependent changes. In the acute phase (< 1 week) hematomas have a signal intensity less than or equal to muscle on T1-weighted images and hypointense on T2-weighted sequences. In large acute hematomas fluid-fluid levels may be demonstrated. Due to the formation of methemoglobin and finally hemosiderin in subacute and chronic hematomas signal intensities will change. In the subacute phase (1-4 weeks) hematomas are very hyperintense in both T1- and T2-weighted images. Chronic hematomas (>4 weeks) are characterized by a hypointense rim (in T1 and T2) due to iron deposition, surrounding a isointense (T1) or hyperintense (T2) core [44].
Abscesses are most predominantly hypoechoic, some primarily solid on ultrasound examination. Gas bubbles producing strong echoes and acoustic shadowing are highly suggestive of an abscess, but, when present, the abnormality must be distinguished from a hernia on the basis of the presence or absence of peristalsis, abdominal wall defect, or accompanying swelling and/or pus. However, gas in an open wound or gas in a fistula connecting bowel to skin surface may have a similar appearance. An abscess is usually more well defined when compared with the more diffuse, ill-defined lateral margins of cellulitis or a phlegmon (figure 24). On CT typical contrast enhancement can be seen. The CT findings of inflammation are nonspecific and include streaky soft-tissue densities, loss of normal intermuscular fat planes, enlargement of abdominal wall muscles, localized masses of varying densities and masses that dissect along fascial planes [44].

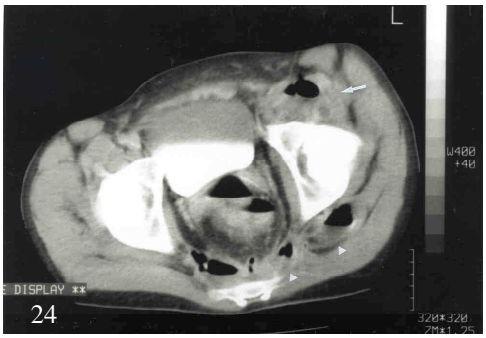

Figure 24
Left-sided psoas abscess (arrow) in a patient with Crohn's disease as demonstrated on contrast enhanced CT. Note the presacral and gluteal extension (arrowheads).

Differentiation between neoplasm, abscess or hematoma may not be possible on diagnostic imaging criteria alone, and clinical correlation is usually necessary. Ultrasound is the imaging modality of first choice for guided percutaneous diagnostic and therapeutic aspiration of fluid collections.
Undescended inguinal testis can be demonstrated ultrasonographically as ovoid hypoechoic masses in the course of the inguinal canal. It often appears smaller than the normal testis. Visualization of the echogenic hilus of a lymphnode should distinguish the structure from a testicle [**15**]. On MRI cryptorchidism can be demonstrated best on T1- and T2-weighted images. Testicular signal is as in normally located testes: intermediate on T1-sequences and bright on T2-weighted images [**45**]. The discussion of testicular pathology is beyond the scope of this paper.
In the past injection therapy with a sclerosing agent has been employed in the treatment of inguinal hernia. This may lead to a dense fibrous reaction in the groin with a CT appearance mimicking a group of enlarged lymphnodes, indistinguishable from malignancy [**46**].
Recently CT findings of medial transfer of the sartorius muscle in patients after lymphadenectomy has been described [**47**]. In such cases differentiation from recurrent lymphadenopathy and from postoperative phlegmon or hematoma may be difficult.

REFERRED PAIN

Patients with pain in the groin, without a palpable mass may suffer from disease located elsewhere. Most frequently encountered are patients with *nephrolithiasis/ureterolithiasis*, or *diverticulitis* (figure 25). Certainly in cases in which no cause for the complaints in the groin is found locally, one should be aware of the possibility of referred pain from disease elsewhere.

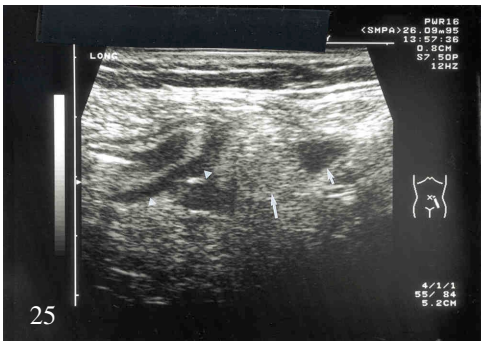

Figure 25
Patient with diverticulitis: ultrasound depicts thickening of the bowel wall (arrowheads), infiltration of adjacent fat (large arrow) and a localized fluid collection (small arrow).

CONCLUSION

Pathology in the groin can be of very diverse etiology, and can thus be puzzling to the clinician. In clinically difficult or doubtful cases a sound working knowledge of groin pathology is mandatory for the radiologist involved, in order to be able to resolve the clinical problems. The role of conventional radiographs, and arthrography seems to be limited presently. Imaging modality of first choice is ultrasound, as it is inexpensive, readily available, and requires only a short examination time. Thus it can have an inventorying and directive function: e.g. differentiation between solid and cystic processes can be made. MRI or CT can be used in further evaluation, depending on findings at ultrasound. In cases of suspicion for an osteoid osteoma or an abscess CT is preferable; when (peri)articular disease is suspected MRI is indicated.

REFERENCES

1. Gitschlag KF, Sandler MA, Madrazo BL, Hricak H, Eyler WR (1982) Disease in the femoral triangle: sonographic appearance. AJR 139:515-519.
2. Deitch EA, Soncrant MC (1981) The value of ultrasound in the diagnosis of nonpalpable femoral hernias. Arch Surg 116:185-187.
3. Arregui ME (1994): The value of ultrasound in the diagnosis of hernias. In: Arregui ME, Nagan RF.Inguinal hernia: advances or controversies? Radcliff Medical Press, Oxford, New York, pp 73-79.
4. Marn CS (1994): Anterior abdominal wall. In: Gore RM, Levine MS and Laufer I. Textbook of gastrointestinal radiology, 1st edition. Saunders, Philadelphia, pp 2401-2410.
5. Ponka JL (1980): Anatomy. In: Ponka JL. Hernias of the abdominal wall. W.B. Saunders, Philadelphia, pp 18-39.

6. Park JM, Charnsangavej C, Yoshimitsu K, Herron DH, Robinson TJ, Wallace S (1994): Pathways of nodal metastasis from pelvic tumors: CT demonstration. Radiographics 14:1309-1321.
7. Wechsler RJ, Kurtz AB, Needleman L, Dick BW, Feld RI, Hilpert PL, Blum L (1989) Cross-sectional imaging of abdominal wall hernias. AJR 153:517-521.
8. Deitch EA, Soncrant MC (1981) Ultrasonic diagnosis of surgical disease in the inguino-femoral region. Surg Gyn Obst 152:319-322.
9. Ekberg O (1981) Inguinal herniography in adults: technique, normal anatomy and diagnostic criteria for hernias. Radiology 138:31-36.
10. Ekberg O, Nordblom I, Fork FTh, Gullmo A (1985) Herniography of femoral,obturator and perineal hernias. Fortschr Röntgenstr 143:193-199.
11. van den Berg JC, Strijk SP (1992) Groin hernia: role of herniography. Radiology 185:191-194.
12. Harrison LA, Keesling CA, Martin NL, Lee KR, Wetzel LH (1995) Abdominal wall hernias: Review of herniography and correlation with cross-sectional imaging. Radiographics 15:315-332.
13. Bijnens E, Broeckx J, Hoffbauer R, Borreman J Ph (1992) Sonographic diagnosis of an incarcerated inguinal hernia containing uterus and left adnex. J Ultrasound Med 11:249-250.
14. Gharemani GG (1994) Hernias. In: Gore RM, Levine MS and Laufer I. Textbook of gastrointestinal radiology, 1st edition. Saunders, Philadelphia, pp 2382-2399.
15. Engel JM, Deitch EE (1981) Sonography of the anterior abdominal wall. AJR 137:73-77.
16. Lee G-H M, Cohen AJ (1993) CT imaging of abdominal hernias. AJR 161:1209-1213.
17. Yeh HC, Lehr-Janus C, Cohen BA, Rabinowitz JG (1984) Ultrasonography and CT of abdominal and inguinal hernias. J Clin Ultrasound 12:479-486.
18. Stallard DJ, Tu RK, Gould MJ, Pozniak MA, Pettersen JC (1994) Minor vascular anatomy of the abdomen and pelvis: a CT atlas. Radiographics 14:493-513.
19. Siewert B, Raptopoulos V (1994) CT of the acute abdomen: findings and impact on diagnosis and treatment. AJR 163:1317-1324.
20. Zarvan NP, Lee FT, Yandow DR, Unger JS (1995) Abdominal hernias: CT findings. AJR 164:1391-1395.
21. Totty WG (1993) MR imaging of the hip. In: Weissman BN. RSNA categorical course in musculoskeletal radiology; Advanced imaging of joints: theory and practice. RSNA, Oakbrook(Ill), pp 127-140.

22. Nguyen KT, Sauerbrei EE, Lewandowski BJ, Nolan RL (1991) The abdominal wall. In: Rumack CM, Wilson SR, Charboneau JW. Diagnostic ultrasound. Mosby Year Book, St. Louis, pp 353-363.
23. Bennett HF, Balfe DM (1995) MR imaging of the peritoneum and abdominal wall. MRI Clinics of North America 3:99-120.
24. Vassallo P, Wernecke K, Roos N, Peters PP (1992) Differentiation of benign from malignant superficial lymphadenopathy: The role of high-resolution US. Radiology 183:215-220.
25. Sutton RS, Reading CC, Charboneau JW, James EM, Grant CS, Hay ID (1988): US-guided biopsy of neck masses in postoperative management of patients with thyroid cancer. Radiology 168: 769-772.
26. Choi MY, Lee JW, Jang KJ (1995) Distinction between benign and malignant causes of cervical, axillary, and inguinal lymphadenopathy: Value of Doppler spectral waveform analysis. AJR 165:981-984.
27. Vincent LM (1992) Peritoneal cavity and abdominal wall. In: Mittelstaedt C. General ultrasound. Churchill Livingstone, New York, pp 639-651.
28. Harms SE, Greenway G (1992) Soft tissue tumors. In: Stark DD, Bradley WG. Magnetic resonance imaging, 2nd edition. Mosby Year Book, St. Louis, pp 2179-2181.
29. van Holsbeeck M, Introcaso JH (1991) Sonography of the dermis, hypodermis, periosteum, and bone. In: van Holsbeeck M, Introcaso JH. Musculoskeletal ultrasound. Mosby Year Book, St. Louis, pp 223-225.
30. Hughes DG, Wilson DJ (1986) Ultrasound appearance of peripheral nerve tumours. Br J Radiology 59:1041-1043.
31. Schmitt von R, Wuttke V, Buchner U, Preger R (1990) Diagnostik posttraumatischer Neurome mittels Sonographie und CT. Fortschr Röntgenstr 152:180-184.
32. Kumar AL, Kuhajda FP, Martinez CR, Fishman EK, Jezic DV, Siegelman SS (1983) Computed tomography of extracranial nerve sheath tumors with pathologic correlation. J Comput Assist Tomogr 7:857-865.
33. Singson RD, Feldman F, Staron R, Fechter D, Gonzalez E, Stein J (1990) MRI of postamputation neuromas. Skeletal Radiol 19:259-262.
34. Suh J, Abenoza P, Galloway HR, Everson LI, Griffiths HJ (1992) Peripheral (extracranial) nerve tumors: correlation of MRI and histologic findings. Radiology 183:341-346.

35. Lund PJ, Nisbet JK, Valencia FG, Ruth JT (1996) Current sonographic applications in orthopedics. AJR 166:889-895.
36. Marchal GJ, van Holsbeeck MT, Raes M, Favril AA, Verbeken EE, Casteels Vandaele M, Baert AL, Lauweryns JM (1987). Transient synovitis of the hip in children: role of US. Radiology 162:825-828.
37. van Holsbeeck M, Introcaso JH (1991) Sonography of bursae. In: van Holsbeeck M, Introcaso JH. Musculoskeletal ultrasound. Mosby Year Book, St. Louis, pp 91-121.
38. Vaccaro JP, Sauser DD, Beals RK (1995) Iliopsoas bursa imaging: Efficacy in depicting abnormal iliopsoas tendon motion in patients with internal snapping hip syndrome. Radiology 197:853-856.
39. Cardinal É, Buckwalter KA, Capello WN, Duval N (1996) US of the snapping iliopsoas tendon. Radiology 198:521-522.
40. Wiese H, Niers BBAM, Huisman PM, Taconis WK (1990) An unusual swelling in the groin. Eur J Radiol 10:156-158.
41. Paulson EK, Kliewer MA, Hertzberg BS, O'Malley CM, Washington R, Carroll BA (1995) Color Doppler sonography of groin complications following femoral artery catheterization. AJR 165:439-444.
42. Middleton MA, Middleton WD (1993) Femoral hernia simulating a pseudoaneurysm on color Doppler sonography. AJR 160:1291-1292.
43. Wales LR, Azose AA (1985) Saphenous varix: ultrasonic diagnosis. J Ultrasound Med 4:143-145.
44. Heiken JP (1989) Abdominal wall and peritoneal cavity. In: Lee JKT, Sagel SS, Stanley RJ. Computed body tomography, 2nd edition. Raven Press, New York, pp 661-666.
45. Mattrey R, Trambert M (1990) Role of MRI in cryptorchidism. In: Edelman RR, Hesselink JR. Clinical magnetic resonance imaging. WB Saunders, Philadelphia, pp 974-977.
46. Widlus DM (1984) Inguinal hernia:CT appearance after injection therapy. Radiology 151:156.
47. Wong JJ, Daly B, Krebs TL, Elias EG, Jacobs SC (1995) Surgical transfer of the sartorius muscle to the groin after lymphadenectomy or debridement: CT findings. AJR 166:109-112.

4

GROIN HERNIA: ROLE OF HERNIOGRAPHY

ABSTRACT

To determine the value of herniography (also known as peritoneography) in the detection of groin hernias, herniographs obtained in 70 consecutive patients with clinically suspected hernias (but with a normal or inconclusive physical examination) were retrospectively evaluated. The radiologic features, complications, and final clinical outcome were reviewed. A total of 30 hernias were found. Sixteen patients underwent surgery; there were no false-positive herniographic diagnoses. No procedure-related complications occurred. These results indicate that herniography is a simple and valuable diagnostic tool in patients with unexplained groin pain or pain in the anterior abdominal wall, with an acceptably low complication rate.

Suspected hernias in the groin may be a diagnostic problem, especially in patients with normal findings at physical examination. Since its introduction by Sternhill and Schwartz [**1**] and Birzle [**2**], herniography (also known as peritoneography) has become a well-accepted diagnostic tool in the detection of groin hernias and hernias of the anterior abdominal wall. To assess its value in patients with unexplained pain in the groin or anterior abdominal wall, a retrospective study of herniographs obtained in 70 patients was performed. Results of this study as well as anatomic characteristics, imaging technique, indications and contraindications for imaging, and diagnostic criteria are described herein.

MATERIALS AND METHODS

Radiologic features and clinical outcome in 70 patients referred for herniography were retrospectively evaluated. All patients had symptoms suggestive of a hernia, but the physical examination was either normal (n=66) or inconclusive (n=4). There were 35 male patients and 35 female patients. The mean patient age was 41.8 years (range, 9-80 years). Twelve patients had previously undergone inguinal herniotomy. Most examinations (68 of 70 examinations) were performed on an out-patient basis.

A standard procedure was used in all cases. The patient was instructed to void and was placed in a supine position on the examination table. After local cleaning of the skin and sterile draping, the peritoneal cavity was punctured in the lower quadrant of the abdomen at the lateral border of the rectus abdominis muscle. A 45-mm-long, 18-gauge intravenous canula (Venflon 2; Vigga Spectramed, Helsingborg, Sweden) or a 22-gauge Chiba needle was used. The former has the advantage of a soft sheath remaining in situ during injection of the contrast medium but is relatively short. The latter was used in obese patients because of its length.

With the head of the table tilted up 20°, 50mL of iohexol (Omnipaque; Nycomed, Oslo {240 mg of iodine per milliliter}) was injected under intermittent fluoroscopic control. The needle was determined to be positioned correctly when contrast medium was seen interspersed between bowel loops. No resistance should be felt during injection. After withdrawal of the canula or needle the patient was placed in the prone position. Care should be taken that enough contrast medium reaches the area to be investigated. Further tilting of the table or turning the patient may be necessary. A standard series of views of both sides was obtained during straining, as follows: posteroanterior, posteroanterior with caudocraniad angulation of the tube (15°), two oblique views, and a lateral view. Spot herniographs can be obtained whenever necessary (it may be of help to ask the patient to point out the location of the pain).

The hernias were classified radiographically as direct and indirect inguinal

hernias and femoral, obturator, and incisional hernias (figure 1). Deep fossa was used to describe local bulging of the inguinal fossa without the existence of a true hernial sac.

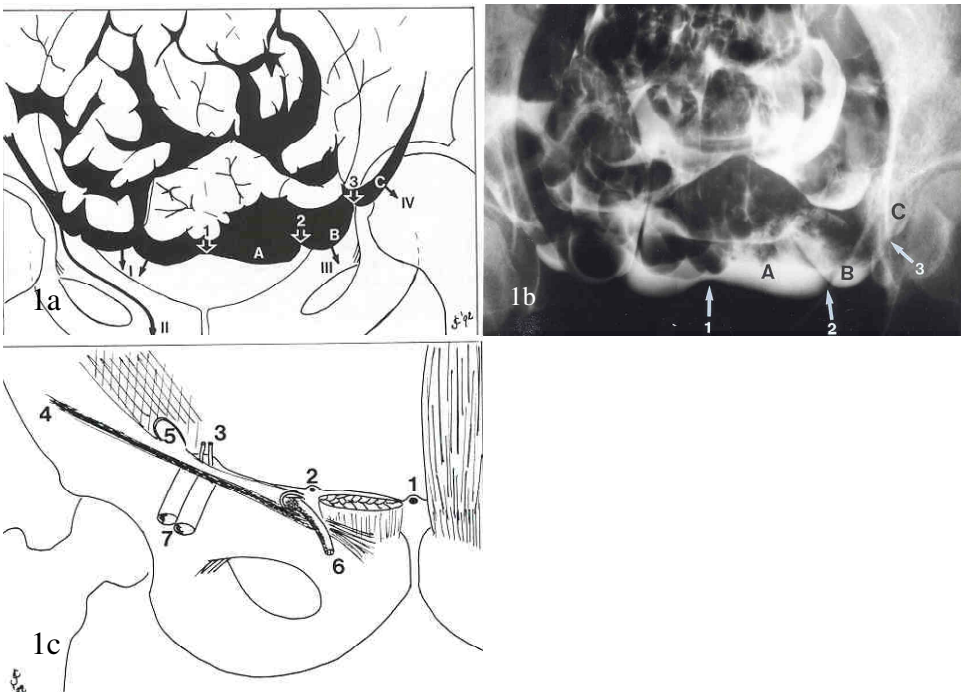

Figure 1
a- Schematic diagram of normal and pathologic findings at herniography. *A*=supravesical fossa, *B*=medial inguinal fossa, *C*= lateral inguinal fossa, *1*= median umbilical fold, *2*=medial umbilical fold, *3*= lateral umbilical fold, *I*=direct inguinal hernia, *II*=indirect inguinal hernia, *III*=femoral hernia, *IV*=obturator hernia. Arrows indicate the pathways followed by the respective hernias.
-b Herniograph shows normal findings. *A*=supravesical fossa, *B*=medial inguinal fossa, *C*=lateral inguinal fossa, *1*= median umbilical fold, *2*=medial umbilical fold, *3*=lateral umbilical fold.
-c Anatomic drawing of the groin region. *1*=median umbilical fold, *2*=medial umbilical fold, *3*=inferior epigastric vessels, *4*=inguinal ligament, *5*=deep inguinal ring, *6*=spermatic cord passing through superficial inguinal ring, *7*= femoral vessels.

RESULTS

Thirty hernias were seen in 25 of the 70 patients (36%). There were 19 indirect inguinal hernias, six direct inguinal hernias, two deep fossae, two femoral hernias, and one incisional hernia. Two of the 70 patients (3%) had a patent vaginal process. The remaining 43 patients (61%) had no radiographically visible abnormalities. Hernias were ipsilateral (i.e., on the symptomatic side) in 17 of the 25 patients; one of these patients also had an incisional hernia. Four of the 25 patients (16%) had a bilateral hernia, and four (16%) had a contralateral hernia (i.e., present on the asymptomatic opposite side). Twenty hernias were detected radiologically in male patients, and 10 were detected in female patients (table 1).

No complications or side effects were seen. In three patients, some contrast medium was inadvertently injected into the anterior abdominal wall. This was not noticed by the patients, and there were no further sequelae. The examination was well tolerated by all patients.

The herniographic diagnosis of hernias was confirmed at surgery in 16 of the 25 patients with hernias. All of these patients' signs and symptoms resolved after surgery. The remaining nine patients with positive radiologic findings were treated conservatively because either the anatomic abnormalities or the clinical situation were not determined to be serious enough to warrant surgery. No patients with normal findings at herniography underwent surgical exploration.

	No. of Patients with Ipsilateral Hernia		No. of Patients with Contralateral Hernia		No. of Patients with Bilateral Hernia	
Herniographic finding	Male	Female	Male	Female	Male	Female
Indirect inguinal hernia	11	2	0	2	1	1
Direct inguinal hernia	2	0	0	0	2	0
Deep fossa	1	1	0	0	0	0
Femoral hernia	0	0	0	2	0	0
Incisional hernia	0	1	0	0	0	0
Total	14	4	0	4	3	1

Table 1
Herniographic findings in male and female patients.

DISCUSSION

Suspected hernias in the groin region or anterior abdominal wall may be a diagnostic problem, especially in patients in whom physical examination reveals no abnormalities. This may be due to the location of the hernia (e.g., obturator hernia [**3**]) or to obesity, which makes the physical examination difficult. Exact figures about the accuracy of physical examination in this regard are not known.

Herniography may be indicated in patients with groin pain or pain in the anterior abdominal wall who are suspected of having a hernia but who have had normal or inconclusive findings at physical examination [**4–6**]. Further indications for herniography are (*a*) to evaluate the contralateral side in patients with a clinically apparent unilateral hernia and (*b*) to evaluate regional anatomic structures in patients in whom a recurrent hernia developed after herniotomy [**5,6**].

The herniographic technique, as described earlier, is a relatively simple and safe procedure. It is contraindicated in patients with known allergies to contrast medium and in the presence of peritonitis, infection of the abdominal wall, urinary retention, gaseous distention of the bowel, peritoneal adhesions, ventriculoperitoneal drain, or bleeding diathesis [**6-8**]. The advent of nonionic contrast media has increased patient tolerance because of the lack of peritoneal irritation. Pain, as described by others [**6,9**], has not been noted by us.

As in other series [**6,9,10**], we encountered no clinical signs of peritonitis. A small amount of contrast medium was injected into the abdominal wall in three of the 70 patients (4%). Injection under fluoroscopic control allows timely recognition. Any resistance felt during injection may be an indication of improper needle positioning. Complications such as puncture of the small bowel, colon, blood vessels, or other retroperitoneal structures, hematoma of the rectus muscle, or inflammation of the abdominal wall, which are said to occur in up to 2.1% of cases [**7,9,11,12**], were not seen in our series.

A number of folds and fossae can be identified with adequately performed herniography (figure1). The median umbilical fold (formed by a remnant of the urachus), the supravesical fossa, the medial umbilical fold (a remnant of the umbilical artery), the medial inguinal fossa, the lateral umbilical fold (formed by the inferior epigastric vessels), and the lateral inguinal fossa are seen lateral to the midline. The pouch of Douglas can be discerned on lateral and oblique views.

Hernias are defined as pathologic protrusions of one of the fossae or of the anterior abdominal wall. The normal medial and lateral inguinal fossa may reach a finger width below the upper pelvic ring [**13**].

Direct (acquired) inguinal hernias usually originate from the medial inguinal fossa (sometimes from the supravesical fossa but always medial to the lateral umbilical fold) and have a broad neck and a course perpendicular to the inguinal channel (figure 2) [**7,11,13,14**].

Figure 2
Herniograph shows direct inguinal hernia protruding from the medial inguinal fossa with bowel contents.

The indirect inguinal hernia, which is of congenital origin, protrudes from the lateral umbilical fossa. It follows the inguinal channel, entering the internal (deep) inguinal ring and sometimes extending beyond the external (superficial) inguinal ring (figure 3) **[5,12]**. Differentiation from a patent vaginal process may be difficult, but the latter tends to have a more slender neck and sometimes a ballooning part distally with a "bird-beaked" end (figure 4) **[6,11,15]**.

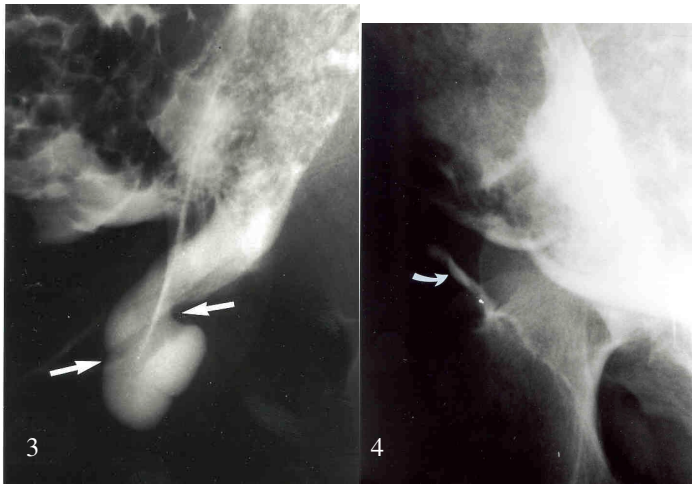

Figures 3,4.
Herniographs show (3) indirect inguinal hernia extending beyond the external inguinal ting (arrows) and (4) patent vaginal process (arrow). Note the slender character of the vaginal process compared with that of the indirect inguinal hernia.

Femoral hernias are often pear shaped and originate below the inguinal ligament (best seen on oblique views) from the inferior aspect of the peritoneal cavity and are therefore best appreciated on the views without angulation of the tube (figure 5). Thus, angulation of the tube is useful in differentiating indirect inguinal from femoral hernias **[5,6,13,16]**.
Obturator hernias are infrequent findings (none were seen in our group of patients), but their characteristic location is in the obturator channel, close to the obturator groove. Filling most frequently occurs in the supine position because of their dorsal reflection from the peritoneal cavity (figure 6) **[5,13,17,18]**.

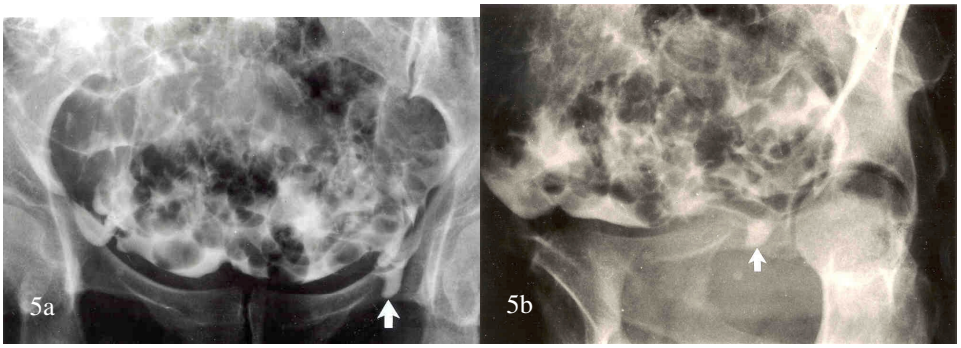

Figure 5
a-Posteroanterior herniograph (obtained without angulation of the tube) of a femoral hernia shows typical pear-shaped configuration (arrow).
b-Oblique herniograph advantageously shows the origin below the inguinal ligament (arrow).

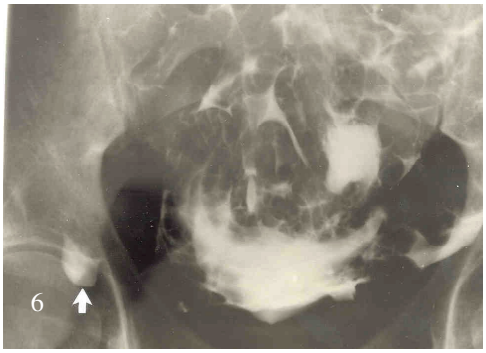

Figure 6
Herniograph shows obturator hernia (arrow). The typical dorsal origin was depicted better with other views (not shown)(Courtesy of D. Wink, MD, Department of Diagnostic Imaging, Diaconessenhuis, Utrecht, The Netherlands.).

Spigelian hernias are even rarer than obturator hernias and originate along the semilunar line (i.e., the lateral border of the rectus abdominis muscle) at the level of the semicircular line [**19**]. Radiologic evaluation is best performed with forced filling of the hernia with the patient in the prone position; imaging is performed with the patient in the lateral decubitus position (with the x-ray beam tangential to the anterior abdominal wall) [**20**]. Alternatively, one can use a horizontal beam with the patient in the knee-elbow position. Umbilical and incisional hernias can be diagnosed analogously [**20**].

The number of hernias found with herniography in our group of patients is in accordance with findings in the literature [**7,9,15,21-23**]. Hernias were found in about one-third of patients (25 patients, 36%). Among these patients, 11 had ipsilateral hernias, four had bilateral hernias, and four had a contralateral hernia.

Because patients with a normal herniographic examination did not undergo surgery, we do not know if there were any false-negative findings. These are

known to occur and can be caused by a filled bladder (which causes distortion of the normal anatomic structures) or filling of the hernial sac with bowel or omentum **[6,17]**.

Although hernias or their contents may be seen during intravenous urography, cystography, or barium examinations of large or small bowel **[7,18,24-26]**, these are not the modalities of choice for the detection of hernias. Ultrasound (US), computed tomography (CT), and magnetic resonance imaging, however may show hernias and are better in depicting other focal abnormalities (e.g., subcutaneous endometriosis or metastases) **[20, 27-29]**. In patients with a positive clinical history for hernia and a negative or inconclusive physical examination, herniography may be the modality of choice. It may advantageously depict anatomic relations of hernias, especially in hernias that are slender and not filled with bowel (the latter may be difficult to discern at CT or US).

Thus herniography, CT, and US can be considered to be complementary in the evaluation of patients with groin pain or pain in the anterior abdominal wall. Herniography is a valuable and simple diagnostic tool in these cases, and when it is accurately performed, the complication rate is acceptably low.

REFERENCES

1. Sternhill V, Schwartz S (1960) Effect of Hypaque on mouse peritoneum. Radiology;75:811-814.
2. Birzle H (1961) Ist die Peritoneographie als röntgenologische Untersuchungsmethode möglich und brauchbar. Fortschr. Röntgenstr.;95:824-829.
3. Cubillo E (1983) Obturator hernia diagnosed by computed tomography. AJR ; 140:735-736.
4. Ekberg O, Abrahamson PA, Kesek P (1988) Inguinal hernia in urological patients: the value of herniography. J.Urol.;139:1253-1255.
5. Ekberg O (1981) Inguinal herniography in adults:technique, normal anatomy and diagnostic criteria for hernias. Radiology;138:31-36.
6. Oh KS, Dorst JP, White JJ, et al. (1973) Positive-contrast peritoneography and herniography. Radiology;108:647-654.
7. Verhaar JAN, Pot JH (1985) De waarde van de herniografie bij onbegrepen pijn in de lies. Ned Tijdschr v Geneeskunde;129:359-362.
8. Meyers MA (1973) Peritoneography, normal and pathologic anatomy. AJR;117:353-365.
9. Ekberg O (1983) Complications after herniography in adults. AJR;140:491-495.

10. Eisenberg AD, Winfield AC, Page DL, Holburn GE, Schifter T, Segars JH (1989) Peritoneal reaction resulting from iodinated contrast material:comparative study. Radiology;172:149-151.
11. Fenn K, Keller G, Kühn R (1982) Die Peritoneographie zum Nachweis nicht tastbarer Hernien.Radiologe;22:166-169.
12. Shackelford GD, McAlister WH (1972) Inguinal herniography. AJR;115:399-407.
13. Gullmo et al (1984) Herniography. Surg Clin North Am; 64:229-244.
14. Ekberg O, Fork FTh, Fritzdorf J (1984) Herniography in atypical inguinal hernia. Br J Radiol ;57:1077-1082.
15. Ekberg O, Kesek P (1987) Herniographic appearance of the lateral inguinal fossa. Acta Radiologica ;28:563-569.
16. Oh KS, Condon VR, Dorst JP, Gralo G (1978) Peritoneographic demonstration of femoral hernia. Radiology;127:209-211.
17. Ekberg O, Nordblom I, Fork FTh, Gullmo Å (1985) Herniography of femoral,obturator and perineal hernias. Fortschr. Röntgenstr.;143:193-199.
18. Carriquiry LA, Pineyro A (1988) Preoperative diagnosis of non-strangulated hernia: the contribution of herniography. Br J Surg;75:785.
19. Balthazar EJ, Subramanyam BR (1983) Radiographic diagnosis of Spigelian hernia. Am J Gastroenterol;78:525-528.
20. Ekberg O, Fork FTh, Aspelin P (1985) Herniography in anterior abdominal wall hernia. Fortschr.Röntgenstr.;143:562-568.
21. Ekberg O, Blomquist P, Fritzdorf J (1984) Herniography in patients with clinically suggested recurrence of inguinal hernia. Acta Radiol Diagn;25:225-229.
22. Smedberg SGG, Broome AEA, Gullmo A, Roos H (1985) Herniography in athletes with groin pain. Am.J.Surg.;149:378-382.
23. Cohen RH,Turkenburg JL,van Dalen A (1990) Herniography in 79 patients with unexplained pain in the groin:a retrospective study. Eur J Radiol;11:184-187.
24. Laurell H (1929) Über die Röntgenuntersuchung von Brüchen, insbesondere klinisch schwer zu diagnostizierende Formen. Acta Radiol; 10:462.
25. Zausner J, Dumont AE, Ring SM (1972) Obturator hernia. AJR;115:408-410.
26. Glicklich M, Eliasoph J (1989) Incarcerated obturator hernia: case diagnosed at barium enema fluoroscopy. Radiology;172:51-52.
27. Maglinte DDT, Miller RE, Lappas JC (1984) Radiological diagnosis of occult incisional hernias of the small intestine. AJR;142:931-932.

28. Gharemani GG, Jimenez MA, Rosenfeld M, et al. (1987) CT diagnosis of occult incisional hernias. AJR;148:139-142.
29. Wechsler RJ, Kurtz AB, Needleman L, et al. (1989) Cross-sectional imaging of abdominal wall hernias.AJR;153:517-521.

5

GROIN HERNIA: CAN DYNAMIC MAGNETIC RESONANCE IMAGING BE OF HELP?

ABSTRACT
This technical note describes the use of dynamic MRI in the diagnosis of groin herniations. A review of the anatomy of the groin is presented and 4 representative cases are described.
This paper indicates that dynamic MRI can be used to confirm the diagnosis in patients with clinically evident groin herniations.

Keywords
Hernia, inguinal
MR, technology
Abdominal wall, abnormalities

INTRODUCTION

In daily clinical practice physical examination is the most important diagnostic modality in the diagnosis of groin hernias. In difficult clinical cases there is a role for additional diagnostic imaging, such as herniography, ultrasound, CT or MRI. Although MRI can visualize herniations of the anterior abdominal wall and the inguinal region, most reports concerning MRI are based on incidental findings [1].

The role of herniography and ultrasound in the diagnosis of groin hernias is well established, herniography being invasive, whereas ultrasound is highly operator-dependent. With this in mind, four patients with clinically evident hernias in the groin were examined using a dynamic magnetic resonance imaging (MRI) protocol (that was developed in 10 volunteers) to determine its capability to visualize groin hernias. In all patients correlation with findings at physical examination and laparoscopic surgery was made. A short review of the anatomical landmarks of interest is presented.

MATERIALS AND METHODS

Four patients (three male, one female; age range 49-72 years), with clinically evident inguinal hernias were investigated using a 0.5T MR system (T5 II; Philips Medical Systems, Best, The Netherlands). All patients were operated irrespective of the findings at MRI. Scan sequences and parameters were optimized in ten healthy volunteers (5 male, 5 female; mean age 32.6 years), resulting in a standard scanning protocol. All scans were interpreted by one observer, without knowledge of the findings at physical examination or at ultrasound that was performed in all cases (except patient no. 4, who was referred for MRI directly after the ultrasound examination).

For the MRI study a body wrap around coil was used, centered over the symphysis. Scanning was performed in the supine position, since image acquisition in the prone position resulted in more respiratory motion artifacts. Furthermore adequate positioning for the dynamic sequences is more difficult in the prone position, due to movement (lifting/tilting) of the pelvis during straining. The protocol consists of a total of four scanning sequences: T-1 weighted volume (FFE), a T-2 weighted (TSE) coronal sequence (turbo factor 16) and two dynamic T-1 W (TFE) sequences, with a scan and reconstruction matrix of 256x256. The latter two sequences were performed during straining (Valsalva maneuver). Scanning parameters are listed in table 1. A large field of view was chosen in order to allow simultaneous visualization of both groins. The (non-dynamic) T-1 and T-2 weighted scans were used for the planning of the dynamic sequences. The centre of the dynamic scans was chosen at the level of the common femoral vessels, at the level of the inguinal ligament. Total scanning time was 8:12

minutes, with an examination time of 20-30 minutes. This makes the method feasible for daily clinical practice.

	survey	T1W/vol	T2W/TSE	Dynamic I	Dynamic II
number of slices	3/3	30	12	2x 3	5
field of view	400	400	400	350	350
slice thickness (mm)	10/10	3	7	7	10
slice gap (mm)	5/5	-	0.7	0.7	1.0
repetition time (ms)	140	44	3855	16	17
echo time (ms)	15	13	150	8	8
flip angle	90	30	90	30	30
no of scan averages	2	1	4	4	2
acquisition time (min)	1:36	2:50	2:41	0:43	0:22

Table 1
MRI protocol.

Attention was paid to visualize the various anatomical structures, that are considered to be crucial in the differentiation of the different types of herniations in the inguinofemoral region. These include the inguinal ligament, the deep and superficial inguinal ring, the inguinal canal and the spermatic cord (in males) and the round ligament (in females), as well as vascular structures (external iliac, femoral and inferior epigastric vein and artery) (figure 1). The inguinal canal is an oblique passage through the abdominal wall, with a length of 3 to 5 cm (figure 1, 2a). It commences at the internal or deep inguinal ring which is a slit-like opening in the transversalis fascia (figure 1, 2a, 5a). The ductus deferens hooks around the lateral side of the inferior epigastric artery (figure 1, 3a), and is joined by vessels and nerves to form the spermatic cord (in the male). The spermatic cord or the round ligament (in the female) traverses the deep inguinal ring and then runs obliquely downward and medially in the inguinal canal. The spermatic cord (or round ligament) emerges through the external or superficial inguinal ring (a triangular opening in the aponeurosis of the external oblique muscle). Hernias are defined as pathologic protrusions of the peritoneal cavity. Medial (direct) and lateral (indirect) inguinal hernias are separated from each other by the inferior epigastric vessels [2].

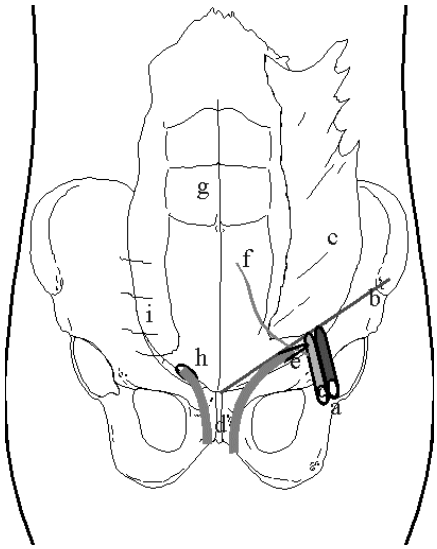

Figure 1
Diagram of anatomy : a=femoral vessels; b=inguinal ligament; c=m. externus obliquus abdominis; d=spermatic cord/round ligament; e=internal inguinal ring; f=inferior epigastric vessels; g=m. rectus abdominis; h=location of external inguinal ring (situated in aponeurosis of m. externus obliquus abdominis); i=m. transversus abdominis.

The normal MR anatomy of the groin was obtained from the MRI studies in the volunteers. In the 4 patients key anatomic structures were identified and hernias were considered to be present when the inguinal canal appeared to be widened (beyond the diameter of the spermatic cord or round ligament) and when there was abnormal contents (fat and/or bowel) within the inguinal canal. Furthermore the presence or absence of herniations was correlated with findings at physical examination and (laparoscopic) surgery.

RESULTS

The examination was easily tolerated by all patients, including the straining test for 20 seconds during the dynamic sequences. All hernias that were present at physical examination could be detected also with dynamic MRI and were confirmed at laparoscopic surgery.

In the first patient an indirect inguinal hernia was found, on the left side containing fat (figure 2). In this patient the right inguinal canal was normal, as compared with the abnormal left side, making identification of the hernia relatively easy.

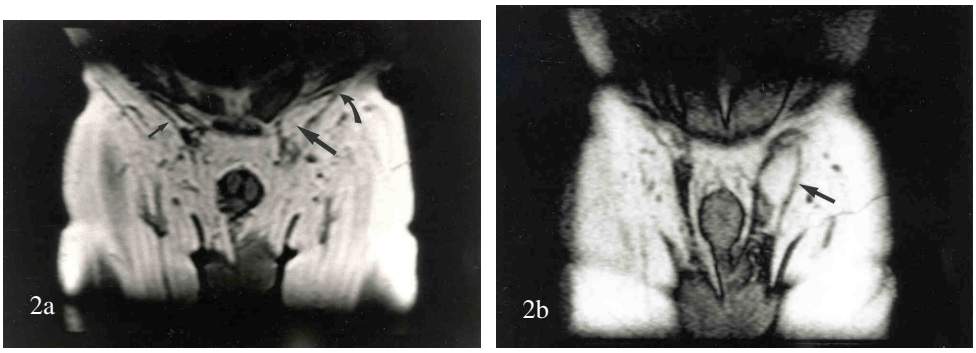

Figure 2
T1-weighted volume scan (a) showing a normal, narrow inguinal canal on the right side (small arrow) and the presence of an indirect hernia on the left (arrow), which can be seen to protrude from the deep inguinal ring (located in the transversalis fascia; curved arrow). The T1-weighted dynamic study, during straining (b) shows an evident increase in diameter of the hernia (arrow).

In the second patient an indirect inguinal hernia was found on the left side as well. This patient showed a wide inguinal canal on the right side (figure 3), however no abnormal contents were seen. At laparoscopy no hernia was found on the right side and the indirect inguinal hernia on the left was confirmed.

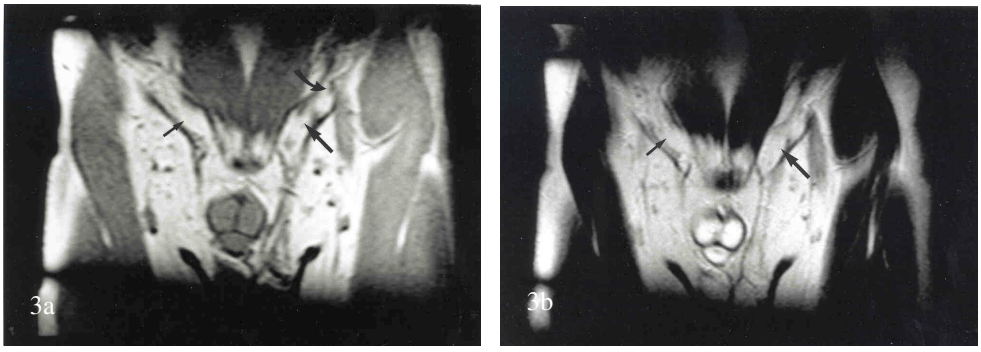

Figure 3
T1-weighted volume scan (a) and T2-weighted images (b) show a relatively wide inguinal canal on the right side (small arrow), however abnormal contents (peritoneum and omental fat) as seen on the left (arrow) is absent on the right. The hernial sac originates lateral to the epigastric vessels (curved arrow), thus the diagnosis of a left indirect inguinal hernia could be made.

In the third patient a right-sided direct inguinal hernia containing fat was diagnosed. Again the dynamic sequences showed the hernia better, partly due to the increase in diameter, partly due to the better visibility of the peritoneal linings caused by using a gradient technique (figure 4).

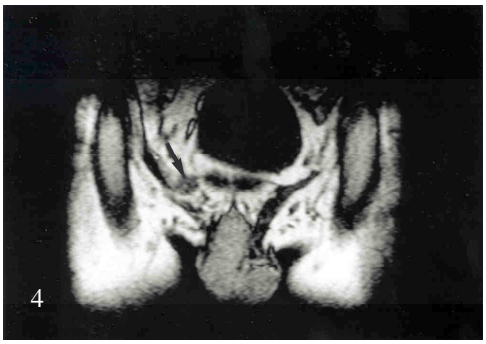

Figure 4
Right-sided direct inguinal hernia (arrow) demonstrated on a T1-weighted dynamic scan, protruding medial into the inguinal canal.

The last patient was referred to our ultrasound department by the nephrologist. The patient was suffering from renal failure, underwent continuous ambulatory peritoneal dialysis and complained of increasing pain in the right groin. At ultrasound an evident indirect inguinal hernia containing fluid was found (not presented). Dynamic MRI showed the herniation clearly on the T1- and T2-weighted images as a fluid filled space with an increase in diameter during straining (figure 5).

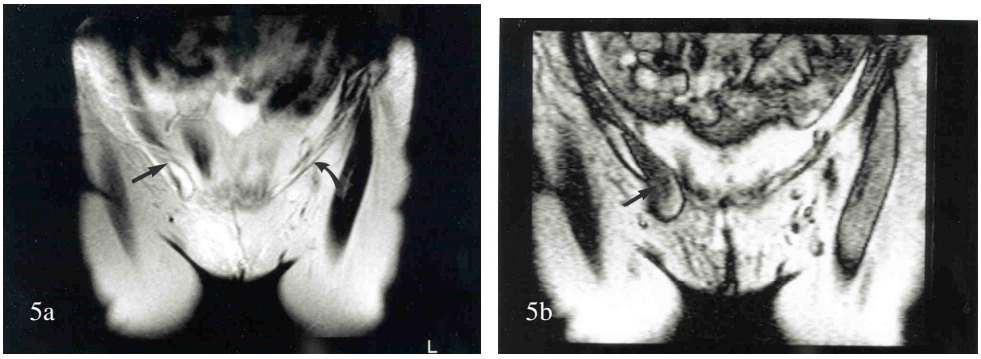

Figure 5
T2-weighted image (a) of a fluid filled indirect inguinal hernia in patient #4: a hyperintense signal is seen within the inguinal canal, originating in the transversalis fascia (arrow), surrounded by a hypointense rim (peritoneum). Note the depiction of the inguinal ligament on the left (curved arrow). The T1-weighted dynamic scan (b) shows an increase in size of the hernial sac (arrow).

DISCUSSION

Surgeons have been diagnosing and treating inguinal hernias for years without resorting to fancy imaging techniques. In some cases, when clinical suspicion of a groin hernia is high, physical examination may reveal no or nonconclusive findings. In other patients the exact nature of a palpable mass in the inguinal region is sometimes difficult to establish. In these cases some kind of imaging, such as ultrasound, CT, MRI or herniography might be

helpful.
Reports concerning CT and MRI of groin hernias are few, and are merely based on description of the appearance of the various types of hernia [1,3,4,5]. Despite its superior soft tissue contrast, MRI has not been used frequently as a diagnostic tool in the evaluation of groin hernias. In our protocol coronal slices were used to examine both groins in one sequence as hernias often occur bilateral [6,7]. Scanning in another plane, e.g. sagittal, or using a smaller field-of-view would increase examination time considerably. In one patient (#4) peritoneal dialysis fluid was used as a contrast agent, a method that can be compared to saline MR peritoneography which has been used in the detection of peritoneal tumor implants [8]. The hernial sac can indeed be seen to advantage. However, when this method is used for the detection of herniations in the groin, the MRI examination becomes as invasive as herniography (with associated risks)[6,9].
This study indicates that in patients with clinically evident herniations MRI can be used to confirm the clinical diagnosis. The relative contribution of each scanning sequence and the diagnostic accuracy will be determined further, in ongoing clinical studies. Until then, all sequences will still be needed. In the future only the dynamic scans may suffice for the diagnosis of groin hernia. The T1- and T2-weighted images may be used to allow the surgeon to differentiate the various types of hernias according to the Nyhus-classification [10], thus offering the possibility to individualization of the surgical approach.

abbreviations: SE (spin echo), FFE (fast field echo), TSE (turbo spin echo), TFE (turbo field echo)

REFERENCES

1. Wechsler RJ, Kurtz AB, Needleman L, Dick BW, Feld RI, Hilpert PL, Blum L (1989) Cross-sectional imaging of abdominal wall hernias.AJR 153:517-521.
2. Rosser J (1994) The anatomical basis for laparoscopic hernia repair revisited. Surgical Laparoscopy & Endoscopy 4:36-44.
3. Harrison LA, Keesling CA, Martin NL, Lee KR, Wetzel LH (1995) Abdominal wall hernias: Review of herniography and correlation with cross-sectional imaging. Radiographics 15:315-332.
4. Zarvan NP, Lee FT, Yandow DR, Unger JS (1995) Abdominal hernias: CT findings. AJR 164:1391-1395.
5. Bennett HF, Balfe DM (1995) MR imaging of the peritoneum and abdominal wall. MRI Clin North Am 3:99-120.

6. Ekberg O (1981) Inguinal herniography in adults: technique, normal anatomy and diagnostic criteria for hernias. Radiology 138:31-36.
7. Chou TY, Chu CC, Diau GY, Wu CJ, Gueng MK (1996) Inguinal hernia in children: US versus exploratory surgery and intraoperative contralateral laparoscopy. Radiology 201:385-388.
8. Magre GR, Terk M, Colletti P, Muggia F, Boswell W (1996) Saline MR peritoneography. AJR 167:749-751.
9. van den Berg JC, Strijk SP (1992) Groin hernia: role of herniography. Radiology 185:191-194.
10. Nyhus LM (1993) Individualisation of hernia repair: a new era. Surgery114:1-2.

6

DYNAMIC MAGNETIC RESONANCE IMAGING IN THE DIAGNOSIS OF GROIN HERNIA

ABSTRACT

Rationale and objective: The authors determine the feasibility of dynamic magnetic resonance (MR) imaging in the diagnosis of groin hernia.

Methods: Ten volunteers and 10 patients with clinically evident and surgically proven herniations were evaluated using T1-, and T2-weighted sequences and 2 dynamic sequences. The visibility of anatomic structures that are crucial for the assessment and the differentiation of inguinofemoral herniations was evaluated.

Results: The inguinal rings could be identified in all subjects. The inferior epigastric vessels could be identified in 85%. In 10 patients 11 hernias were found at MR imaging, whereas at surgery and physical examination 13 herniations were diagnosed (84.6%). The two hernias, that were missed initially could be identified retrospectively on MR imaging. One volunteer showed a small bilateral inguinal hernia on MR imaging, that could be confirmed on physical examination.

Conclusions: The anatomic structures that are crucial for the assessment and the differentiation of inguinofemoral herniations can be identified prospectively with MR imaging.

Keywords

Magnetic resonance imaging
Hernia, inguinal
Peritoneum
Abdominal wall

In clinical cases suspected of hernias in the groin region, additional diagnostic imaging studies are indicated only in patients in whom physical examination reveals no abnormalities, or in whom there are inconclusive findings. Although magnetic resonance (MR) imaging can visualize herniations of the anterior abdominal wall and the inguinal region, most reports concerning MR imaging are based on incidental findings [1]. In this paper the results of dynamic MR imaging in 10 healthy volunteers and 10 patients with clinically obvious and surgically proven inguinal herniations will be discussed. A short review of the anatomic landmarks of interest is presented.

MATERIALS AND METHODS

Ten healthy volunteers (5 male, 5 female; mean age 32.6 years, range 19-47 years) and 10 patients (all male; mean age 55.6 years, range 36-73 years), with clinically evident inguinal hernias were investigated using a 0.5 tesla (T) MR system (T5 II; Philips Medical Systems, Best, The Netherlands). Informed consent for the study was obtained in all patients and volunteers. In all cases a body wrap-around coil was used, centered over the symphysis. Scan sequences and parameters were optimized in two volunteers, resulting in a standard scanning protocol. Scanning was performed in the supine position, because image acquisition in the prone position resulted in more respiratory motion artifacts. The protocol consists of four scanning sequences: T1-weighted volume (fast field echo), a T2-weighted (turbo spin echo) coronal sequence (turbo factor 16), and two dynamic T1-weighted (turbo field echo) sequences, with a scan and reconstruction matrix of 256 x 256. The latter two sequences were performed during straining (Valsalva maneuver). Scanning parameters are listed in table 1. The (non-dynamic) T1- and T2-weighted scans were used for the planning of the dynamic sequences. The center of the dynamic scans was chosen at the level of the common femoral vessels, at the level of the inguinal ligament. All scans were interpreted by one observer, without knowledge of the findings at physical examination. Attention was paid to the visualization of various anatomic structures (figure 1), considered to be crucial in the differentiation of the different types of herniations in the inguinofemoral region. These included the inguinal ligament, the deep and superficial inguinal ring, the inguinal canal and the spermatic cord (in the male) and the round ligament (in the female), as well as vascular structures (external iliac, femoral, and inferior epigastric vein and artery). Furthermore the presence or absence of (inguinal or femoral) herniations was evaluated and correlated with the findings at physical examination or laparoscopic surgery.

	survey	T2W/TSE	T1W/vol	dynamic I	dynamic II
slice orientation	cor/ transv	coronal	coronal	coronal	coronal
number of slices	3/3	12	30	2x 3	5
slice thickness (mm)	10/10	7	3	7	10
slice gap (mm)	5/5	0.7	-	0.7	1.0
field of view	400	400	400	350	350
scan technique	SE	TSE	FFE	TFE	TFE
repetition time (ms)	140	3855	44	16	17
echo time (ms)	15	150	13	8	8
flip angle (▯)	90	90	30	30	30
no of scan averages	2	4	1	4	2
acquisition time (min:sec)	1:36	2:41	2:50	0:43	0:22

Table 1
Magnetic Resonance Imaging scanning protocol; total scanning time 8 minutes, 12 seconds
abbreviations: SE (spin echo), FFE (fast field echo), TSE (turbo spin echo), TFE (turbo field echo).

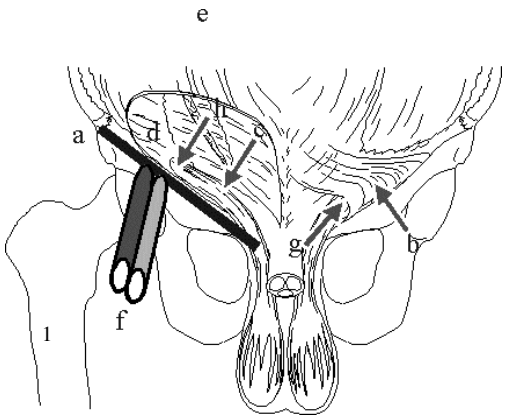

Figure 1
Schematic diagram of anatomic findings (in the male): a=inguinal ligament; b=m. externus obliquus abdominis; c=spermatic cord; d=transversalis fascia; e=inferior epigastric vessels; f=femoral vessels; g=external inguinal ring; h=internal inguinal ring.

Hernias were considered to be present when the inguinal canal appeared to be widened (beyond the diameter of the spermatic cord or round ligament),

with abnormal contents (fat or bowel) within the inguinal canal (figure 2).

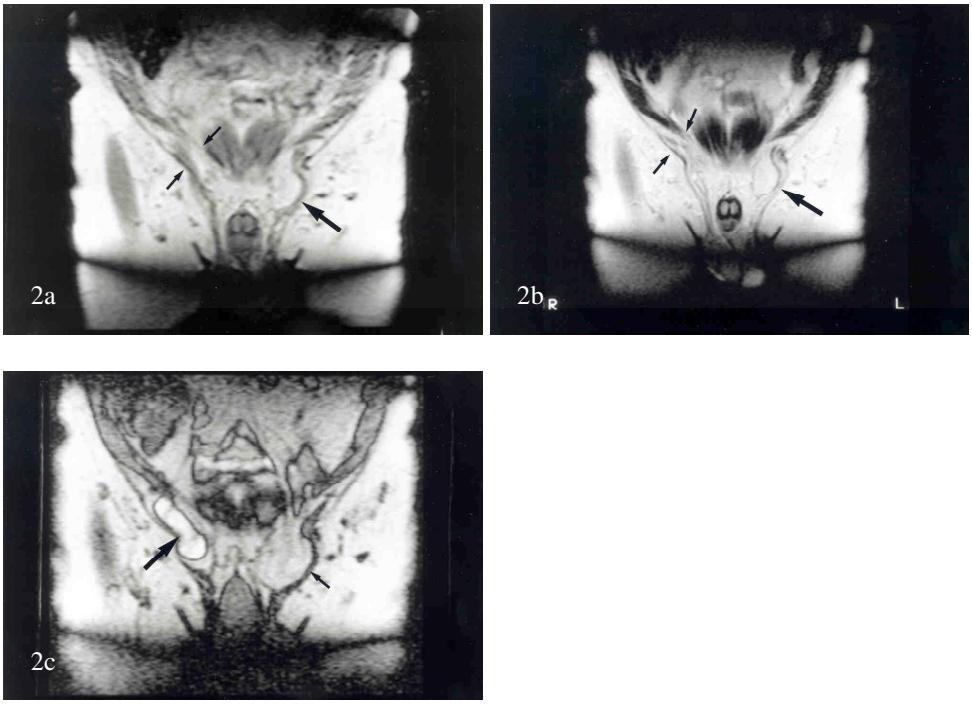

Figure 2
T1- (fig 2a), and T2-weighted (fig 2b) image of inguinal hernia containing fat on the left (arrow), on the right side subtle widening of the inguinal canal is noted (small arrows); the dynamic scan (fig 2c) performed during straining revealed a bilateral hernia. An evident increase in size is seen on the left (small arrow); on the right a herniated bowel is now evident (large arrow).

The overall accuracy of all sequences was evaluated. In this feasibility study no further determination was made of the diagnostic accuracy of the different sequences, and when a hernia was found no further determination of location, size, and contents was made. In case of disagreement between findings at surgery and at MR imaging, the MR scans were reviewed.

RESULTS

The examination was well tolerated by the 20 volunteers and patients, including the straining test of 20 seconds during the dynamic sequences. The visibility of various anatomic structures is summarized in table 2. The median and medial umbilical fold could not be identified in anyone.

In 10 patients, 11 hernias (9 unilateral, 1 bilateral) were found at MR imaging, whereas at laparoscopic surgery and physical examination, 13 herniations (7 unilateral, 3 bilateral) were diagnosed. Discrepancies occurred in two patients. In retrospect, these two hernias were identified on the MR scans. In one of the volunteers the MR image demonstrated small bilateral

inguinal hernias, which were confirmed on physical examination. This volunteer also appeared to have longstanding, intermittent complaints consistent with groin hernia such as pain with coughing. All other volunteers were asymptomatic for hernias.

	T1 vol	T2 (TSE)	Dynamic I	dynamic II
Annulus inguinalis internus	40	38	26	26
Annulus inguinalis externus	40	40	26	26
Ligamentum inguinale	40	40	28	26
a./v. epigastrica inferior	34	30	14	12
a./v. femoralis communis	40	40	40	40
a./v. iliaca externa	40	40	40	40
Peritoneum	4	4	36	36
m. externus obliquus abdominis	40	40	8	8
Transversalis fascia	40	38	26	26
Spermatic cord	30/30	30/30	26/30	26/30
Round ligament	6/10	4/10	4/10	2/10

Table 2
Anatomic structures as visualized in 40 groin sites on different scanning sequences using the protocol as described in table 1.

DISCUSSION

Hernias are defined as pathologic protrusions of the peritoneal cavity. At the caudad lining of the peritoneal cavity a number of important anatomic structures can be identified: the median, medial, and lateral umbilical folds formed by a remnant of the urachus, remnants of the umbilical artery, and the inferior epigastric vessels, respectively. The inguinal canal is an oblique passage, 3 to 5 cm long, through the abdominal wall. It contains the spermatic cord in males and the round ligament of the uterus in females as well as the ilioinguinal nerve. The inguinal canal commences at the internal or deep inguinal ring (situated in the transversalis fascia) and ends and the external or superficial ring, a triangular opening in the aponeurosis of the external oblique muscle. The ductus deferens hooks around the lateral side of the inferior epigastric artery, separating medial (direct) and lateral (indirect) inguinal hernias [2].

When clinical suspicion of a groin hernia is high, physical examination may be negative or indeterminate. In other patients the exact nature of a palpable mass in the inguinal region is sometimes difficult to establish. This necessitates the use of ultrasound, computed tomography (CT), MR imaging or herniography.

Herniography is a valuable diagnostic tool in patients with unexplained groin pain [**3,4,5**], but has the disadvantage of being invasive, using contrast medium and ionizing radiation. It lacks the ability to visualize abnormalities of neighboring structures [**1,6,7**]. Therefore ultrasound, CT, and MR imaging are preferred in the diagnosis of groin hernias. The main advantage of ultrasound, CT, and MR imaging is their ability to depict pathologic conditions other than hernias that may be responsible for the patient's symptoms.

The role of ultrasound has been documented extensively in the surgical literature, and this modality appears to have a high diagnostic accuracy in the evaluation of groin disease. Deitch and Soncrant [**8,9**] showed that in 68 out of 70 patients the preoperative ultrasonic diagnosis was proved to be correct at surgery. Ultrasound is able to visualize herniations in patients despite a negative physical examination, and to diagnose abnormalities other than hernias, e.g. femoral artery aneurysm [**8,9**]. Being a real-time examination, it has the capability of facilitating the diagnosis of hernias by showing movement of any herniated contents or by using a Valsalva maneuver, or by examining the patient in the upright position [**5**]. The disadvantage of ultrasound is the high operator dependency.

Reports concerning CT and MR imaging of groin hernias are few, and are based merely on the descriptions of the appearances of the various types of hernias [**1,5,10,11**].

The role of CT seems to be narrow because its ability to depict abnormalities in any required plane (and during straining) is limited. This might be overcome with the use of helical CT scanning, which offers the ability to perform multiplanar reconstruction, even during straining. Furthermore hernias can remain undetected at CT because the patient usually is scanned in the supine position [**5**].

Despite its superior soft tissue contrast, MR imaging has not been used as a primary diagnostic imaging tool in the evaluation of groin hernias. The authors propose a scanning protocol, requiring an examination time of 20 to 30 minutes, scanning time 8:12 minutes, which is acceptable for daily clinical practice. In our protocol coronal slices were used to examine both groins in one sequence as hernias often are bilateral [**4,12**]. Scanning in another plane, e.g. sagittal, would double examination time, because only one groin could be examined at a time.

In this study, the median and medial umbilical folds could not be identified in

any of the individuals examined. From a diagnostic point of view this is not important, because neither structure plays a role in the differentiation of the various forms of hernias, (i.e. direct hernias), which originate either from the supravesical fossa, bounded by the median umbilical fold and the medial umbilical fold, or the medial inguinal fossa, bordered by the medial and lateral umbilical fold. The inferior epigastric vessels, which can be identified easily on herniography as the lateral umbilical folds, and on CT, could not be identified in every subject in this study (table 2) [**3,4**]. This probably relates to the fact that the MR scanning was performed in the coronal plane. The epigastric vessels are a major landmark in the differentiation between direct and indirect inguinal hernias. However, the course of the spermatic cord or round ligament, which could be identified on MR, were used to lead the way to the location of the internal and external inguinal ring. This was a successful alternative way to differentiate direct from indirect inguinal hernias.

The inguinal ligament is of importance in differentiating femoral from inguinal hernias. It was identifiable in all cases. It was not surprising that smaller anatomic structures, such as the epigastric vessels, were poorly visualized on the dynamic, relatively thick sliced, sequences. Although the dynamic sequences showed less anatomic detail, the pronounced depiction of the peritoneal linings, due to the gradient technique, was considered an advantage. Straining during the examination was essential. Hernias were considered to be present when the inguinal canal was wide and showed abnormal contents. Chou et al [**12**] considered a value of 4 mm as an upper limit of the diameter of the inguinal canal in children using ultrasound. The normal size of the inguinal canal in adults is not known to our knowledge, and could be determined with a larger study population.

This feasibility study demonstrated that in patients with clinically evident herniations, MR can clearly identify the structures that are crucial for the assessment and differentiation of inguinofemoral hernias. The diagnostic accurracy of MR in identifying the presence or absence of inguinal hernias is promising. Prospectively, 11 of 13 hernias (i.e. 84.6 %) were diagnosed correctly, with the two missed herniations still visible retrospectively. The two herniations that were missed initially appeared to be small (<10 mm), early stage, precursor hernias, i.e. hernia incipiens, containing only fat. This probably reflects the learning curve of the single observer. No false-positive findings occurred in the patient group.

The relative contribution of each scanning sequence will be further evaluated in an ongoing prospective clinical trial. The present study does suggest that dynamic MR imaging should be reserved for patients with unclear or doubtful clinical findings.

REFERENCES

1. Wechsler RJ, Kurtz AB, Needleman L, Dick BW, Feld RI, Hilpert PL, Blum L (1989) Cross-sectional imaging of abdominal wall hernias. AJR 153:517-521.
2. Rosser J (1994) The anatomical basis for laparoscopic hernia repair revisited. Surgical Laparoscopy & Endoscopy 4:36-44.
3. van den Berg JC, Strijk SP (1992) Groin hernia: role of herniography. Radiology 185:191-194.
4. Ekberg O (1981) Inguinal herniography in adults: technique, normal anatomy and diagnostic criteria for hernias. Radiology 138:31-36.
5. Harrison LA, Keesling CA, Martin NL, Lee KR, Wetzel LH (1995) Abdominal wall hernias: Review of herniography and correlation with cross-sectional imaging. Radiographics 15:315-332.
6. Maglinte DDT, Miller RE, Lappas JC (1984) Radiological diagnosis of occult incisional hernias of the small intestine. AJR 142:931-932.
7. Gharemani GG, Jimenez MA, Rosenfeld M, Rochester D (1987) CT diagnosis of occult incisional hernias. AJR 148:139-142.
8. Deitch EA, Soncrant MC (1981) The value of ultrasound in the diagnosis of nonpalpable femoral hernias. Arch Surg 116:185-187.
9. Deitch EA, Soncrant MC (1981) Ultrasonic diagnosis of surgical disease in the inguino-femoral region. Surg Gyn Obst 152:319-322.
10. Zarvan NP, Lee FT, Yandow DR, Unger JS (1995) Abdominal hernias: CT findings. AJR 164:1391-1395.
11. Bennett HF, Balfe DM (1995) MR imaging of the peritoneum and abdominal wall. MRI Clin North Am 3:99-120.
12. Chou TY, Chu CC, Diau GY, Wu CJ, Gueng MK (1996) Inguinal hernia in children: US versus exploratory surgery and intraoperative contralateral laparoscopy. Radiology 201:385-388.

7

DETECTION OF GROIN HERNIA WITH PHYSICAL EXAMINATION, ULTRASOUND AND MRI AS COMPARED TO LAPAROSCOPIC FINDINGS

ABSTRACT

Objective: To determine the diagnostic accuracy of physical examination, ultrasound and dynamic MRI in patients with inguinal hernia.

Methods: In 41 patients with clinically evident herniations, 82 groins were evaluated using a standard ultrasound and MRI protocol, the latter including T1-, and T2-weighted sequences as well as two dynamic sequences. All ultrasound examinations and MRI scans were reviewed without knowledge of clinical findings. In all cases, correlation with findings at laparoscopic surgery was made.

Results: At surgery, 55 inguinal herniations were found. Physical examination revealed 42 herniations (one false-positive finding), whereas ultrasound made the diagnosis of a hernia in 56 cases (five false-positive and four false-negative findings). MRI diagnosed 53 herniations (one false-positive and 3 false-negative findings). Thus sensitivity and specificity figures were 74.5%, and 96.3% for physical examination, 92.7% and 81.5% for ultrasound, and 94.5% and 96.3% for MRI.

Conclusions: In patients with clinically uncertain herniations, MRI is a valid diagnostic tool with a high positive predictive value.

Keywords

Hernia, inguinal
MRI
Ultrasound
Abdominal wall, abnormalities

INTRODUCTION

The clinical diagnosis of inguinal and femoral hernias is usually made straightforward, and in the most cases further imaging is unnecessary and expensive. A few hernias, however present a diagnostic problem. This diagnostic difficulty is usually encountered in obese patients or in patients with reducible hernias that are not protruding at the time of physical examination. Ultrasound and MRI can depict inguinal hernias, but their sensitivity and specificity are not known. To determine the diagnostic accuracy of both ultrasound and MRI in the diagnosis of groin hernia, 41 consecutive patients with inguinofemoral herniations found at physical examination were evaluated prospectively. Findings were correlated with those at laparoscopic surgery.

METHODS

Forty-one consecutive patients, all referred to the Department of Surgery for suspected inguinal hernias, were included, after obtaining informed consent. All patients (37 men, 4 women; mean age 57.5 years, [range 28.1-77.2 years]), had uni- or bilateral reducible masses in the groin region at physical examination. All patients were scheduled for hernia repair because of their complaints. During the preoperative waiting period, ultrasound and MRI examinations were performed on the same day in all cases. Both groins were examined. Patients were evaluated for the presence of herniations; no differentiation was made between direct and indirect inguinal hernias. The ultrasound examination, using a 7-MHz linear array transducer (Acuson 128 XP/10, computed sonography system; Acuson, Mountain View, CA), was performed by one radiologist unaware of the localization of the complaints of the patient. Patients were examined in supine and upright positions, at rest, and during straining (Valsalva's maneuver).

The MRI examination was performed on an 0.5 Tesla MR system (T5 II; Philips Medical Systems, Best, The Netherlands), according to a well-circumscribed protocol [**1**], evaluating both groins. The protocol consisted of a T1-weighted volumetric sequence (used to make 3-mm-thick coronal reconstructions), and a T2-weighted sequence (table 1). The two dynamic sequences (7- and 10-mm slices, respectively) were focused on the inguinal canal, as demonstrated on the previous T1- and T2-weighted sequences and were performed during straining. Hard copies of the MRI without any demographic data were studied by the same radiologist, at a later date, to avoid any effect on the interpretation of findings at MRI by the recent ultrasound examination (the hard copies were randomized).

A hernia was defined as abnormal ballooning of the anteroposterior diameter of the inguinal canal and/or simultaneous protrusion of fat and/or bowel within the inguinal canal (either originating from the posterior wall of the

inguinal canal or through the internal inguinal ring). An example of an inguinal hernia as demonstrated by ultrasound and MRI is shown in figure 1.

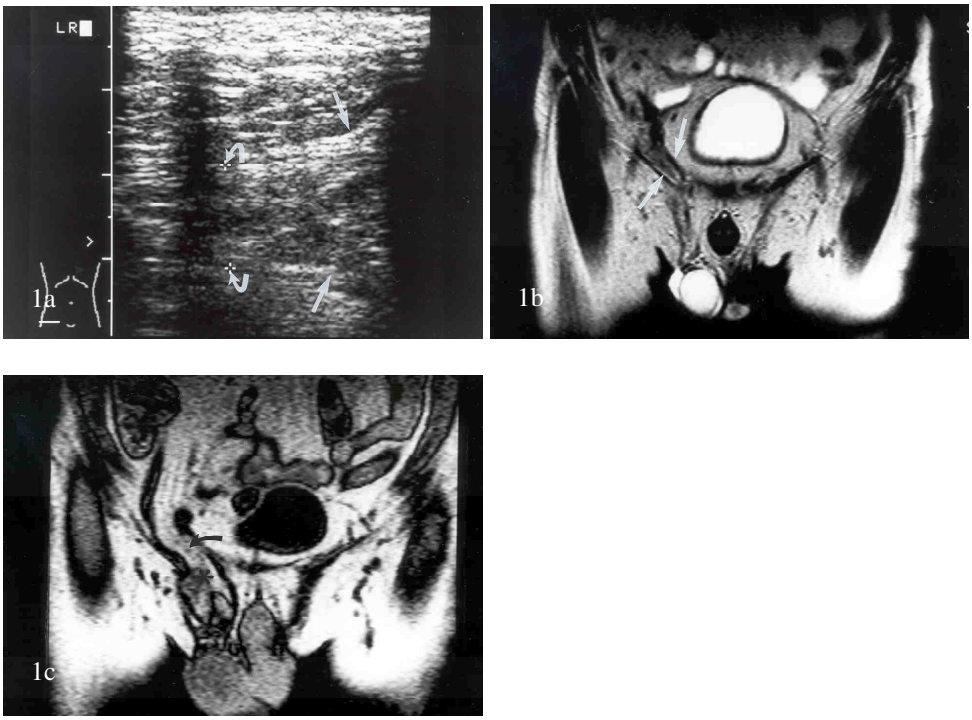

Figure 1
a- Ultrasound appearance of a right inguinal hernia during straining in the supine position (at rest no abnormalities were found); note the abnormal widening of the inguinal canal and abnormal fat content is present (curved arrows); the hernia is widened more distally at the level of the external inguinal ring (arrows).
b- T2- weighted MRI image in the same patient, obtained at rest; note minimal but distinct widening of the right inguinal canal (arrows) as compared to the right side.
c- Dynamic T1-weighted MRI in the same patient during straining: the inguinal hernia is now demonstrated to advantage (curved arrow); as with ultrasound the widening distally from the external inguinal ring can be seen (asterisk).

The gold standard for the diagnosis of inguinal hernia was the presence of a *symptomatic* abdominal wall defect at diagnostic laparoscopy, eventually followed by laparoscopic, transabdominal hernia repair. In all study subjects, both groins were evaluated laparoscopically without prior knowledge of the results from ultrasound and MRI examinations. Findings from the physical examination, ultrasound, and MRI were correlated with the findings at laparoscopic surgery.

	survey	T2W/TSE	T1W/vol	dynamic I	dynamic II
slice orientation	cor/ transv	coronal	coronal	coronal	coronal
number of slices	3/3	12	30	2x 3	5
slice thickness (mm)	10/10	7	3	7	10
scan technique	SE	TSE	FFE	TFE	TFE
repetition time (ms)	140	3855	44	16	17
echo time (ms)	15	150	13	8	8
flip angle	90	90	30	30	30
acquisition time (min)	1:36	2:41	2:50	0:43	0:22

Table 1
MRI scanning protocol; total scanning time of all sequences <10 minutes (SE=spin echo;TSE=turbo spin echo; FFE=fast field echo; TFE=turbo field echo).

RESULTS

In all patients, ultrasound and MRI evaluation of both groins was performed (82 groins). The interval between physical examination and ultrasound/MRI was 1 day to 27 weeks (mean 6 weeks). The patients underwent surgery 1 day to 43.4 weeks (mean 8 weeks) after diagnostic imaging. On physical examination, 42 herniations (6 bilateral, 30 unilateral) were found; on ultrasound 56 (15 bilateral, 26 unilateral) were found; on MRI 53 (12 bilateral, 29 unilateral) were found. Surgery revealed 55 groin herniations (14 bilateral, 27 unilateral). Table 2 summarizes the findings at the different diagnostic modalities. Table 3 shows the sensitivity and specificity, and the accuracy and positive and negative predictive value of the diagnostic modalities, including physical examination.

All herniations missed by physical examination (n=14) were small (but were repaired because of complaints). The one false-positive finding occurred in a patient with a preperitoneal lipoma.

The four herniations missed on ultrasound were all very small (two of these were also missed on MRI). Four of the false-positive findings by ultrasound consisted of findings of minimal bulging of the peritoneum, obviously misinterpreted as being of clinical significance. The other false-positive finding by ultrasound occurred in the beginning of the series, and in this case an enlarged lymph node in the inguinal region was interpreted as a hernia.

One of the false-negative findings on MRI was caused by insufficient scanning technique in the dynamic sequences (the anterior part of the

inguinal canal was not visualized adequately). In the other two patients, a small hernia could be noted on one of the dynamic sequences in retrospect. The false-positive finding on MRI was caused by the presence of a preperitoneal lipoma, which was surgically resected (same patient as described above). In retrospect, there was no increase in the diameter of the inguinal canal during straining, and sliding of the fat inside the inguinal canal occurred.

		Laparoscopy	
		Positive	Negative
Physical examination	Positive	41	1
	Negative	14	26
Ultrasound	Positive	51	5
	Negative	4	22
MRI	Positive	52	1
	Negative	3	26

Table 2
Findings at laparoscopy, physical examination, ultrasound and MRI.

DISCUSSION

In day-to-day clinical practice, the diagnosis of inguinal herniations is generally made by physical examination. However, clinicians sometimes need to use diagnostic imaging in doubtful cases (such as obese patients, or those who have previously had surgery). The diagnostic accuracy of physical examination is not known. Further, there are reports that hernias can be present in up to one-third of asymptomatic patients [**2**]. The relatively poor diagnostic accuracy of physical examination in this series cannot be explained, although clinicians may tend to examine the groin that is clinically less or not involved in an insufficient way. However retrospective evaluation of the physical examination is impossible.

Herniography and ultrasound are of established value in diagnosing herniations of the groin, especially because the examination can be performed during straining [**3,4,5,6,7,8**]. A relative drawback of herniography is its invasiveness. With the arrival of fast MR imaging techniques, dynamic imaging (performed during straining) has become possible. To establish the diagnostic accuracy of ultrasound and MRI in patients with questionable findings of a groin hernia, one must determine the sensitivity and specificity

of both modalities in patients with clinically evident herniations. After this, further investigation of the diagnostic accuracy in patients with questionable findings at physical examination must be performed. A clinical trial in which the negative predictive value is established properly would be very difficult, or even impossible to perform, because it is impossible, from an ethical viewpoint, to perform exploratory surgery in all patients with doubtful clinical findings and negative findings on adjunctive diagnostic imaging.

Some of these problems have been overcome in this study by evaluating both groins in a group of patients with clinically evident uni- or bilateral herniations who would undergo laparoscopy (evaluating both groins), eventually followed by surgery. By scanning the "healthy" groin as well, one also gets an impression of the number of false positives and true negative findings. The drawback is the bias of the examiner, who knows that at least one hernia must be present, thus, the pretest probability of the presence of a hernia is high. Because in this study we intended to evaluate the accuracy of ultrasound and MRI in diagnosing groin herniations (findings being compared with the presence of an abdominal wall defect at surgery), the ability of these modalities to differentiate between direct and indirect inguinal herniations was not examined separately.

The relatively long interval between physical examination, imaging, and surgery is caused by the presence of a waiting list. The major risk of not performing direct elective surgery for inguinal hernia is strangulation. The cumulative probability of strangulation of an inguinal hernia has been reported to be 2.8% at 3 months [**9**]. In our group, no strangulation occurred. Other features of the natural history of groin hernias are not known in the current literature.

Ultrasound is noninvasive and, like herniography, allows examination of the patient in a physiologic manner; however, it is operator-dependent [**10**]. Operator errors can be minimized by highly standardizing the ultrasound examination. The interobserver variability was not addressed to in this study. In the study by Deitch and Soncrant [**4**] the ultrasonographer was not blinded to the findings of physical examination, which might explain the higher sensitivity (97.1%). In our series, a lower sensitivity was achieved. Specificity cannot be compared because in the study by Deitch and Soncrant an additional 25 patients were included with negative findings at ultrasound. These patients did not undergo surgery, and thus specificity cannot be calculated. From table 3 one can see that ultrasound should be performed dynamically and in the upright and supine positions to obtain the highest accuracy. With ultrasound, even incipient hernias can be detected [**5**]. A pitfall causing a false-positive finding is a lipoma of the spermatic cord or a preperitoneal lipoma (as in our series, both on ultrasound and MRI). A cord lipoma appears as a smooth, finger-like projection of fat parallel to the cord

vessels at rest. During straining, longitudinal sliding occurs. Unlike indirect inguinal hernias, the anteroposterior diameter of the inguinal canal does not increase during Valsalva's maneuver [5]. False-negative findings on ultrasound occur and can be partly attributed to the intermittent nature of the herniation. In a series of 70 patients with surgical correlation, Deitch and Soncrant [4] had 2 false-negative ultrasound findings; in both patients a small, only intermittently palpable, indirect inguinal herniation was present. Another cause of false-negative findings on ultrasound is the application of too much pressure on the scanhead during the procedure, or insufficient patient cooperation [5]. Incipient (direct) inguinal hernias cause only a convex anterior bulge of the posterior inguinal wall and ballooning of the spermatic cord in its craniocaudal diameter [5]. Four (out of five) of the false-positive findings and all four false-negative findings on ultrasound in our series were in the difficult gray area between normal and pathologic conditions.

The diagnostic accuracy of the dynamic MRI, as presented in this paper, is very promising. No other reports dealing with the sensitivity and specificity of MRI of groin hernias are known. The false-negative findings in our series were caused by insufficient scanning technique (n=1) or by the learning curve of the new technique (n=2), because the herniations could be demonstrated in retrospect. The preperitoneal lipoma (which does not have to be treated surgically) causing the only false-positive result remains a difficult issue. The most important feature differentiating preperitoneal lipomas from inguinal hernias is the absence of an increase in the transverse diameter of the inguinal canal during straining. Sliding of the lipoma, however, does occur.

In our protocol, coronal sequences were used because of the lack of knowledge as to the symptomatic side of the patient and because inguinal hernias often occur bilaterally. In the future, more dedicated scanning focused on the side involved (e.g. sagittal or sagittal oblique slices) might yield an even higher accuracy. Table 3 indicates that combining dynamic MRI of the groin with static imaging sequences leads to the detection of more herniations than if the separate sequences were used alone. Thus, all 4 sequences are still needed to demonstrate the presence or absence of a hernia. If one is interested only in determining the exact nature of a clinically evident hernia, the number of sequences may be reduced (thus reducing imaging time considerably). This is the subject of further investigation. The sensitivity and specificity of MRI might be increased by the use of intraperitoneal contrast agents (saline or gadolinium), as for the staging of gynecological malignancies or demonstration of peritoneal dissemination [11]. However, this is invasive and more costly.

This study indicates that both ultrasound and MRI examinations of the groin

are more sensitive than physical examination. The specificity of physical examination in identifying a groin mass as a hernia equals that of MRI and is higher than that of ultrasound. Therefore, ultrasound and MRI seem to merit a place in diagnostic workup of doubtful clinical cases. Because the positive and negative predictive values of MRI is higher than that of ultrasound (table 3), MRI seems to be the modality of choice from a clinician's point of view. Factors still to be evaluated are the optimal technique in the MR-imaging of herniations, inter-observer variability, and the role of the modality in pre-operative planning. In the future, the role of additional diagnostic imaging can be extended to help determine the exact nature of a hernia in clear-cut clinical cases. This would assist in optimal preoperative planning, because recent reports indicate that the best laparoscopic surgical approaches differ considerably for direct and indirect inguinal hernias [**12,13**] (this finding, however, was not reproduced by others [**14**]).

Our study indicates that MRI and ultrasound can be used as final diagnostic modalities in clinically doubtful cases. Ultrasound should be the diagnostic modality of choice merely because of its low-cost and its availability. The high operator dependency of ultrasound (reflected by the high number of false-positive findings caused by borderline "herniations" in our series) remains a problem. The reproducibility of the ultrasound technique must be examined further.

In conclusion, physical examination will remain the cornerstone in the diagnosis of groin herniations in clinical practice. At present, there is no place for the routine use of ultrasound or MRI (which costs up to $500) in patients with clear-cut inguinal hernias. MRI and to a lesser extent ultrasound can be used to diagnose groin herniations accurately, in patients with negative or uncertain findings at physical examination but with a history suspicious for a groin hernia.

	Physical examination	US supine		US upright		US-total	T-1	T-2	dynamic I	dynamic II	MRI-total
		Rest	Straining	Rest	Straining						
Sensitivity	74.5	58.2	80.0	81.8	90.9	92.7	81.8	76.4	78.2	74.5	94.5
Specificity	96.3	92.6	85.2	85.2	85.2	81.5	100	96.3	100	96.3	96.3
Accuracy	81.7	69.5	81.7	82.9	89.0	89.0	87.8	82.9	82.9	81.7	95.1
PPV	97.6	94.1	91.7	91.8	92.6	91.1	100	97.7	100	97.6	98.1
NPV	65.0	52.1	69.7	69.7	82.1	84.6	73	66.7	69.2	65	89.7

Table 3
Diagnostic performance of all modalities
PPV= positive predictive value; NPV= negative predictive value.

REFERENCES

1. van den Berg JC, de Valois JC, Go PMNYH, Rosenbusch G (1997) Dynamic magnetic resonance imaging in the diagnosis of groin hernia. Invest Radiol 32:644-647.
2. Kald A, Nilsson E, Anderberg B, et al (1998) Reoperation as surrogate endpoint in hernia surgery. Eur J Surg 164:45-50.
3. Ekberg O (1981) Inguinal herniography in adults: technique, normal anatomy and diagnostic criteria for hernias. Radiology 138:31-36.
4. Deitch EA, Soncrant MC (1981) Ultrasonic diagnosis of surgical disease in the inguino-femoral region. Surg Gyn Obstet 152:319-322.
5. Orchard JW, Read JW, Neophyton J, Garlick D (1998) Groin pain associated with ultrasound finding of inguinal canal posterior wall deficiency in Australian Rules footballers. Br J Sports Med 32:134-139.
6. van den Berg JC, Strijk SP (1992) Groin hernia: role of herniography. Radiology 185:191-194.
7. Jones RL, Wingate JP (1998) Pictorial review: herniography in the investigation of groin pain in adults. Clinical Radiology 53:805-808.
8. Vincent LM (1992) Peritoneal cavity and abdominal wall. In: Mittelstaedt C, ed. General ultrasound. New York: Churchill Livingstone 639-651.
9. Gallegos NC, Dawson J, Jarvis M, Hobsley M (1991) Risk of strangulation in groin hernias. Br J Surg 78:1171-1173.
10. Harrison LA, Keesling CA, Martin NL, Lee KR, Wetzel LH (1995) Abdominal wall hernias: Review of herniography and correlation with cross-sectional imaging. Radiographics 15:315-332.
11. Magre GR, Terk M, Colletti P, Muggia F, Boswell W (1996) Saline MR peritoneography. AJR 167:749-751.
12. Liem MSL, van Vroonhoven ThJMV (1996). Laparoscopic inguinal hernia repair. Br J Surg 83:1197-1204.
13. Nyhus LM (1993) Individualization of hernia repair: a new era. Surgery 114: 1-2.
14. Beets GL, Oosterhuis KJ, Go, PMNYH, Baeten CGMI, Kootstra G (1997) Longterm follow-up (12-15 years) of a randomized controlled trial comparing Bassini-Stetten, Shouldice, and high ligation with narrowing of the internal ring for primary inguinal hernia repair. J Am Coll Surg 185:352-357.

8

PREOPERATIVE AND POSTOPERATIVE ASSESSMENT OF LAPAROSCOPIC INGUINAL HERNIA REPAIR USING DYNAMIC MRI

ABSTRACT

Rationale and Objectives:

To determine the value of dynamic MRI for seroma detection, hernia recurrence and mesh placement in patients after laparoscopic inguinal hernia repair.

Methods:

Thirteen inguinal hernias in 10 consecutive patients were evaluated before and after surgery by using an MRI protocol consisting of coronal T1-weighted (fast field echo), T2-weighted (turbo spin echo) images and two sequences obtained during straining (turbo field echo gradient technique). All patients underwent a transabdominal preperitoneal laparoscopic inguinal hernia repair. MRI scans were reviewed for the presence of postoperative fluid collections, recurrent hernia and mesh localisation.

Results:

In all patients an inguinal hernia was identified on the pre-operative MRI, and was absent on the post-operative MRI. In all patients treated laparoscopically the mesh and its position were clearly identified. Three small fluid collections were found on the post-operative MRI scans.

Conclusions:

Dynamic MRI can demonstrate small, post-operative fluid collections and a sufficient hernioplasty by showing the proper position of the mesh and the absence of a hernia.

Keywords

Abdominal wall, abnormalities
Hernia, inguinal
Laparoscopic hernia repair
MRI

In laparoscopic inguinal hernia repair a prosthetic mesh is placed in the pre-peritoneal space to cover the abdominal wall defect. Insufficient mesh placement (i.e. in a position not covering the hernial defect completely) may result in an early postoperative recurrence. In addition, seroma may be noticed in the inguinal region around the mesh. With physical examination, it is sometimes difficult to differentiate between recurrence or mesh seroma. Dynamic MRI allows functional studies of the pelvis. Its role is well established in the evaluation of functional pelvic floor abnormalities (e.g. MR defecography)[1]. It has been successfully used to identify inguinal hernias [2]. The aim of this study was to compare the preoperative dynamic MRI with the postoperative study of patients undergoing laparoscopic inguinal hernia repair with regard to seroma formation, hernia recurrence and mesh placement.

METHODS

Ten consecutive patients (nine men, one woman; mean age 58.1 years, range 28-74) with 13 palpable hernias at physical examination (7 unilateral, 3 bilateral) underwent a laparoscopic inguinal hernia repair. This was the transabdominal pre-peritoneal repair with the use of a 10 x 12-cm. Polyprolene mesh (Prolene mesh®, Ethicon, Amersfoort, The Netherlands). Pre- and postoperative dynamic MRI scans were obtained in all patients, after obtaining informed consent. The interval between surgery and the post-operative MRI averaged 12 weeks (range, 6-35). All MRI examinations were performed on a 0.5-T MR system (T5 II; Philips Medical Systems, Best, The Netherlands), according to a defined protocol, which included scanning both groins in the coronal plane. The protocol consisted of a T1-weighted volumetric sequence (fast field echo; repetition time (TR) 44 ms, echo time (TE) 13 ms, slice thickness 3 mm, duration 2 minutes and 41 seconds; field-of-view 400), a T-2 weighted sequence (turbo spin echo; TR 3855 ms, TE 150 ms, slice thickness 10 mm, duration 2 minutes and 50 seconds; field of view 400), and two dynamic sequences (turbo field echo; for the first, TR 16 ms, TE 8 ms, 6 slices with a slice thickness 7 mm, duration 43 seconds; for the second, TR 17 ms, TE 8 ms, 5 slices with a slice thickness 10 mm, duration 22 seconds; field of view for both 350) obtained during straining. The matrix size for all sequences was 256 x 256. Total examination time was 15 to 20 minutes. One observer, who was aware of the hernia location and side operated on, reviewed all MRI scans. The observer was unaware to the surgical results and clinical outcome. Any pre-operative anomalies were noted. After surgery, the visibility of seroma, the presence of recurrent hernia and the mesh location were evaluated.

RESULTS

During surgery all 13 hernias were found and treated laparoscopically. No postoperative complications occurred. In all 13 groins the presence of an inguinal hernia was confirmed on the pre-operative scan, including the five recurrences (figure 1). In three patients a left-sided inguinal hernia was present; four patients had a right-sided groin herniation. The other three patients had bilateral inguinal herniations. In all cases findings consisted of a hernial sac containing fat. In none of the patients were bowel structures present within the hernial sac. In the MRI scan of four groins a scrotal fluid collection (hydrocele) was present.

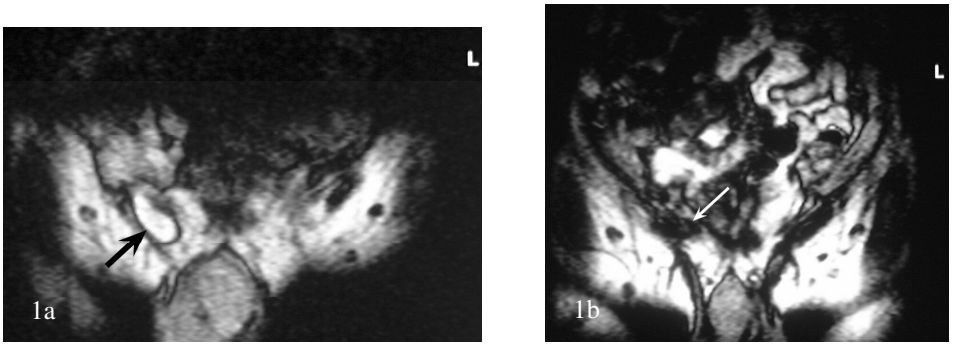

Figure 1
Preoperative (a) and postoperative (b) dynamic MRI (turbo field echo) scans of the groin in a patient with a recurrence after inguinal hernia repair on the right. Recurrence of a hernial sac, containing fat, is clearly seen before surgery (arrow); on the postoperative image no hernial sac is seen, and the mesh can be seen as a relatively broad, hypointense band (arrow).

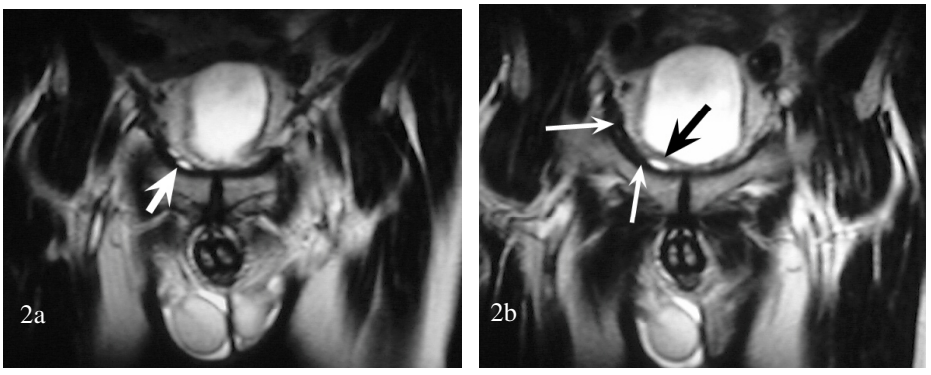

Figure 2
Postoperative T2-weighted image after right-sided laparoscopic inguinal hernia repair demonstrating a small fluid collection (arrow) near the medial insertion of the mesh, at the level of the pubic bone (a) and the hypointense mesh (between the white arrows) and an adjacent hyperintense fluid collection (black arrow) at a level more posteriorly located (b); note the difference with the left side.

On the post-operative MRI scans all four hydroceles were still present. No signs of hernia recurrence were demonstrated. In three groins a small unilateral fluid collection near the insertion of the mesh was found (figure 2)

In two patients a postoperative seroma was detected at the pubic bone at 6 and 12 weeks. In one patient a seroma in the inguinal canal was found at 6 weeks. The polypropylene mesh was visualised in all patients as a hypointense linear structure reaching from the pubic bone and overlying the internal inguinal ring in all sequences.

DISCUSSION

There is little need for diagnostic imaging after inguinal hernia repair. Only patients suspected of having a hernia recurrence or post-operative complications may be referred for radiological evaluation, which includes ultrasound, CT and MRI.

Ultrasound and CT are of established value in patients with seromas or abscesses [3-6]. Ultrasound can demonstrate postoperative changes such as seromas, abscesses and neuromas. CT can demonstrate globular, tubular or multilobular fluid collections. In the immediate post-operative period these fluid collections may even show rim enhancement (mimicking abscess formation) or air-fluid levels (mimicking recurrent hernia). With MRI, especially in T2-weighted sequences, it is relatively easy to detect small fluid collections (they appear hyperintense) [7]. MRI, like CT, has the advantage of producing an exact reproducible depiction of anatomical structures and reconstructions in various planes [4]. In none of the patients were direct post-operative complications, such as seromas and abscesses, suspected; thus in practical terms it did not matter whether they were detected or not However, this study indicates that MRI can demonstrate even small fluid collections (seromas) at the medial insertion of the mesh.

The key to success in laparoscopic hernia repair is the placement of the mesh far enough medially (i.e. over the pubic bone). The mesh is placed in the preperitoneal space without the use of hernia staplers and is covered by peritoneum [8]. Inappropriate positioning or dislodgement of the mesh might occur, resulting in an immediate recurrence. In the early post-operative period an adequate physical examination to assess the presence or absence of a recurrence is sometimes difficult to perform. The use of MRI in the postoperative evaluation of laparoscopic hernia repair has not been described before. Herniography has been used, but it has the disadvantage of being more invasive, and using ionising radiation (like CT) [9]. With CT postoperative fluid loculations can be easily mistaken for hernia recurrence [3]. The visibility of the mesh on CT scanning varies with the type of mesh from hardly discernible (Surgipro Mesh®, United States Surgical, Norwalk, CT) to readily seen (Bard Composix Mesh®, Davol, Cranston, RI)[6]. Our results demonstrated that the material commonly used in laparoscopic hernia repair in our hospital (Prolene® mesh) is readily identified on MRI scans.

Neither CT nor ultrasound has been used to evaluate the efficacy and

sufficiency of inguinal hernia repair, although helical CT and ultrasound can be performed during straining (like MRI, as used in our protocol). The technique used in this study (with easily reproducible sequences in the coronal plane, thus allowing both groins to be evaluated simultaneously) has been shown to be accurate in identifying the key anatomic structures of the inguinal canal [**2**]. It appears to be more accurate than ultrasound in the primary diagnosis of groin hernias [**10**], especially when the two dynamic sequences are added. This study indicates that not only the presence, but also the exact location of the mesh can be determined adequately. By demonstrating medial positioning of the mesh, and the absence of a previously present hernia sac, immediate recurrence of an inguinal hernia can be ruled out. A limitation of this series is the fact that no recurrences after transabdominal pre-peritoneal hernia repair were seen. However, dynamic MRI seems able to demonstrate recurrence of herniations after previous surgery, as demonstrated in the preoperative scans of five patients in this series.

In conclusion, this study indicates that dynamic MRI can reveal small, post-operative fluid collections after surgical repair. It can demonstrate a sufficient laparoscopic hernioplasty by showing the proper position of the mesh in the absence of a hernia. A larger study involving longer follow-up and comparing clinical examination, MRI, and an inexpensive, readily available radiological examination such as ultrasound is required to evaluate fully the utility of MRI in demonstrating hernia recurrence.

REFERENCES

1. Vanbeckevoort D, Van Hoe L, Oyen R, Ponette E, De Ridder D, Deprest J (1999) Pelvic floor descent in females: comparative study of colpocystodefecography and dynamic fast MR imaging. J Magn Reson Imaging 9: 373-377.
2. van den Berg JC, de Valois JC, Go PMNYH, Rosenbusch G (1997) Dynamic magnetic resonance imaging in the diagnosis of groin hernia. Invest Radiol 32:644-647.
3. Lin BHJ, Vargish T, Dachman AH (1999) CT findings after laparoscopic repair of ventral hernia. AJR 172: 389-392.
4. Furtschegger A, Sandbichler P, Judmaier W, Gstir H, Steiner E, Egender G (1995) Sonography in the postoperative evaluation of laparoscopic inguinal hernia repair. J Ultrasound Med 14: 679-684.
5. Hergan K, Scheyer M, Oser W, Zimmermann G (1995) CT- und Ultraschallnormalbefunde nach laparoskopischer Leistenhernien-operation. RöFo 162:29-32.

6. Archer A, Choyke PL, O'Brien W, Maxted WC, Grant EG (1988) Scrotal enlargement following inguinal herniorrhaphy: ultrasound evaluation. Urol Radiol 9:249-252.
7. Noone TC, Semelka RC, Worawattanakul S, Marcos HB (1998) Intraperitoneal abscesses: diagnostic accuracy of and appearances at MR imaging. Radiology 208: 525-528.
8. McIntyre IMC (1998) Does the mesh require fixation? Semin Laparosc Surg 5:224-226.
9. Ekberg O, Blomquist P, Fritzdorf J (1984) Herniography in patients with clinically suggested recurrence of inguinal hernia. Acta Radiol Diagn 25:225-229.
10. van den Berg JC, de Valois JC, Go PMNYH, Rosenbusch G (1999) Detection of groin hernia with physical examination, ultrasound, and MRI compared with laparoscopic findings. Invest Radiol 34:739-743.

9

GENERAL DISCUSSION AND CONCLUSIONS

Groin hernia is seen frequently in general surgical practice. However, both incidence and prevalence of groin hernias remain unknown [**1**]. Prevalence in adults is known to increase with age (from 1% in men aged 17-44 years, to 3.8% for those 45-64 years of age). Furthermore the distribution according to sex shows a high male preponderance for inguinal hernias (90% male, 10% female), while femoral herniations occur mostly in women (70% female, 30% male) [**1**]. Exact figures of the need of radiological examination in the diagnosis of groin hernia are not known, and additional investigation is mostly restricted to clinically doubtful cases, or in cases where the origin of pain in the groin can not be elucidated by medical history and physical examination.

In this thesis the role of diagnostic imaging in inguinofemoral disease in general, and inguinal and femoral herniations in specific is discussed.

The role of diagnostic imaging in the primary diagnosis of inguinal disease is changing. Herniography, ultrasound and to a lesser extent CT were already used in the diagnosis of inguinal hernias in clinically unclear or doubtful cases. This thesis reflects the development of the role of additional diagnostic imaging in the diagnosis of inguinofemoral hernia, not only because of the rapid development of imaging techniques (e.g. high resolution ultrasound and dynamic MRI), but also because of new (laparoscopic) surgical techniques requiring more imaging pre- and or postoperatively.

Basic issues in radiology are knowledge of the anatomy of the groin region (gross and radiological), and differential diagnosis of disease in the inguinofemoral triangle. Finally radiologists should be able to answer the question which modality is best suited for a specific clinical problem.

After description of the anatomy of the inguinal canal and it's neighbouring structures in chapter 2, an overview of disease in the groin region is presented in chapter 3. In the following chapters attention is focused on the diagnosis of inguinofemoral herniations using herniography, ultrasound and Miring the last chapter the use of dynamic MRI of the groin after surgical inguinal hernia repair will be discussed.

Knowledge of the anatomy of the groin is the key to success in diagnosing disease in the inguinofemoral region. Description of the anatomy is based on data obtained from anatomical literature, with a special interest for laparoscopic surgical anatomy [**2**]. Main anatomic structures, that can be identified at gross anatomy and are also of surgical interest, are the inguinal canal and inguinal ligament, the deep and superficial inguinal rings, and the inferior epigastric vessels and finally the parietal peritoneum. On herniography only the bony structures can be depicted directly. Other structures, like peritoneum and the inferior epigastric vessels, can be discerned in an indirect way by means of intraperitoneal contrast (e.g. inguinal fossae and lateral umbilical fold). Advantage of herniography is the

relatively easy interpretation, disadvantage it's invasiveness (with potentially lethal complications) [**3**].

Ultrasound, CT and MRI delineate anatomical structures in a direct fashion. Using these imaging techniques the nervous, muscular and small vascular structures (e.g. inferior epigastric vessels) of the inguinofemoral region can be easily identified. The disadvantage of ultrasound is its operator dependency, disadvantage of MRI its availability. The absence of MR facilities or ultrasound experience therefore still leaves a role for herniography, and CT [**4,5**]. All diagnostic modalities mentioned above are capable of obtaining images in a dynamic way (i.e. during straining). Imaging of internal hernias (e.g. obturator hernia) seems to be restricted to herniography and CT [**6,7,8,9**].

Pathology in the groin can be of very diverse etiology. Therefore diseases of the groin were classified into several differential diagnostic entities including herniations, neoplasms, joint disease and vascular abnormalities. In evaluating groin disease in general the role of conventional radiographs, and arthrography seems to be limited presently. All other imaging modalities used should be considered complementary in the diagnostic work-up of groin pathology. Imaging modality of first choice is ultrasound, as it is inexpensive, readily available, and requires only a short examination time. It can be used as an inventorying and directive technique: e.g. differentiation between solid and cystic processes can be made. MRI or CT should be used only when necessary in further evaluation. For the diagnosis of inguinofemoral herniations herniography, ultrasound, CT and MRI are suited [**6,8,9,10,11,12**], and their respective value is described hereafter.

To determine the value of herniography in detecting groin hernias, in chapter 4, herniographs obtained in 70 consecutive patients with clinically suspected hernias (but with a normal or inconclusive physical examination) were retrospectively evaluated. In this group a total of 30 herniations was found. In sixteen of 25 patients with an inguinofemoral hernia, surgical correlation was obtained, without any false-positive findings (that are known to occur) [**13**]. Procedure-related complications as described in literature (e.g. puncture of bowel or retroperitoneal structures, hematoma of rectus muscle etcetera [**3,14,15,16,17**]) were not seen.

These results, that are consistent with more recent reports [**4**] indicate that herniography is a simple and valuable diagnostic tool in patients with unexplained groin pain or pain in the anterior abdominal wall. It may advantageously delineate anatomic relations of hernias, especially in hernias that are small and not filled with bowel (the latter may be difficult to discern at CT or US).

(Spiral) CT scanning is known to be of value in the clinical diagnosis of inguinal herniations, especially in obese patients or patients that already

underwent laparotomy [18]. It can clearly demonstrate the location of the anatomical site of the hernial sac, and its content. Furthermore CT can depict occlusive bowel complications due to incarceration or strangulation in patients with acute symptoms [18]. Herniography and CT both have the disadvantage that the patient is exposed to a certain amount of ionizing radiation. Ultrasound and MRI do not have these limitations. Therefore we prospectively studied the role of the latter two imaging modalities.

Chapter 5 describes, as a technical note, the preliminary experience using dynamic MRI in the diagnosis of groin herniations. Reports in literature using MRI in the diagnosis of inguinal hernias are scarse [8] and are merely case reports. Adding a dynamic sequence to the MRI protocol might increase sensitivity and may obviate the use of herniography (proven to be reliable but invasive) or ultrasound (diagnostically accurate but highly operator dependent [6,19,20]). Patients with clinically evident inguinal hernias were investigated using a MRI protocol (consisting of T1-, and T2-weighted sequences and 2 dynamic sequences) that had proven to yield diagnostic images in volunteers. In all cases the clinical and surgical diagnosis could be confirmed.

Encouraged by these promising results a feasibility study was conducted (presented in chapter 6) that included description of the anatomy of the inguinal canal as depicted on coronal MRI (using the same protocol). Furthermore the feasibility of dynamic MRI in the diagnosis of groin hernia was investigated. This study evaluated 10 volunteers and 10 patients with surgically proven herniations. Larger anatomic structures like the inguinal rings and greater vessels could be identified more easily than smaller ones (e.g. inferior epigastric vessels; 100% versus 85%). On a total of 13 surgically proven hernias two herniations were not diagnosed prospectively on MRI (i.e. 84.6 % was diagnosed correctly). However, the two herniations missed initially could be diagnosed in retrospect. Thus, this feasibility study demonstrated that in patients with clinically evident herniations, MRI can clearly identify the structures that are crucial for the assessment and differentiation of inguinofemoral hernias. The diagnostic accurracy of MRI in identifying the presence or absence of inguinal hernias was judged to be promising enough to warrant a study determining the diagnostic accuracy of dynamic MRI in a larger group of patients with inguinal herniations. As little is known about the accuracy of physical examination and ultrasound in diagnosing hernias [11,21,22], these modalities were evaluated as well. This study, which is described in chapter 7, included 41 patients with clinically evident herniations, 82 groins were evaluated using a standard ultrasound and MRI protocol. All ultrasound examinations and MRI scans were reviewed without knowledge of clinical findings. In all cases, correlation with findings at laparoscopic surgery was made. Sensitivity and specificity figures

were 74.5%, and 96.3% for physical examination, 92.7% and 81.5% for ultrasound, and 94.5% and 96.3% for MRI. Physical examination will remain the cornerstone in the diagnosis of groin herniations in clinical practice. At present, there is no place for the routine use of ultrasound or MRI in patients with clear-cut inguinal hernias. However, this study indicates that MRI and to a lesser extent ultrasound (that has lower cost and higher availability) can be used to diagnose groin herniations accurately, in patients with negative or uncertain findings at physical examination but with a history suspicious for a groin hernia. In this study the role of various ultrasound scanning techniques (supine versus erect, with or without straining) and the different MRI sequences (T1, T2 and dynamic sequences) was evaluated. It was found that in order to achieve adequate diagnostic accuracy all techniques or sequences are still necessary. For example using all ultrasound techniques, a sensitivity of 92.7% could be reached, while sensitivity obtained using one sequence only ranged from 58.2% to 90.9%. These results are comparable with findings in literature [**23,24**]. For MRI the range was 74.5% to 81.8% with an overall sensitivity of 94.5%.
The last study in this thesis evaluates dynamic MRI in patients treated surgically for an inguinal hernia. Reports dealing with ultrasound and CT findings after (laparoscopic) inguinal hernia repair indicate that the role of imaging in the postoperative period after laparoscopic surgery for inguinal hernias is increasing [**19,25,26**]. In 10 patients, who underwent laparoscopic inguinal hernia repair using a polypropylene mesh, 13 groins were evaluated pre- and post-operatively, using the dynamic MRI protocol. As could be expected from our previous studies the inguinal hernias could be identified on the pre-operative MRI. Small post-operative fluid collections could be revealed, and sufficient hernioplasty could be demonstrated by showing the proper position of the mesh and the absence of a hernia.

A practical guide to the work-up of the patient suspected of groin hernia will be given, although a lot depends on the "couleur locale" in a hospital. Not only the availability of equipment plays a role, but also the specific demands of the surgeon and skills or preferences of the radiologist are of importance. The latter is reflected by the existing differences as described in literature. Some surgeons want to be informed about the nature of the hernia (because this changes the surgical approach) [**27,28**], while others are only interested in the fact whether a hernia is present or not [**29**]. The nature of the hernia can be determined using herniography, ultrasound or MRI [**30,31,32,33**]. The presence of a hernia can be diagnosed with herniography, CT, ultrasound and MRI. Herniography and CT have the disadvantage of using ionizing radiation and being invasive. Herniography and CT are only indicated in cases of suspected obturator hernias and when experience using

ultrasound, or MRI equipment is not available [34,35]. When ultrasound experience is sufficient a positive test will obviate the need for further investigations. In all other situations MRI is the modality of choice, also because MRI is a good method to visualize musculoskeletal structures, and may reveal an origin of pain in the groin region other than herniations [36,37].

The work-up of a patient suspected of groin hernia should consist of medical history and physical examination followed, when doubt about the diagnosis exists, by ultrasound. MRI can be used as a final examination when ultrasound does not clarify the origin of the complaints.

CONCLUSIONS

- A sound working knowledge of groin anatomy and pathology is mandatory when evaluating groin disease and more specifically inguinofemoral herniation.
- Herniography, although one of the conventional radiological tools, still is a valuable diagnostic modality in the diagnosis of inguinal hernia in clinically equivocal cases.
- Dynamic MRI is able to depict inguinal hernias and is able to diagnose small hernias that are not detected by physical examination.
- Ultrasound has a slightly lower diagnostic accuracy than dynamic MRI, but a higher diagnostic yield than physical examination in this group of patients and is imaging method of first choice.
- Dynamic MRI is able to depict the postoperative changes following inguinal hernia repair and can play a role in patients when doubt exists about the sufficiency of hernioplasty.

REFERENCES

1. Rutkow IM (1996) Epidemiologic, economic, and sociologic aspects of hernia surgery in the United States in the 1990s. Surg Clin North Am 78:941-951.
2. Rosser J (1994) The anatomical basis for laparoscopic hernia repair revisited. Surgical Laparosopy & Endoscopy 4:36-44.
3. Butsch JL, Kuhn JO (1978) Intramural hematoma of the small bowel: a possible lethal complication of herniography. Surgery 83:121-122
4. Jones RL, Wingate JP (1998) Herniography in the investigation of groin pain in adults. Clin Radiol 53:805-808.
5. Hamlin JA, Kahn AM (1998) Herniography: a review of 333 herniograms. Am Surg 64:965-969.

6. Harrison LA, Keesling CA, Martin NL, Lee KR, Wetzel LH (1995) Abdominal wall hernias: Review of herniography and correlation with cross-sectional imaging. Radiographics 15:315-332.
7. Ekberg O (1981) Inguinal herniography in adults:technique, normal anatomy and diagnostic criteria for hernias. Radiology 138:31-36.
8. Wechsler RJ, Kurtz AB, Needleman L, et al (1989) Cross-sectional imaging of abdominal wall hernias. AJR 153:517-521.
9. Zarvan NP, Lee FT, Yandow DR, Unger JS (1995) Abdominal hernias: CT findings. AJR 164:1391-1395.
10. Ekberg O, Fork FT (1979) Röntgenologische Leistenbruchdiagnostik-Erfahrungen mit intraperitonealer Jodkontrastinstillation. Fortschr. Röntgenstr 131: 166-168.
11. Deitch EA, Soncrant MC (1981) Ultrasonic diagnosis of surgical disease in the inguino-femoral region. Surg Gyn Obst 152:319-322.
12. Lee G-H M, Cohen AJ (1993) CT imaging of abdominal hernias. AJR 161:1209-1213.
13. Oh KS, Dorst JP, White JJ, Haller JA, Heller RM, James AE, Johnson BA, Strife JL (1973) Positive-contrast peritoneography and herniography. Radiology 108:647-654.
14. Verhaar JAN, Pot JH (1985) De waarde van de herniografie bij onbegrepen pijn in de lies. Ned Tijdschr v Geneeskunde 129:-359-362.
15. Ekberg O (1983) Complications after herniography in adults.AJR 140:491-495.
16. Fenn K, Keller G, Kühn R (1982) Die Peritoneographie zum Nachweis nicht tast-barer Hernien.Radiologe 22-:166-169.
17. Shackelford GD, McAlister WH (1972) Inguinal herniography. AJR 115:399-407.
18. Stabile Ianora AA, Midiri M, Vinci R, Rotondo A, Angelelli G. (2000) Abdominal wall hernias: imaging with spiral CT. Eur Radiol 10:914-919.
19. Furtschegger A, Sandbichler P, Judmaier W, Gstir H, Steiner E, Egender G (1995) Sonography in the postoperative evaluation of laparoscopic inguinal hernia repair. J Ultrasound Med 14: 679-684.
20. Orchard JW, Read JW, Neophyton J, Garlick D (1998) Groin pain associated with ultrasound finding of inguinal canal posterior wall deficiency in Australian Rules footballers. Br J Sports Med 32:134-139.
21. Arregui ME (1994) The value of ultrasound in the diagnosis of hernias. In: Arregui ME, Nagan RF.Inguinal hernia: advances or controversies? Radcliff Medical Press, Oxford, New York, pp 73-79.

22. Machan L, Cooperberg PL (1984) A femoral hernia diagnosed by ultrasonography and fine-needle aspiration biopsy. J Ultrasound Med 3:379-380.
23. Erez I, Schneider N, Glaser E, Kovalivker M (1992) Prompt diagnosis of 'acute groin' conditions in infants. Eur J Radiology 15:185-189.
24. Chou TY, Chu CC, Diau GY, Wu CJ, Gueng MK (1996) Inguinal hernia in children: US versus exploratory surgery and intraoperative contralateral laparoscopy. Radiology 201:385-388.
25. Lin BHJ, Vargish T, Dachman AH (1999) CT findings after laparoscopic repair of ventral hernia. AJR 172: 389-392.
26. Hergan K, Scheyer M, Oser W, Zimmermann G (1995) CT- und Ultraschallnormalbefunde nach laparoskopischer Leistenhernien-operation. Fortschr. Röntgenstr 162:29-32.
27. Liem MSL, van Vroonhoven ThJMV (1996) Laparoscopic inguinal hernia repair. Br J Surg 83:1197-1204.
28. Nyhus LM (1993) Individualization of hernia repair: a new era. Surgery 114: 1-2.
29. Beets GL, Oosterhuis KJ, Go, PMNYH, Baeten CGMI, Kootstra G (1997) Longterm follow-up (12-15 years) of a randomized controlled trial comparing Bassini-Stetten, Shouldice, and high ligation with narrowing of the internal ring for primary inguinal hernia repair. J Am Coll Surg 185:352-357.
30. Sanders FBM, Pierie JPEN, Hoynck van Papendrecht AAGM (1997) Duplex-echografie ter differentiatie van mediale en laterale liesbreuken. Memorad 2:25-26 (abstr).
31. van der Ben EJM, van den Berg JC, de Valois JC, Go PMNYH (1999) Dynamische MRI ter evaluatie van inguino-femorale breuken. Memorad 4:38 (abstr).
32. Ekberg O (1981) Inguinal herniography in adults:technique, normal anatomy and diagnostic criteria for hernias.Radiology 138:31-36.
33. Gullmo A et al (1984) Herniography. Surg Clin North Am 64:229-244.
34. Zausner J, Dumont AE, Ring SM (1972) Obturator hernia.AJR 115:408-410.
35. Glicklich M, Eliasoph J (1989) Incarcerated obturator hernia: case diagnosed at barium enema fluoroscopy. Radiology 172:51-52.
36. Tuite MJ, DeSmet AA (1994) MRI of selected sports injuries: muscle tears, groin pain, and osteochondritis dissecans. Semin Ultrasound CT MR 15:318-340.
37. Ekberg O, Sjoberg S Westlin N (1996) Sports-related groin pain: evaluation with MR imaging. Eur Radiol 6:52-55.

10

DISCUSSIE EN CONCLUSIES

Liesbreuken komen in de algemene chirurgische praktijk veel voor. Exacte gegevens over incidentie en prevalentie van liesbreuken ontbreken echter. De prevalentie bij volwassenen neemt toe bij het stijgen van de leeftijd (van 1% bij mannen in de leeftijd van 17-44 jaar, tot 3.8% voor mannen in de leeftijdsgroep van 45-64 jaar). Tevens is bekend dat liesbreuken (hernia inguinalis) veel vaker voorkomen bij mannen (90% bij mannen, 10% bij vrouwen), terwijl dijbeenbreuken (hernia femoralis) meer voorkomen bij vrouwen (70% bij vrouwen, 30% bij mannen). Exacte cijfers over de noodzaak van aanvullend radiologisch onderzoek bij het stellen van de diagnose liesbreuk zijn niet bekend, en aanvullend onderzoek blijft meestal beperkt tot klinisch twijfelachtige gevallen, of tot die gevallen waarbij pijn in de liesregio niet voldoende kan worden verklaard door bevindingen bij anamnese en lichamelijk onderzoek.
In dit proefschrift wordt de rol van diagnostische beeldvorming bij pathologie van de liesregio in het algemeen, en bij lies- en dijbeenbreuken in het bijzonder besproken.
De rol van beeldvorming bij de primaire diagnostiek van liesbreuken is aan verandering onderhevig. Herniografie, echografie en, in mindere mate, CT werden al gebruikt bij de diagnostiek van liesbreuken in klinisch onduidelijke of twijfelachtige gevallen. Dit proefschrift weerspiegelt de ontwikkeling van de rol van aanvullende beeldvorming bij het stellen van de diagnose van inguinofemorale breuken, niet alleen ten gevolge van de snelle ontwikkeling van beeldvormende technieken (bijvoorbeeld echografie met hoge resolutie en dynamische MRI), maar ook ten gevolge van nieuwe (laparoscopische) chirurgische technieken die meer pre- en postoperatieve beeldvorming vereisen.
Grondbeginselen in de radiologie zijn kennis van de anatomie van de liesregio (zowel macroscopische anatomie als radiologisch), en kennis van de differentiële diagnostiek van afwijkingen van de inguinofemorale driehoek. Tenslotte dienen radiologen in staat te zijn om de vraag te beantwoorden, welke modaliteit het best geschikt is voor het oplossen van een specifiek klinisch probleem.
Na beschrijving van de anatomie van het lieskanaal en de aangrenzende structuren in hoofdstuk 2, wordt in hoofdstuk 3 een overzicht gegeven van de pathologie van de liesregio. In de daarop volgende hoofdstukken wordt de aandacht gericht op de diagnostiek van inguinofemorale liesbreuken met behulp van herniografie, echografie en MRI. In het laatste hoofdstuk wordt het gebruik van dynamische MRI van de lies na chirurgische correctie van een liesbreuk besproken.
Kennis van de anatomie van de lies is de sleutel tot succes in de diagnostiek van afwijkingen in de inguinofemorale regio. Beschrijving van de anatomie wordt gebaseerd op gegevens uit anatomische literatuur, met speciale

aandacht voor de laparoscopische chirurgische anatomie. Belangrijke anatomische structuren, die chirurgisch van belang zijn en macroscopisch kunnen worden herkend, zijn het lieskanaal en het ligament van Poupart, de diepe en oppervlakkige inguinale ring en de a. en v. epigastrica inferior en tenslotte het peritoneum parietale. Met behulp van herniografie kunnen slechts de benige structuren direct worden afgebeeld. Andere structuren, zoals het peritoneum en de epigastrische vaten kunnen indirect zichtbaar worden gemaakt door middel van intraperitoneaal toegediend contrast (bijvoorbeeld de inguinale fossae en de plica umbilicalis lateralis). Voordeel van herniografie is de relatief eenvoudige interpretatie, nadeel de invasiviteit (met mogelijk dodelijke complicaties).
Echografie, CT en MRI beelden anatomische structuren af op een directe wijze. Met behulp van deze beeldvormende modaliteiten kunnen de zenuw-, spier- en vaatstructuren (bijvoorbeeld a. en v. epigastrica inferior) van de inguinofemorale driehoek makkelijk worden geïdentificeerd. Nadeel van echografie is de sterke onderzoekersafhankelijkheid, nadeel van MRI de beperkte beschikbaarheid. Bij ontbreken van mogelijkheden tot MRI of gebrek aan echografische expertise is er nog steeds een rol voor herniografie of CT. Alle voornoemde diagnostische modaliteiten zijn in staat om op dynamische wijze afbeeldingen te verkrijgen (dat wil zeggen, tijdens persen). Het afbeelden van inwendige hernias (bijvoorbeeld hernia obturatoria) lijkt alleen mogelijk te zijn met behulp van herniografie en CT
Pathologie in de lies kan een sterk varierende aetiologie hebben. Derhalve worden afwijkingen van de lies ingedeeld in diverse differentiaal diagnostische entiteiten, waaronder hernias, neoplasma's, gewrichtsafwijkingen en vaatafwijkingen. Heden ten dage is de rol van conventionele röntgenopnamen, en arthrografie bij de evaluatie van afwijkingen in de liesregio beperkt. In de diagnostische work-up van liespathologie dienen de overige modaliteiten als complementair te worden beschouwd. Modaliteit van eerste keuze is echografie aangezien het goedkoop is en makkelijk beschikbaar en slechts weinig onderzoekstijd behoeft. Het kan worden gebruikt ter inventarisatie en ter sturing van het verdere diagnostische proces: bijvoorbeeld het maken van onderscheid tussen solide en cysteuze processen is mogelijk. MRI en CT dienen alleen te worden gebruikt indien nodig bij nadere evaluatie. Voor de diagnostiek van inguinofemorale herniaties zijn herniografie, echografie, CT en MRI geschikte modaliteiten, en hun waarde wordt hieronder beschreven.
In hoofdstuk 4 wordt een retrospectieve analyse gemaakt van herniografieën verkregen bij 70 opeenvolgende patiënten die klinisch werden verdacht van het hebben van een liesbreuk (maar bij wie de bevindingen bij lichamelijk onderzoek normaal waren of niet-conclusief), teneinde de waarde te bepalen van herniografie bij de detectie van liesbreuken. In deze groep werden in

totaal 30 hernia's gevonden. Bij 16 van de 25 patiënten met een inguinofemorale breuk werd chirurgische bevestiging verkregen, en er waren geen fout-positieve bevindingen (waarvan bekend is dat deze voorkomen). Aan de procedure verbonden complicaties zoals beschreven in de literatuur (aanprikken van darm of retroperitoneale structuren, rectus hematoom, et cetera) werden niet gezien.
Deze resultaten die overeenkomen met recente publicaties tonen aan dat herniografie een eenvoudig en waardevol diagnostisch hulpmiddel is bij patiënten met onverklaarde pijn in de liesstreek of voorste buikwand. Bijkomend voordeel is de gebleken geschiktheid om de anatomische verhoudingen weer te geven, met name bij kleine breuken en bij breuken die niet gevuld zijn met darmlissen (deze laatste zijn moeilijk aan te tonen met behulp van bij CT en echografie).
(Spiraal) CT is van bewezen waarde bij het stellen van de diagnose liesbreuk, met name bij adipeuze patiënten, of bij patiënten die al eerder een laparotomie ondergingen. CT kan de anatomische localisatie en de inhoud van een breuk zeer duidelijk afbeelden. Tevens kan CT bij patiënten met acute symptomen obstructieve darmproblematiek ten gevolge van inklemming of strangulatie aantonen. Zowel herniografie als CT hebben het nadeel dat de patiënt wordt blootgesteld aan een bepaalde hoeveelheid ioniserende straling. Echografie en MRI kennen deze beperkingen niet. Derhalve werd het belang van deze laatste twee modaliteiten nader onderzocht.
Hoofdstuk 5 beschrijft, in de vorm van een zogenaamde technische notitie, de eerste ervaringen met het gebruik van dynamische MRI bij de diagnostiek van liesbreuken. In de literatuur is het gebruik van MRI bij het stellen van de diagnose liesbreuk slechts mondjesmaat beschreven en meestal beperkt tot beschrijving van incidentele gevallen. Het toevoegen van een aanvullende dynamische serie aan het MRI protocol zou de sensitiviteit van het MRI onderzoek kunnen verhogen. Het gebruik van herniografie (betrouwbaar doch invasief) of echografie (diagnostisch nauwkeurig maar erg onderzoekersafhankelijk) zou hierdoor achterwege kunnen blijven). Patiënten met op klinische gronden duidelijke hernias werden onderzocht met behulp van een MRI protocol dat had bewezen diagnostisch adequate opnamen op te leveren bij vrijwilligers (bestaande uit een T1- en T2-gewogen sequentie en 2 dynamische sequenties). In alle gevallen kon de klinische en chirurgische diagnose worden bevestigd.
Aangespoord door deze bemoedigende resultaten werd een onderzoek naar de geschiktheid van MRI uitgevoerd (beschreven in hoofdstuk 6), waarbij onder andere de anatomie van het lieskanaal zoals zichtbaar op coronale MRI afbeeldingen (verkregen met hetzelfde voornoemde protocol) wordt besproken. Tevens werd de bruikbaarheid van dynamische MRI bij de

diagnose liesbreuk bestudeerd. Dit onderzoek omvatte evaluatie van 10 vrijwilligers en 10 patiënten met (chirurgisch) bewezen hernias. Grotere anatomische structuren als de annulus inguinalis en de grote vaten konden makkelijker worden geidentificeerd dan kleine structuren (bijvoorbeeld epigastrische vaten; 100% versus 85%). Op een totaal van 13 chirurgisch bewezen hernias, werden 2 breuken prospectief niet gediagnostiseerd met behulp van MRI (d.w.z. 84,6% werd juist gediagnostiseerd). De twee aanvankelijk gemiste hernia's konden retrospectief echter wel worden gevonden. Deze haalbaarheidsstudie toonde aan dat, althans bij patiënten met klinisch duidelijke hernias, MRI de structuren van belang bij het aantonen en differentiatie van inguinofemorale breuken duidelijk kan afgrenzen. De diagnostische nauwkeurigheid van MRI om een liesbreuk aan te tonen of uit te sluiten werd voldoende groot geacht om een studie naar de diagnostische betrouwbaarheid van dynamische MRI in een grotere groep patiënten met liesbreuken te rechtvaardigen. Aangezien weinig bekend is met betrekking tot de nauwkeurigheid van lichamelijk onderzoek en echografie in de diagnose van hernias, werden deze modaliteiten ook onderzocht.
Deze studie die wordt beschreven in hoofdstuk 7, omvatte 41 patiënten met klinisch evidente hernias, waarbij 82 liesregio's werden onderzocht met een standaard echografie- en MRI onderzoek. Alle echografische en MRI onderzoeken werden beoordeeld zonder kennis van de klinische bevindingen. In alle gevallen werd een correlatie verkregen met de bevindingen bij laparoscopische chirurgie. Sensitiviteit en specificiteit waren 74.5%, en 96.3% voor lichamelijk onderzoek, 92.7% en 81.5% voor echografie, en 94.5% en 96.3% voor MRI. In de dagelijkse praktijk zal lichamelijk onderzoek de hoeksteen blijven in de liesbreuk diagnostiek. Op dit moment is er geen plaats voor routinematig gebruik van echografie of MRI bij patiënten met duidelijke hernias. Deze studie toont echter wel aan dat MRI, en in mindere mate echografie (dat overigens goedkoper en makkelijker beschikbaar is) kunnen worden gebruikt om op betrouwbare wijze hernias te diagnostiseren bij patiënten met afwezige of onduidelijke bevindingen bij lichamelijk onderzoek maar met een anamnese die verdacht is voor een liesbreuk. In dit onderzoek werd de rol van de diverse echografische technieken (liggend versus staand, tijdens of zonder persen) en de verschillende MRI technieken (T1, T2 en dynamische sequenties) onderzocht. De hierbij verkregen bevindingen tonen aan dat, teneinde voldoende diagnostische betrouwbaarheid te krijgen, alle technieken of sequenties nodig zijn. Bijvoorbeeld kon met gebruik van alle echografische technieken een sensitiviteit van 92,7% worden bereikt, terwijl bij gebruik van slechts één techniek de sensitiviteit varieerde van 58,2% tot 90,9%. Deze resultaten komen overeen met bevindingen uit de literatuur. Voor MRI liep de sensitiviteit uiteen voor iedere sequentie van 74,5% tot 81,8%, met een totale

sensitiviteit van 94,5%.
De laatste studie in dit proefschrift bepaalt de rol van dynamische MRI bij patiënten die chirurgisch zijn behandeld wegens een liesbreuk. Artikelen die de echografische en CT bevindingen na laparoscopische liesbreukchirurgie beschrijven geven aan dat de rol van beeldvormende diagnostiek in het postoperatieve beloop na laparoscopische correctie van liesbreuken toeneemt. Bij 10 patiënten, die een laparoscopische liesbreukcorrectie met behulp van een polypropylene matje ondergingen, werden 13 liezen pre- en postoperatief met een dynamische MRI bestudeerd. Zoals kon worden verwacht op grond van eerdere studies konden alle inguinale breuken worden herkend op de pre-operatieve MRI. Kleine postoperatieve vochtcollecties konden worden aangetoond, en een sufficiënte hernioplastiek kon worden aangetoond door middel van het afbeelden van een goede positie van het matje en de afwezigheid van een breuk.

Een praktische handleiding voor het analyseren van een patiënt verdacht van het hebben van een liesbreuk zal hieronder worden gegeven, alhoewel veel afhangt van de locale situatie in een ziekenhuis. Niet alleen de beschikbaarheid van bepaalde apparatuur speelt een rol, maar ook de specifieke vragen/eisen van de chirurg en de ervaring of voorkeur van de radioloog. Dit laatste wordt ook weerspiegeld in de bestaande verschillen zoals beschreven in de literatuur. Sommige chirurgen willen van tevoren op de hoogte zijn van de aard van de liesbreuk (omdat dit de chirurgische benadering wijzigt), terwijl anderen slechts willen weten of er een hernia aanwezig is of niet. De aard van een hernia kan worden bepaald met behulp van herniografie, echografie of MRI. De aanwezigheid van een liesbreuk kan worden aangetoond met behulp van herniografie, CT, echografie en MRI. Het nadeel van herniografie en CT is het gebruik van ioniserende straling en de invasiviteit. Herniografie en CT zijn slechts geïndiceerd in gevallen waarbij verdenking bestaat op een hernia obturatoria, en wanneer er gebrek is aan ervaring met echografie of wanneer MRI niet beschikbaar is. Indien er voldoende echografische expertise aanwezig is, zal een positieve bevinding verder onderzoek onnodig maken. In alle andere gevallen is MRI de modaliteit van keuze, mede omdat MRI een goede methode is om spier- en skeletstructuren af te beelden en op die wijze ook andere oorzaken van de pijn kunnen worden aangetoond.
De beoordeling van een patiënt die wordt verdacht van een liesbreuk dient te bestaan uit het afnemen van de anamnese en het verrichten van een lichamelijk onderzoek, gevolgd door echografie in die gevallen waarbij twijfel over de diagnose bestaat. MRI kan worden gebruikt als sluitstuk van de diagnostiek, als echografie de oorzaak van de klachten niet kan verklaren.

CONCLUSIES

- Goede kennis van de liesanatomie en de in deze regio voorkomende pathologie is vereist wanneer afwijkingen in het liesgebied, met name liesbreuken, worden beoordeeld.
- Herniografie is nog steeds een waardevolle diagnostische modaliteit bij het stellen van de diagnose liesbreuk in klinisch onduidelijke situaties, ook al is het één van de conventionele radiologische technieken.
- Dynamische MRI is in staat om liesbreuken aan te tonen, en om kleine liesbreuken vast te stellen die bij lichamelijk onderzoek onopgemerkt blijven.
- Echografie heeft een iets lagere diagnostische betrouwbaarheid dan dynamische MRI maar een hogere diagnostische opbrengst dan lichamelijk onderzoek in deze groep patiënten, en is daarom beeldvormende techniek van eerste keuze.
- Dynamische MRI is in staat om de veranderingen na chirurgische liesbreukcorrectie af te beelden, en kan een rol spelen bij patiënten bij wie twijfel bestaat over de sufficiëntie van een hernioplastiek.

DANKWOORD

Dit proefschrift is het resultaat van enige jaren bloed, zweet, en tranen. Toch heb ik deze tranen niet alleen geplengd, of dit leed alleen hoeven dragen. Op deze plaats wil ik een aantal personen danken voor hun steun of bijdrage in de realisatie van dit proefschrift.

Hooggeleerde Rosenbusch, beste Gerd. Jij hebt als één der weinigen van het begin af in de haalbaarheid van dit onderzoek geloofd. Ook nadat ik het AZN voor het AZN verruild had, ben jij een grote stimulans voor mijn wetenschappelijke activiteiten gebleven. Dat het uiteindelijk zolang heeft moeten duren, lag deels aan mijn langzaam aan verschuivende belangstelling, deels aan jouw streven tot perfectie. Dank voor je steun.

Hooggeleerde Janssen, beste Jan. Als tweede promotor is je bijdrage aan één der hoofdstukken, alsmede advies met betrekking tot de inleiding en discussie van groot belang geweest. Met name het zetten van de laatste stap was zonder jou niet mogelijk geweest.

Frank Joosten: als co-promotor heb je een wezenlijke bijdrage geleverd in de totstandkoming van inleiding en discussie, ook al had je zelf het idee "er op het laatste moment bij gesleept te zijn". Juist jouw commentaar van afstand heeft de discussie meer diepgang gegeven.

Leden van de manuscriptcommissie, prof. dr. M.A.M. Feldberg, prof. dr. van J.H.J.M. van Krieken en prof. dr. Th. Wobbes. Dank voor de tijd genomen voor de beoordeling van dit proefschrift. Met name de hooggeleerde Wobbes heeft als voorzitter van de manuscriptcommissie nog een taalzuiverende werking gehad met betrekking tot de Nederlandse vertaling van de samenvatting en discussie.

Van mijn vroegere collegae in het St. Radboud Ziekenhuis (thans UMC Nijmegen) wil ik met name Simon Strijk noemen. Niet slechts als co-auteur van één der artikelen uit dit proefschrift, maar ook, en vooral, om je ondersteuning bij mijn eerste schreden op het pad van de interventieradiologie. Dank voor je vertrouwen destijds.

Leden van de maatschap Radiologie van het St. Antonius Ziekenhuis, beste maten, Hans, Hans, Hans, Jiri, Tim en Wouter, en mijn oud-maten Jan en Pierre. Bij onze kennismaking in 1994 is het totstandkomen van een proefschrift reeds ter sprake gekomen. Zeven jaar later is het dan eindelijk zover, en zou je kunnen zeggen dat ik aan de destijds geuite wens heb voldaan. Ik heb één en ander echter nooit als een verplichting gevoeld, en dit geeft denk ik ook de sfeer binnen onze groep goed weer. Het wederzijds respect en het stimuleren van de ontwikkeling van ieders sterke kanten heeft er voor gezorgd dat ik me thuis voel. Hans de Valois, als primus inter pares en co-auteur wil ik met name danken voor de uitbundige correcties in de diverse manuscripten.

Peter Go wil ik bedanken voor zijn inzet, niet alleen als co-auteur, maar vooral als stuwende kracht bij het werven van de patiënten voor dit

onderzoek. Jij hebt hierdoor mogelijk gemaakt wat eerder niet van de grond te krijgen was.
Jan Verwoerd, met behulp van jouw kennis en kunde kon een reeds in Nijmegen ten dele ontwikkeld MRI protocol tot een werkbare Nieuwegeinse vorm worden gesmeed. Dank voor je bijdrage hieraan.
Uiteraard wil ik de vrijwilligers en de patiënten danken voor hun deelname aan dit onderzoek, en de MRI laboranten voor hun inzet. Zonder hun bijdrage was dit boekje nooit gerealiseerd.
Dames van de postkamer: jullie directe berichtgeving en oprechte belangstelling wanneer er weer eens enveloppe binnen kwam, is en blijft hartverwarmend.
Alle medewerkers van de afdeling Medische Fotografie. Dank voor jullie geduld, want ik ben me bewust dat ik een kritische klant ben (geweest). Het digitale tijdperk zal het leven een stuk veranderen.
Matthieu Rutten, samen hebben we al vele projecten op de rails gezet, overigens niet altijd met succes. Met het voltooien van dit boekje komt er zeker geen einde aan onze samenwerking. Dank voor al je tijd, plannen, gezelligheid etc.
Louis Meiss, onze vriendschap dateert van de bestuurstijd in de Aspirant Sectie. Jou wil ik danken voor je aanwezigheid en betrokkenheid op de juiste momenten.
Cara Barbara. Grazie per aver fatto ricominciare la mia vita quasi tre anni fa: senza te non avrei sicuramente avuto la forza per portare a termine l'impegno di questa tesi. Spero tu possa adattarti alla vita in Olanda, con tutti.....gli Olandesi. Soprattutto grazie per il grande regalo che mi hai fatto (Lucone) e perchè accetti anche Aernout e Jacobine.
Luca, Jacobine en Aernout: nu is het de hoogste tijd voor iets echt leuks.

CURRICULUM VITAE

De schrijver van dit proefschrift werd op 20 september 1961 geboren te Leiden. Na het behalen van het eindexamen VWO (Chr. Lyceum dr. W.A. Visser 't Hooft, Leiden), werd in 1979 begonnen met de studie Geneeskunde aan de Rijksuniversiteit te Leiden. In 1986 werd het artsexamen behaald, waarna de militaire dienstplicht werd vervuld op de afdeling Radiologie van het Militair Hospitaal "Dr. A. Mathijssen" te Utrecht (hoofd van de afdeling dr. J.M.H. Blom). Vanaf 1988 tot 1994 was hij werkzaam in het St. Radboud Ziekenhuis te Nijmegen, alwaar de opleiding tot radioloog werd gevolgd (opleider prof.dr. J.H.J. Ruijs). Tijdens de opleiding publiceerde hij diverse artikelen op het gebied van de gastro-enterologische radiologie, en ontstond een speciale belangstelling voor interventie-radiologie en echografie van het steun- en bewegingsapparaat. Als assistent in opleiding was hij secretaris en later voorzitter van het bestuur van de Aspirant-Sectie van de Nederlandse Vereniging voor Radiologie. Vanaf april 1994, na het voltooien van de opleiding Radiologie, is de schrijver van dit proefschrift werkzaam als radioloog in het St. Antonius Ziekenhuis te Nieuwegein in associatie met J.W.B.M. Casparie, dr. H.W. van Es, dr. J.P.M. van Heesewijk, T.Th.C. Overtoom, dr. J.C. de Valois en dr. J. Zapletal. Zijn huidige aandachtsgebieden zijn de vasculaire interventieradiologie en echografie van het steun- en bewegingsapparaat. Hij is actief lid van de Nederlandse werkgroep voor echografie van het steun- en bewegingsapparaat en bestuurslid van het Endovasculair Forum.